

Top-Down Holographic G -Structure Glueball Spectroscopy at (N)LO in N and Finite Coupling

Karunava Sil¹, Vikas Yadav² and Aalok Misra³

Department of Physics, Indian Institute of Technology, Roorkee - 247 667, Uttarakhand, India

Abstract

The top-down type IIB holographic dual of large- N thermal QCD as constructed in [1] involving a fluxed resolved warped deformed conifold, its delocalized type IIA SYZ mirror as well as its M-theory uplift constructed in [2] - both in the finite coupling ($g_s \lesssim 1$)/‘MQGP’ limit of [2] - were shown explicitly to possess a local $SU(3)/G_2$ -structure in [3]. Glueballs spectra in the *finite-gauge-coupling limit* (and not just large- t ’t Hooft coupling limit) - a limit expected to be directly relevant to strongly coupled systems at finite temperature such as QGP [4] - has thus far been missing in the literature. In this paper, we fill this gap by calculating the masses of the $0^{++}, 0^{-+}, 0^{--}, 1^{++}, 2^{++}$ (‘glueball’) states (which correspond to fluctuations in the dilaton or complexified two-forms or appropriate metric components) in the aforementioned backgrounds of G -structure in the ‘MQGP’ limit of [2]. We use WKB quantization conditions on one hand and impose Neumann/Dirichlet boundary conditions at an IR cut-off (‘ r_0 ’)/horizon radius (‘ r_h ’) on the solutions to the equations of motion on the other. We find that the former technique produces results closer to the lattice results. We also discuss $r_h = 0$ -limits of all calculations. In this context we also calculate the $0^{++}, 0^{--}, 1^{++}, 2^{++}$ glueball masses up to NLO in N and find a $\frac{g_s M^2}{N}(g_s N_f)$ -suppression similar to and further validating a similar semi-universality of NLO corrections to transport coefficients, observed in [5].

arXiv:1703.01306v2 [hep-th] 15 May 2017

¹e-mail: krusldph@iitr.ac.in

²email: viitr.dph2015@iitr.ac.in

³e-mail: aalokfph@iitr.ac.in

1 Introduction

The AdS/CFT correspondence [6] remarkably establishes an equivalence between the partition functions of a five dimensional gravitational theory (bulk theory) and a four dimensional supersymmetric and scale invariant gauge theory (boundary theory). A generalization of the AdS/CFT correspondence is necessary to explore more realistic gauge theories (less supersymmetric and non-conformal) such as QCD with $SU(3)$ gauge group. The top-down model that we have considered in this work is motivated to capture QCD-like gauge theories from a suitable gravitational background. QCD is a strongly coupled theory at low energies. The low energy dynamics of QCD involves the color neutral bound states of gluons, known as glueballs. Hence, the non-perturbative aspects of QCD can be largely understood from the glueball sector of the theory. Moreover, the plasma phase of QCD (QGP) occurs at high temperatures $T > T_c$. In QGP medium the quarks and the gluons stay in a deconfined state due to Debye screening. However, the recent RHIC experiments indicate strongly that non-perturbative effects of QCD are present in the plasma phase. In fact the lattice results of [7] conclude that QGP must be non-perturbative in the temperature regime $T_c \leq T \leq 5T_c$. This is precisely the reason why we concentrate on the glueball spectra in the *finite-gauge-coupling limit* (and not just large-t'Hooft coupling limit) - a limit expected to be directly relevant to strongly coupled systems at finite temperature such as QGP [4].

QCD is a non-abelian gauge theory, in which gauge fields play the role of dynamical degrees of freedom. Non-abelian nature of QCD allows the gauge bosons to form color-neutral bound states of gluons known as glueballs (gg, ggg, etc.). Therefore, the study of glueballs and their spectra enables us to gain a better understanding of the non-perturbative regime of QCD. Glueball state is represented by quantum numbers J^{PC} , where J, P and C correspond to total angular momentum, parity and charge conjugation respectively

Different generalized versions of the AdS/CFT correspondence has thus far been proposed to study non-supersymmetric field theories with a running gauge coupling constant. The original proposal was given by Witten to obtain a gravity dual for non-supersymmetric field theories. As per Witten's formalism, non-supersymmetric Yang-Mills theory can be obtained by compactifying one of the spatial direction on a circle and imposing antiperiodic boundary conditions on the fermions around this circle. This makes the fermions and scalars massive and they get decoupled leaving only gauge fields as degrees of freedom. The gravity dual of this compactified theory was asymptotically AdS. In a particular case of $\mathcal{N} = 4$ $SU(N)$ super-Yang-Mills theory dual to type IIB string theory on $AdS_5 \times S^5$, the procedure described above gives an effective model of three dimensional Yang-Mills theory, i.e., QCD_3 .

The gravity dual of non-supersymmetric theories in the low energy limit is typically given by supergravity backgrounds involving $AdS_p \times M_q$ where AdS is the anti de Sitter space with dimension p and M_q is the internal manifold with dimension q . In the supergravity theory the Kaluza-Klein modes on M_q can be classified according to the spherical harmonics of the M_q , which forms representations of the isometry group of M_q . The states carrying the non-trivial isometry group quantum numbers are heavier and do not couple to the pure gluonic operators on the boundary. Thus the glueballs are identified with singlet states of the isometry group.

In the past decade, glueballs have been studied extensively to gain new insight into the non-perturbative regime of QCD. Various holographic setups such as soft-wall model, hard wall model, modified soft wall model, etc. have been used to obtain the glueball's spectra. In [8, 9] a soft wall holographic model was used to study the glueball spectrum. In [8] glueballs and scalar mesons were studied at finite temperature. It was found that the masses of the hadronic states decreases and the widths become broader as T increases. But for temperature range of the order of 40-60 MeV, states

disappear from the glueball and meson spectral function. Both hard wall and soft wall holographic models were considered [10, 11] to obtain the glueball correlation functions to study the dynamics of QCD. Decay rates were obtained for glueballs in both models. Dynamical content of the correlators was investigated [11] by obtaining their spectral density and relating it with various other quantities to obtain the estimates for three lowest dimensional gluon condensate. In [12] a two-flavor quenched dynamical holographic QCD model was considered with two different forms for the dilaton field given as: $\Phi = \mu_G^2 z^2$ and $\Phi = \mu_G^2 z^2 \tanh(\mu_G^4 z^2 / \mu_G^2)$, (z being a radial coordinate). In [13] an AdS₅ mass renormalization was implemented in a modified holographic softwall model to obtain the spectrum of scalar and higher even glueball spin states with $P = C = +1$. In [14, 15] a bottom-up approach was used to obtain the mass spectra of the scalar and vector glueballs. In this case, the Vector glueball masses were found to be heavier than that of the scalar glueballs while higher values for both were reported in other approaches. In [16] holographic description was used for supersymmetric and non-supersymmetric, non-commutative dipole gauge theory in 4D. WKB approximation was used to obtain the mass by solving the dilaton and antisymmetric tensor field equations in the bulk. For the supersymmetric theory, dipole length plays the role of an intrinsic scale while for non-supersymmetric theory the same role is played by the temperature. Two different phases for baryons were found, a big baryon dual to the static string and a small baryon dual to a moving string. In [17] spectrum for scalar, vector and tensor two-gluon and trigluon glueballs were obtained in 5-D holographic QCD model with a metric structure deformed by the dilaton field. The spectrum was compared with the results obtained from both soft-wall and hard-wall holographic QCD models. Here, the spectra of the two-gluon glueball was found to be in agreement with the lattice data. For trigluon glueballs, the masses for $1^{\pm-}, 2^{--}$ were matched while masses for $0^{--}, 0^{+-}$ and 2^{+-} were lighter than lattice data which indicates that the latter glueballs are dominated by three-gluon condensate. In [18] holographic glueball spectrum was obtained in the singlet sector of $\mathcal{N}=1$ supersymmetric Klebanov-Strassler model. States containing the bifundamental A_i and B_i fields were not considered. Comparison with the lattice data showed a nice agreement for 1^{+-} and 1^{--} states while 0^{+-} results were different because of its fermionic component.

Glueballs appear in the meson spectra of QCD and difficulty in their identification in the meson spectra is largely due to lack of information about their coupling with mesons in strongly coupled QCD. Lattice QCD gives an estimate for the masses but it does not give any information about the glueball couplings and their decay widths both of which are required for identification of glueballs. Holographic approach gives a better understanding of glueball decay rates than lattice QCD. Various holographic models such as Witten-Sakai-Sugimoto model, Soft wall model and supersymmetric Klebanov-Strassler model, etc. have been used to obtain the coupling between mesons and glueballs to obtain expressions for the glueball decay widths.

In [19, 20, 21, 22, 23, 24] top-down Witten-Sakai-Sugimoto model was used as a holographic setup for low energy QCD to obtain the coupling of scalar glueballs to mesons and subsequently obtain their decay widths. Results obtained were compared with the experimental data available for lattice counterparts $f_0(1500)$ and $f_0(1710)$ of scalar glueballs. In [19] results obtained for decay widths and branching ratios for scalar glueball decays were found to be consistent with experimental data for $f_0(1500)$ state in [19] while in [21] results favored $f_0(1710)$ as scalar glueball candidate instead of $f_0(1500)$. Decay patterns were obtained for scalar glueball candidate $f_0(1710)$ in top-down holographic Witten-Sakai-Sugimoto model for low energy QCD in [20]. It was shown that there exists a narrow pseudoscalar glueball heavier than the scalar glueball whose decay pattern involves η and η' mesons. In [22, 23, 24] Witten-Sakai-Sugimoto model was used to study the phenomenology of scalar glueball states. A dilaton and an exotic mode were obtained as two sets of scalar glueball states in [22, 23].

Calculation of mass spectra showed that out of two modes, dilaton mass is quite close to both $f_0(1710)$ and $f_0(1500)$ scalar glueball candidates while calculation of decay width showed that $f_0(1710)$ is the favored glueball candidate corresponding to dilaton mode. In [25] the holographic top-down Witten-Sakai-Sugimoto model was used to study the tensor 2^{++} glueball mass spectrum and decay width. Decay width was found to be above 1 GeV for glueball mass $M_T=2400$ MeV while for $M_T=2000$ MeV it was reduced to 640 MeV. In [26] modified holographic soft-wall model was used to calculate the mass spectrum and Regge trajectories of lightest scalar glueball and higher spin glueball states. Results were obtained for both even and odd spins glueball states.

In this paper, we use a large- N top-down holographic dual of QCD to obtain the spin $2^{++}, 1^{++}, 0^{++}, 0^{--}, 0^{-+}$ glueball spectrum explicitly for QCD₃ from type IIB, type IIA and M theory perspectives. Now for the computation of the glueball masses, we need to introduce a scale in our theory. In other words, the conformal invariance has to be broken. This can be done in two different ways. The first approach, after Witten [27], corresponds to the compactification of the time direction on a circle of finite radius, forming a black hole in the background. In this case the masses are determined in units of the horizon radius r_h of the black hole. The other approach is to consider a cut-off at $r = r_0$ in the gravitational background (r being the non-compact radial direction)[28]. This forbids the arbitrary low energy excitations of the boundary field theory and hence breaks the conformal invariance. So, in this case the required scale to address strong interaction is introduced by the IR cut-off r_0 . From a top-down perspective this IR cut-off will in fact be proportional to two-third power of the Ouyang embedding parameter obtained from the minimum radial distance (corresponding to the lightest quarks) requiring one to be at the South Poles in the $\theta_{1,2}$ coordinates, in the holomorphic Ouyang embedding of flavor $D7$ -branes. In the spirit of [27], the time direction for both cases will be compact with fermions obeying anti-periodic boundary conditions along this compact direction, and hence we will be evaluating three-dimensional glueball masses.

Glueball masses can be obtained by evaluating the correlation functions of gauge invariant local operator. The first step to obtain the glueball spectrum in QCD₃ is to identify the operators in the gauge theory that have quantum number corresponding to the glueballs of interest. According to the gauge/gravity duality each supergravity mode corresponds to a gauge theory operator. This operator couples to the supergravity mode at the boundary of the AdS space, for example, the lowest dimension operator with quantum numbers $J^{PC} = 0^{++}$ is $\text{Tr}F^2 = \text{Tr}F_{\mu\nu}F^{\mu\nu}$ and this operator couples to the dilaton mode on the boundary. To calculate 0^{++} glueball mass we need to evaluate the correlator $\langle \text{Tr}F^2(x)\text{Tr}F^2(y) \rangle = \sum_i c_i e^{-m_i|x-y|}$, where m_i give the value for glueball mass. However the masses can also be obtained by solving the wave equations for supergravity modes which couples to the gauge theory operators on the boundary. The latter approach is used in this paper.

The 11D metric obtained as the uplift of the delocalized SYZ type IIA metric, up to LO in N , can be interpreted as a black $M5$ -brane wrapping a two-cycle, i.e. a black $M3$ -brane [29, 3]. Taking this as the starting point, compactifying again along the M-theory circle, we land up at the type IIA metric and then compactifying again along the periodic temporal circle (with the radius given by the reciprocal of the temperature), one obtains QCD₃ corresponding to the three non-compact directions of the black $M3$ -brane world volume. The Type IIB background of [1], in principle, involves $M_4 \times \text{RWDC}$ (\equiv Resolved Warped Deformed Conifold); asymptotically the same becomes $AdS_5 \times T^{1,1}$. To determine the gauge theory fields that would couple to appropriate supergravity fields a la gauge-gravity duality, ideally one should work the same out for the $M_4 \times \text{RWDC}$ background (which would also involve solving for the Laplace equation for the internal RWDC). We do not attempt to do the same here. Motivated however by, e.g.,

(a) asymptotically the type IIB background of [1] and its delocalized type IIA mirror of [2] consist of

AdS_5

and

(b) terms of the type $Tr(F^2(AB)^k), (F^4(AB)^k)$ where $F^2 = F_{\mu\nu}F^{\mu\nu}, F^4 = F_{\mu_1}^{\mu_2}F_{\mu_2}^{\mu_3}F_{\mu_3}^{\mu_4}F_{\mu_4}^{\mu_1} - \frac{1}{4}(F_{\mu_1}^{\mu_2}F_{\mu_2}^{\mu_1})^2$, A, B being the bifundamental fields that appear in the gauge theory superpotential corresponding to $AdS_5 \times T^{1,1}$ in [30], form part of the gauge theory operators corresponding to the solution to the Laplace equation on $T^{1,1}$ [31] (the operator TrF^2 which shares the quantum numbers of the 0^{++} glueball couples to the dilaton and TrF^4 which also shares the quantum numbers of the 0^{++} glueball couples to trace of metric fluctuations and the four-form potential, both in the internal angular directions),

we calculate in this paper:

- type IIB dilaton fluctuations, which we refer to as 0^{++} glueball
- type IIB complexified two-form fluctuations that couple to $d^{abc}Tr(F_{\mu\rho}^a F_{\lambda}^b{}^\rho F^c{}^\lambda{}_\nu)$, which we refer to as 0^{--} glueball
- type IIA one-form fluctuations that couple to $Tr(F \wedge F)$, which we refer to as 0^{-+} glueball
- M-theory metric's scalar fluctuations which we refer to as another (lighter) 0^{++} glueball
- M-theory metric's vector fluctuations which we refer to as 1^{++} glueball,

and

- M-theory metric's tensor fluctuations which we refer to as 2^{++} glueball.

All holographic glueball spectra calculations done thus far, have only considered a large t'Hooft coupling limit: $g_{YM}^2 N \gg 1, N \gg 1$. However, holographic duals of thermal QCD laboratories like sQGP also require a finite gauge coupling [4]. This was addressed as part of the 'MQGP limit' in [2]. It is in this regard that results of this paper - which discusses supergravity glueball spectra at finite string coupling - are particularly significant. Also, the recent observation - see, e.g., [32] - that the non-perturbative properties of quark gluon plasma can be related to the change of properties of scalar and pseudoscalar glueballs, makes the study of glueballs quite important.

The rest of the paper is organized as follows. In Sec. **2**, via five sub-sections, we summarize the top-down type IIB holographic dual of large- N thermal QCD of [1], its delocalized SYZ type IIA mirror and its M theory uplift of [2, 3]. In Sec. **3**, we discuss a supergravity calculation of the spectrum of 0^{++} glueball at finite horizon radius r_h (**3.1**) and setting $r_h = 0$ (**3.2**). The $r_h \neq 0$ computations are given in **3.1**, corresponding to use of WKB quantization conditions using coordinate/field redefinitions of [34]. The $r_h = 0$ calculations are subdivided into sub-section **3.2.1** corresponding to solving the 0^{++} equation of motion up to LO in N and imposing Neumann/Dirichlet boundary condition at the horizon, and sub-section **3.2.2** corresponding to WKB quantization conditions inclusive of non-conformal/NLO-in- N corrections using the redefinitions of [34]. Sec. **4** has to do with the 0^{-+} glueball spectrum. Further therein, **4.1.1** and **4.1.2** respectively are on obtaining the $r_h \neq 0$ spectrum and its $r_h = 0$ limit using Neumann/Dirichlet boundary conditions on the solutions up to LO in N respectively at the horizon and the IR cutoff. Then subsections **4.2.1** and **4.2.2** respectively are on WKB quantization at finite and zero r_h up to LO in N , using redefinitions of [34]. Sec. **5** is on 0^{--} glueball spectrum. Therein, subsections **5.1** and **5.2** are on getting the spectrum by imposing Neumann/Dirichlet boundary condition on the solutions up to LO in N to the EOM respectively at the horizon and the IR cut-off. Subsection **5.3** has to do with obtaining the spectrum using WKB quantization up to LO in N at $r_h \neq 0$ using the redefinitions of [34]; **5.4** has to do with a similar calculation in the $r_h = 0$ limit at LO in N in **5.4.1** and up to NLO in N in **5.4.2**. Section **6** has to do with M-theory calculations of $0^{++}, 1^{++}, 2^{++}$ glueballs arising from appropriate metric fluctuations. Subsection **6.1** is on such a 0^{++} glueball spectrum (imposing Neumann/Dirichlet boundary conditions at the horizon/IR cut-off in **6.1.1**, and using WKB quantization conditions and the redefinitions of

[34] at finite/zero horizon radius in **6.1.2**). Subsection **6.2** is on such a 2^{++} glueball spectrum (via imposing Neumann/Dirichlet boundary conditions at the horizon/IR cut-off in **6.2.1/6.2.2**, and via WKB quantization conditions using redefinitions of [34] at LO in N at $r_h \neq 0$ in **6.2.3** and zero r_h in **6.2.4** as well as up to NLO in N in the $r_h = 0$ -limit, in **6.2.5**). Subsection **6.3** is on such a 1^{++} glueball spectrum (via WKB quantization conditions using the redefinitions of [34] up to LO in N in the finite/zero horizon radius limit in **6.3.1/6.3.2**, and up to NLO in N in the zero-horizon limit in **6.3.3**). From the point of view of comparing string theory and M theory glueball spectrum calculations, we obtain the 2^{++} glueball spectrum arising from tensor mode of metric fluctuations in the type IIB background of [1] in Sec. **7**. Subsection **7.1** has to do with a supergravity calculation (via Neumann/Dirichlet boundary conditions at the horizon in **7.1.1** and WKB quantization condition using redefinitions of [34] in **7.1.2**), and **7.2** has to do with zero-horizon radius limit calculation (WKB quantization condition using redefinitions of [34] at LO in N in **7.2.1** and up to NLO in N in **7.2.2**). Section **8** contains a summary of and discussion on the results obtained in this paper. There a appendix **A** on the square of different fluxes that appear in EOM relevant to spin-two perturbations of the type IIB metric.

2 Background: A Top-Down Type IIB Holographic Large- N Thermal QCD and its M-Theory Uplift in the ‘MQGP’ Limit

In this section, via five sub-sections we will:

- provide a short review of the type IIB background of [1] which is supposed to provide a UV complete holographic dual of large- N thermal QCD, as well as their precursors in subsection **2.1**,
- discuss the ‘MQGP’ limit of [2] and the motivation for considering the same in subsection **2.2**,
- briefly review issues as discussed in [2] pertaining to construction of delocalized S(trominger) Y(au) Z(aslow) mirror and approximate supersymmetry, in subsection **2.3**,
- briefly review the new results of [3] and [5] pertaining to construction of explicit $SU(3)$ and G_2 structures respectively of type IIB/IIA and M-theory uplift,
- briefly discuss the new Physics-related results of [3] and [5], in subsection **2.4**

2.1 Type IIB Dual of Large- N Thermal QCD

In this subsection, we will discuss a UV complete holographic dual of large- N thermal QCD as given in Dasgupta-Mia et al [1]. As partly mentioned in Sec. **1**, this was inspired by the zero-temperature Klebanov-Witten model [30], the non-conformal Klebanov-Tseytlin model [35], its IR completion as given in the Klebanov-Strassler model [36] and Ouyang’s inclusion [37] of flavor in the same ⁴, as well as the non-zero temperature/non-extremal version of [38] (the solution however was not regular as the non-extremality/black hole function and the ten-dimensional warp factor vanished simultaneously at the horizon radius), [39] (valid only at large temperatures) of the Klebanov-Tseytlin model and [40]

⁴See [70] for earlier attempts at studying back-reacted $D3/D7$ geometry at zero temperature; we thank L. Zayas for bringing [70, 40] to our attention.

(addressing the IR), in the absence of flavors.

(a) Brane construction

In order to include fundamental quarks at non-zero temperature in the context of type IIB string theory, to the best of our knowledge, the following model proposed in [1] is the closest to a UV complete holographic dual of large- N thermal QCD. The KS model (after a duality cascade) and QCD have similar IR behavior: $SU(M)$ gauge group and IR confinement. However, they differ drastically in the UV as the former yields a logarithmically divergent gauge coupling (in the UV) - Landau pole. This necessitates modification of the UV sector of the KS model apart from inclusion of non-extremality factors. With this in mind and building up on all of the above, the type IIB holographic dual of [1] was constructed. The setup of [1] is summarized below.

- From a gauge-theory perspective, the authors of [1] considered N black $D3$ -branes placed at the tip of six-dimensional conifold, M $D5$ -branes wrapping the vanishing two-cycle and M $\overline{D5}$ -branes distributed along the resolved two-cycle and placed at the outer boundary of the IR-UV interpolating region/inner boundary of the UV region.
- More specifically, the M $\overline{D5}$ are distributed around the antipodal point relative to the location of M $D5$ branes on the blown-up S^2 . If the $D5/\overline{D5}$ separation is given by $\mathcal{R}_{D5/\overline{D5}}$, then this provides the boundary common to the outer UV-IR interpolating region and the inner UV region. The region $r > \mathcal{R}_{D5/\overline{D5}}$ is the UV. In other words, the radial space, in [1] is divided into the IR, the IR-UV interpolating region and the UV. To summarize the above:

- $r_0/r_h < r < |\mu_{\text{Ouyang}}|^{\frac{2}{3}}(r_h = 0)/\mathcal{R}_{D5/\overline{D5}}(r_h \neq 0)$: the IR/IR-UV interpolating regions with $r \sim \Lambda$: deep IR where the $SU(M)$ gauge theory confines
- $r > |\mu_{\text{Ouyang}}|^{\frac{2}{3}}(r_h = 0)/\mathcal{R}_{D5/\overline{D5}}(r_h \neq 0)$: the UV region.

- N_f $D7$ -branes, via Ouyang embedding, are holomorphically embedded in the UV (asymptotically $AdS_5 \times T^{1,1}$), the IR-UV interpolating region and dipping into the (confining) IR (up to a certain minimum value of r corresponding to the lightest quark) and N_f $\overline{D7}$ -branes present in the UV and the UV-IR interpolating (not the confining IR). This is to ensure turning off of three-form fluxes, constancy of the axion-dilaton modulus and hence conformality and absence of Landau poles in the UV.
- The resultant ten-dimensional geometry hence involves a resolved warped deformed conifold. Back-reactions are included, e.g., in the ten-dimensional warp factor. Of course, the gravity dual, as in the Klebanov-Strassler construct, at the end of the Seiberg-duality cascade will have no $D3$ -branes and the $D5$ -branes are smeared/dissolved over the blown-up S^3 and thus replaced by fluxes in the IR.

The delocalized S(trominger) Y(au) Z(aslow) type IIA mirror of the aforementioned type IIB background of [1] and its M-theory uplift had been obtained in [2, 3, 5].

(b) Seiberg duality cascade, IR confining $SU(M)$ gauge theory at finite temperature and $N_c = N_{\text{eff}}(r) + M_{\text{eff}}(r)$

1. **IR Confinement after Seiberg Duality Cascade:** Footnote numbered 3 shows that one effectively adds on to the number of $D3$ -branes in the UV and hence, one has $SU(N + M) \times SU(N + M)$ color gauge group (implying an asymptotic AdS_5) and $SU(N_f) \times SU(N_f)$ flavor

gauge group, in the UV: $r \geq \mathcal{R}_{D5/\overline{D5}}$. It is expected that there will be a partial Higgsing of $SU(N+M) \times SU(N+M)$ to $SU(N+M) \times SU(N)$ at $r = \mathcal{R}_{D5/\overline{D5}}$ [41]. The two gauge couplings, $g_{SU(N+M)}$ and $g_{SU(N)}$ flow logarithmically and oppositely in the IR:

$$4\pi^2 \left(\frac{1}{g_{SU(N+M)}^2} + \frac{1}{g_{SU(N)}^2} \right) e^\phi \sim \pi; \quad 4\pi^2 \left(\frac{1}{g_{SU(N+M)}^2} - \frac{1}{g_{SU(N)}^2} \right) e^\phi \sim \frac{1}{2\pi\alpha'} \int_{S^2} B_2. \quad (1)$$

Had it not been for $\int_{S^2} B_2$, in the UV, one could have set $g_{SU(M+N)}^2 = g_{SU(N)}^2 = g_{YM}^2 \sim g_s \equiv \text{constant}$ (implying conformality) which is the reason for inclusion of M $\overline{D5}$ -branes at the common boundary of the UV-IR interpolating and the UV regions, to annul this contribution. In fact, the running also receives a contribution from the N_f flavor $D7$ -branes which needs to be annulled via N_f $\overline{D7}$ -branes. The gauge coupling $g_{SU(N+M)}$ flows towards strong coupling and the $SU(N)$ gauge coupling flows towards weak coupling. Upon application of Seiberg duality, $SU(N+M)_{\text{strong}} \xrightarrow{\text{Seiberg Dual}} SU(N - (M - N_f))_{\text{weak}}$ in the IR; assuming after repeated Seiberg dualities or duality cascade, N decreases to 0 and there is a finite M , one will be left with $SU(M)$ gauge theory with N_f flavors that confines in the IR - the finite temperature version of the same is what was looked at by [1].

2. **Obtaining $N_c = 3$, and Color-Flavor Enhancement of Length Scale in the IR:** So, in the IR, at the end of the duality cascade, what gets identified with the number of colors N_c is M , which in the ‘MQGP limit’ to be discussed below, can be tuned to equal 3. One can identify N_c with $N_{\text{eff}}(r) + M_{\text{eff}}(r)$, where $N_{\text{eff}}(r) = \int_{\text{Base of Resolved Warped Deformed Conifold}} F_5$ and $M_{\text{eff}} = \int_{S^3} \tilde{F}_3$ (the S^3 being dual to $e_\psi \wedge (\sin \theta_1 d\theta_1 \wedge d\phi_1 - B_1 \sin \theta_2 \wedge d\phi_2)$, wherein B_1 is an asymmetry factor defined in [1], and $e_\psi \equiv d\psi + \cos \theta_1 d\phi_1 + \cos \theta_2 d\phi_2$) where $\tilde{F}_3 (\equiv F_3 - \tau H_3) \propto M(r) \equiv 1 - \frac{e^{\alpha(r - \mathcal{R}_{D5/\overline{D5}})}}{1 + e^{\alpha(r - \mathcal{R}_{D5/\overline{D5}})}}$, $\alpha \gg 1$ [42]. The effective number N_{eff} of $D3$ -branes varies between $N \gg 1$ in the UV and 0 in the deep IR, and the effective number M_{eff} of $D5$ -branes varies between 0 in the UV and M in the deep IR (i.e., at the end of the duality cascade in the IR). Hence, the number of colors N_c varies between M in the deep IR and a large value [even in the MQGP limit of (11) (for a large value of N)] in the UV. Hence, at very low energies, the number of colors N_c can be approximated by M , which in the MQGP limit is taken to be finite and can hence be taken to be equal to three. However, in this discussion, the low energy or the IR is relative to the string scale. But these energies which are much less than the string scale, can still be much larger than T_c . Therefore, for all practical purposes, as regard the energy scales relevant to QCD, the number of colors can be tuned to three.

In the IR in the MQGP limit, with the inclusion of terms higher order in $g_s N_f$ in the RR and NS-NS three-form fluxes and the NLO terms in the angular part of the metric, there occurs an IR color-flavor enhancement of the length scale as compared to a Planckian length scale in KS for $\mathcal{O}(1) M$, thereby showing that quantum corrections will be suppressed. Using [1]:

$$\begin{aligned} N_{\text{eff}}(r) &= N \left[1 + \frac{3g_s M_{\text{eff}}^2}{2\pi N} \left(\log r + \frac{3g_s N_f^{\text{eff}}}{2\pi} (\log r)^2 \right) \right], \\ M_{\text{eff}}(r) &= M + \frac{3g_s N_f M}{2\pi} \log r + \sum_{m \geq 1} \sum_{n \geq 1} N_f^m M^n f_{mn}(r), \\ N_f^{\text{eff}}(r) &= N_f + \sum_{m \geq 1} \sum_{n \geq 0} N_f^m M^n g_{mn}(r). \end{aligned} \quad (2)$$

it was argued in [3] that the length scale of the OKS-BH metric in the IR will be given by:

$$\begin{aligned}
L_{\text{OKS-BH}} &\sim \sqrt{M} N_f^{\frac{3}{4}} \sqrt{\left(\sum_{m \geq 0} \sum_{n \geq 0} N_f^m M^n f_{mn}(\Lambda) \right) \left(\sum_{l \geq 0} \sum_{p \geq 0} N_f^l M^p g_{lp}(\Lambda) \right)^{\frac{1}{4}}} g_s^{\frac{1}{4}} \sqrt{\alpha'} \\
&\equiv N_f^{\frac{3}{4}} \sqrt{\left(\sum_{m \geq 0} \sum_{n \geq 0} N_f^m M^n f_{mn}(\Lambda) \right) \left(\sum_{l \geq 0} \sum_{p \geq 0} N_f^l M^p g_{lp}(\Lambda) \right)^{\frac{1}{4}}} L_{\text{KS}} \Bigg|_{\Lambda: \log \Lambda < \frac{2\pi}{3g_s N_f}}, \quad (3)
\end{aligned}$$

which implies that in the IR, relative to KS, there is a color-flavor enhancement of the length scale in the OKS-BH metric. Hence, in the IR, even for $N_c^{\text{IR}} = M = 3$ and $N_f = 2$ (light flavors) upon inclusion of $n, m > 1$ terms in M_{eff} and N_f^{eff} in (2), $L_{\text{OKS-BH}} \gg L_{\text{KS}} (\sim L_{\text{Planck}})$ in the MQGP limit involving $g_s \lesssim 1$, implying that the stringy corrections are suppressed and one can trust supergravity calculations. As a reminder one will generate higher powers of M and N_f in the double summation in M_{eff} in (2), e.g., from the terms higher order in $g_s N_f$ in the RR and NS-NS three-form fluxes that become relevant for the aforementioned values of g_s, N_f .

- Further, the global flavor group in the UV-IR interpolating and UV regions, due to presence of N_f $D7$ and N_f $\overline{D7}$ -branes, is $SU(N_f) \times SU(N_f)$, which is broken in the IR to $SU(N_f)$ as the IR has only N_f $D7$ -branes.

Hence, the following features of the type IIB model of [1] make it an ideal holographic dual of thermal QCD:

- the theory having quarks transforming in the fundamental representation, is UV conformal and IR confining with the required chiral symmetry breaking in the IR and restoration at high temperatures
- the theory is UV complete with the gauge coupling remaining finite in the UV (absence of Landau poles)
- the theory is not just defined for large temperatures but for low and high temperatures
- (as will become evident in Sec. 3) with the inclusion of a finite baryon chemical potential, the theory provides a lattice-compatible QCD confinement-deconfinement temperature T_c for the right number of light quark flavors and masses, and is also thermodynamically stable; given the IR proximity of the value of the lattice-compatible T_c , after the end of the Seiberg duality cascade, the number of quark flavors approximately equals M which in the ‘MQGP’ limit of (11) can be tuned to equal 3
- in the MQGP limit (11) which requires considering a finite gauge coupling and hence string coupling, the theory was shown in [2] to be holographically renormalizable from an M-theory perspective with the M-theory uplift also being thermodynamically stable.

(d) Supergravity solution on resolved warped deformed conifold

The working metric is given by :

$$ds^2 = \frac{1}{\sqrt{h}} (-g_1 dt^2 + dx_1^2 + dx_2^2 + dx_3^2) + \sqrt{h} \left[g_2^{-1} dr^2 + r^2 d\mathcal{M}_5^2 \right]. \quad (4)$$

g_i 's are black hole functions in modified OKS(Ouyang-Klebanov-Strassler)-BH (Black Hole) background and are assumed to be: $g_{1,2}(r, \theta_1, \theta_2) = 1 - \frac{r_h^4}{r^4} + \mathcal{O}\left(\frac{g_s M^2}{N}\right)$ where r_h is the horizon, and the (θ_1, θ_2) dependence come from the $\mathcal{O}\left(\frac{g_s M^2}{N}\right)$ corrections. The h_i 's are expected to receive corrections of $\mathcal{O}\left(\frac{g_s M^2}{N}\right)$ [41]. We assume the same to also be true of the 'black hole functions' $g_{1,2}$. The compact five dimensional metric in (4), is given as:

$$\begin{aligned} d\mathcal{M}_5^2 = & h_1(d\psi + \cos \theta_1 d\phi_1 + \cos \theta_2 d\phi_2)^2 + h_2(d\theta_1^2 + \sin^2 \theta_1 d\phi_1^2) + \\ & + h_4(h_3 d\theta_2^2 + \sin^2 \theta_2 d\phi_2^2) + h_5 \cos \psi (d\theta_1 d\theta_2 - \sin \theta_1 \sin \theta_2 d\phi_1 d\phi_2) + \\ & + h_5 \sin \psi (\sin \theta_1 d\theta_2 d\phi_1 + \sin \theta_2 d\theta_1 d\phi_2), \end{aligned} \quad (5)$$

$r \gg a, h_5 \sim \frac{(\text{deformation parameter})^2}{r^3} \ll 1$ for $r \gg (\text{deformation parameter})^{\frac{2}{3}}$, i.e. in the UV/IR-UV interpolating region. The h_i 's appearing in internal metric as well as M, N_f are not constant and up to linear order depend on g_s, M, N_f are given as below:

$$\begin{aligned} h_1 = \frac{1}{9} + \mathcal{O}\left(\frac{g_s M^2}{N}\right), \quad h_2 = \frac{1}{6} + \mathcal{O}\left(\frac{g_s M^2}{N}\right), \quad h_4 = h_2 + \frac{a^2}{r^2}, \\ h_3 = 1 + \mathcal{O}\left(\frac{g_s M^2}{N}\right), \quad h_5 \neq 0, \quad L = (4\pi g_s N)^{\frac{1}{4}}. \end{aligned} \quad (6)$$

One sees from (5) and (6) that one has a non-extremal resolved warped deformed conifold involving an S^2 -blowup (as $h_4 - h_2 = \frac{a^2}{r^2}$), an S^3 -blowup (as $h_5 \neq 0$) and squashing of an S^2 (as h_3 is not strictly unity). The horizon (being at a finite $r = r_h$) is warped squashed $S^2 \times S^3$. In the deep IR, in principle one ends up with a warped squashed $S^2(a) \times S^3(\epsilon)$, ϵ being the deformation parameter. Assuming $\epsilon^{\frac{2}{3}} > a$ and given that $a = \mathcal{O}\left(\frac{g_s M^2}{N}\right) r_h$ [41], in the IR and in the MQGP limit, $N_{\text{eff}}(r \in \text{IR}) = \int_{\text{warped squashed } S^2(a) \times S^3(\epsilon)} F_5(r \in \text{IR}) \ll M = \int_{S^3(\epsilon)} F_3(r \in \text{IR})$; we have a confining $SU(M)$ gauge theory in the IR.

The warp factor that includes the back-reaction, in the IR is given as:

$$h = \frac{L^4}{r^4} \left[1 + \frac{3g_s M_{\text{eff}}^2}{2\pi N} \log r \left\{ 1 + \frac{3g_s N_f^{\text{eff}}}{2\pi} \left(\log r + \frac{1}{2} \right) + \frac{g_s N_f^{\text{eff}}}{4\pi} \log \left(\sin \frac{\theta_1}{2} \sin \frac{\theta_2}{2} \right) \right\} \right], \quad (7)$$

where, in principle, $M_{\text{eff}}/N_f^{\text{eff}}$ are not necessarily the same as M/N_f ; we however will assume that up to $\mathcal{O}\left(\frac{g_s M^2}{N}\right)$, they are. Proper UV behavior requires [41]:

$$\begin{aligned} h = \frac{L^4}{r^4} \left[1 + \sum_{i=1} \frac{\mathcal{H}_i(\phi_{1,2}, \theta_{1,2}, \psi)}{r^i} \right], \quad \text{large } r; \\ h = \frac{L^4}{r^4} \left[1 + \sum_{i,j;(i,j) \neq (0,0)} \frac{h_{ij}(\phi_{1,2}, \theta_{1,2}, \psi) \log^i r}{r^j} \right], \quad \text{small } r. \end{aligned} \quad (8)$$

In the IR, up to $\mathcal{O}(g_s N_f)$ and setting $h_5 = 0$, the three-forms are as given in [1]:

$$\begin{aligned}
(a) \tilde{F}_3 &= 2MA_1 \left(1 + \frac{3g_s N_f}{2\pi} \log r \right) e_\psi \wedge \frac{1}{2} (\sin \theta_1 d\theta_1 \wedge d\phi_1 - B_1 \sin \theta_2 d\theta_2 \wedge d\phi_2) \\
&\quad - \frac{3g_s MN_f}{4\pi} A_2 \frac{dr}{r} \wedge e_\psi \wedge \left(\cot \frac{\theta_2}{2} \sin \theta_2 d\phi_2 - B_2 \cot \frac{\theta_1}{2} \sin \theta_1 d\phi_1 \right) \\
&\quad - \frac{3g_s MN_f}{8\pi} A_3 \sin \theta_1 \sin \theta_2 \left(\cot \frac{\theta_2}{2} d\theta_1 + B_3 \cot \frac{\theta_1}{2} d\theta_2 \right) \wedge d\phi_1 \wedge d\phi_2, \\
(b) H_3 &= 6g_s A_4 M \left(1 + \frac{9g_s N_f}{4\pi} \log r + \frac{g_s N_f}{2\pi} \log \sin \frac{\theta_1}{2} \sin \frac{\theta_2}{2} \right) \frac{dr}{r} \\
&\quad \wedge \frac{1}{2} \left(\sin \theta_1 d\theta_1 \wedge d\phi_1 - B_4 \sin \theta_2 d\theta_2 \wedge d\phi_2 \right) + \frac{3g_s^2 MN_f}{8\pi} A_5 \left(\frac{dr}{r} \wedge e_\psi - \frac{1}{2} de_\psi \right) \\
&\quad \wedge \left(\cot \frac{\theta_2}{2} d\theta_2 - B_5 \cot \frac{\theta_1}{2} d\theta_1 \right).
\end{aligned} \tag{9}$$

The asymmetry factors in (9) are given by: $A_i = 1 + \mathcal{O}\left(\frac{a^2}{r^2} \text{ or } \frac{a^2 \log r}{r} \text{ or } \frac{a^2 \log r}{r^2}\right) + \mathcal{O}\left(\frac{\text{deformation parameter}^2}{r^3}\right)$, $B_i = 1 + \mathcal{O}\left(\frac{a^2 \log r}{r} \text{ or } \frac{a^2 \log r}{r^2} \text{ or } \frac{a^2 \log r}{r^3}\right) + \mathcal{O}\left(\frac{\text{deformation parameter}^2}{r^3}\right)$. As in the UV, $\frac{(\text{deformation parameter})^2}{r^3} \ll \frac{(\text{resolution parameter})^2}{r^2}$, we will assume the same three-form fluxes for $h_5 \neq 0$.

Further, to ensure UV conformality, it is important to ensure that the axion-dilaton modulus approaches a constant implying a vanishing beta function in the UV. This was discussed in detail in appendix B of [3], wherein in particular, assuming an F-theory uplift involving, locally, an elliptically fibered $K3$, it was shown that UV conformality and the Ouyang embedding are mutually consistent.

2.2 The ‘MQGP Limit’

In [2], we had considered the following two limits:

$$\begin{aligned}
&(i) \text{weak}(g_s) \text{coupling} - \text{large } t' \text{Hooft coupling limit :} \\
&g_s \ll 1, g_s N_f \ll 1, \frac{g_s M^2}{N} \ll 1, g_s M \gg 1, g_s N \gg 1 \\
&\text{effected by : } g_s \sim \epsilon^d, M \sim (\mathcal{O}(1)\epsilon)^{-\frac{3d}{2}}, N \sim (\mathcal{O}(1)\epsilon)^{-19d}, \epsilon \ll 1, d > 0
\end{aligned} \tag{10}$$

(the limit in the first line though not its realization in the second line, considered in [1]);

$$\begin{aligned}
&(ii) \text{MQGP limit : } \frac{g_s M^2}{N} \ll 1, g_s N \gg 1, \text{finite } g_s, M \\
&\text{effected by : } g_s \sim \epsilon^d, M \sim (\mathcal{O}(1)\epsilon)^{-\frac{3d}{2}}, N \sim (\mathcal{O}(1)\epsilon)^{-39d}, \epsilon \lesssim 1, d > 0.
\end{aligned} \tag{11}$$

Let us enumerate the motivation for considering the MQGP limit which was discussed in detail in [3]. There are principally two.

1. Unlike the AdS/CFT limit wherein $g_{\text{YM}} \rightarrow 0, N \rightarrow \infty$ such that $g_{\text{YM}}^2 N$ is large, for strongly coupled thermal systems like sQGP, what is relevant is $g_{\text{YM}} \sim \mathcal{O}(1)$ and $N_c = 3$. From the

discussion in the previous paragraphs specially the one in point (c) of sub-section **2.1**, one sees that in the IR after the Seiberg duality cascade, effectively $N_c = M$ which in the MQGP limit of (11) can be tuned to 3. Further, in the same limit, the string coupling $g_s \lesssim 1$. The finiteness of the string coupling necessitates addressing the same from an M theory perspective. This is the reason for coining the name: ‘MQGP limit’. In fact this is the reason why one is required to first construct a type IIA mirror, which was done in [2] a la delocalized Strominger-Yau-Zaslow mirror symmetry, and then take its M-theory uplift.

2. From the perspective of calculational simplification in supergravity, the following are examples of the same and constitute therefore the second set of reasons for looking at the MQGP limit of (11):

- In the UV-IR interpolating region and the UV, $(M_{\text{eff}}, N_{\text{eff}}, N_f^{\text{eff}}) \stackrel{\text{MQGP}}{\approx} (M, N, N_f)$
- Asymmetry Factors A_i, B_j (in three-form fluxes) $\stackrel{\text{MQGP}}{\rightarrow} 1$ in the UV-IR interpolating region and the UV.
- Simplification of ten-dimensional warp factor and non-extremality function in MQGP limit

With $\mathcal{R}_{D5/\overline{D5}}$ denoting the boundary common to the UV-IR interpolating region and the UV region, $\tilde{F}_{lmn}, H_{lmn} = 0$ for $r \geq \mathcal{R}_{D5/\overline{D5}}$ is required to ensure conformality in the UV. Near the $\theta_1 = \theta_2 = 0$ -branch, assuming: $\theta_{1,2} \rightarrow 0$ as $\epsilon^{\gamma\theta} > 0$ and $r \rightarrow \mathcal{R}_{\text{UV}} \rightarrow \infty$ as $\epsilon^{-\gamma r} < 0$, $\lim_{r \rightarrow \infty} \tilde{F}_{lmn} = 0$ and $\lim_{r \rightarrow \infty} H_{lmn} = 0$ for all components except $H_{\theta_1\theta_2\phi_{1,2}}$; in the MQGP limit and near $\theta_{1,2} = \pi/0$ -branch, $H_{\theta_1\theta_2\phi_{1,2}} = 0 / \left. \frac{3g_s^2 M N_f}{8\pi} \right|_{N_f=2, g_s=0.6, M=(\mathcal{O}(1)g_s)^{-\frac{3}{2}}} \ll 1$. So, the UV nature too is captured near $\theta_{1,2} = 0$ -branch in the MQGP limit. This mimics addition of $\overline{D5}$ -branes in [1] to ensure cancellation of \tilde{F}_3 .

2.3 Approximate Supersymmetry, Construction of the Delocalized SYZ IIA Mirror and Its M-Theory Uplift in the MQGP Limit

A central issue to [2, 29] has been implementation of delocalized mirror symmetry via the Strominger Yau Zaslow prescription according to which the mirror of a Calabi-Yau can be constructed via three T dualities along a special Lagrangian T^3 fibered over a large base in the Calabi-Yau. This sub-section is a quick review of precisely this.

To implement the quantum mirror symmetry a la S(trominger)Y(au)Z(aslow) [43], one needs a special Lagrangian (sLag) T^3 fibered over a large base (to nullify contributions from open-string disc instantons with boundaries as non-contractible one-cycles in the sLag). Defining delocalized T-duality coordinates, $(\phi_1, \phi_2, \psi) \rightarrow (x, y, z)$ valued in $T^3(x, y, z)$ [2]:

$$x = \sqrt{h_2} h^{\frac{1}{4}} \sin\langle\theta_1\rangle\langle r\rangle\phi_1, \quad y = \sqrt{h_4} h^{\frac{1}{4}} \sin\langle\theta_2\rangle\langle r\rangle\phi_2, \quad z = \sqrt{h_1}\langle r\rangle h^{\frac{1}{4}}\psi, \quad (12)$$

using the results of [44] it was shown in [29, 5] that the following conditions are satisfied:

$$\begin{aligned} i^* J|_{\text{RC/DC}} &\approx 0, \\ \Im m(i^* \Omega)|_{\text{RC/DC}} &\approx 0, \\ \Re e(i^* \Omega)|_{\text{RC/DC}} &\sim \text{volume form}(T^3(x, y, z)), \end{aligned} \quad (13)$$

for the T^2 -invariant sLag of [44] for a deformed conifold. Hence, if the resolved warped deformed conifold is predominantly either resolved or deformed, the local T^3 of (12) is the required sLag to effect SYZ mirror construction.

Interestingly, in the ‘delocalized limit’ [45] $\psi = \langle \psi \rangle$, under the coordinate transformation:

$$\begin{pmatrix} \sin\theta_2 d\phi_2 \\ d\theta_2 \end{pmatrix} \rightarrow \begin{pmatrix} \cos\langle \psi \rangle & \sin\langle \psi \rangle \\ -\sin\langle \psi \rangle & \cos\langle \psi \rangle \end{pmatrix} \begin{pmatrix} \sin\theta_2 d\phi_2 \\ d\theta_2 \end{pmatrix}, \quad (14)$$

and $\psi \rightarrow \psi - \cos\langle \bar{\theta}_2 \rangle \phi_2 + \cos\langle \theta_2 \rangle \phi_2 - \tan\langle \psi \rangle \ln \sin \bar{\theta}_2$, the h_5 term becomes $h_5 [d\theta_1 d\theta_2 - \sin\theta_1 \sin\theta_2 d\phi_1 d\phi_2]$, $e_\psi \rightarrow e_\psi$, i.e., one introduces an isometry along ψ in addition to the isometries along $\phi_{1,2}$. This clearly is not valid globally - the deformed conifold does not possess a third global isometry.

To enable use of SYZ-mirror duality via three T dualities, one also needs to ensure a large base (implying large complex structures of the aforementioned two two-tori) of the $T^3(x, y, z)$ fibration. This is effected via [46]:

$$\begin{aligned} d\psi &\rightarrow d\psi + f_1(\theta_1) \cos \theta_1 d\theta_1 + f_2(\theta_2) \cos \theta_2 d\theta_2, \\ d\phi_{1,2} &\rightarrow d\phi_{1,2} - f_{1,2}(\theta_{1,2}) d\theta_{1,2}, \end{aligned} \quad (15)$$

for appropriately chosen large values of $f_{1,2}(\theta_{1,2})$. The three-form fluxes remain invariant. The fact that one can choose such large values of $f_{1,2}(\theta_{1,2})$, was justified in [2]. The guiding principle is that one requires the metric obtained after SYZ-mirror transformation applied to the non-Kähler resolved warped deformed conifold is like a non-Kähler warped resolved conifold at least locally. Then $G_{\theta_1\theta_2}^{IIA}$ needs to vanish [2]. This was explicitly shown in [3].

As in Klebanov-Strassler construction, a single T-duality along a direction orthogonal to the $D3$ -brane world volume, e.g., z of (12), yields $D4$ branes straddling a pair of $NS5$ -branes consisting of world-volume coordinates (θ_1, x) and (θ_2, y) . Further, T-dualizing along x and then y would yield a Taub-NUT space from each of the two $NS5$ -branes [47]. The $D7$ -branes yield $D6$ -branes which get uplifted to Kaluza-Klein monopoles in M-theory [48] which too involve Taub-NUT spaces. Globally, probably the eleven-dimensional uplift would involve a seven-fold of G_2 -structure, analogous to the uplift of $D5$ -branes wrapping a two-cycle in a resolved warped conifold [49].

2.4 G -Structures

The mirror type IIA metric after performing three T-dualities, first along x , then along y and finally along z , utilizing the results of [45] was worked out in [2]. The type IIA metric components were worked out in [2].

Now, any metric-compatible connection can be written in terms of the Levi-Civita connection and the contorsion tensor κ . Metric compatibility requires $\kappa \in \Lambda^1 \otimes \Lambda^2$, Λ^n being the space of n -forms. Alternatively, in d complex dimensions, since $\Lambda^2 \cong so(d)$, κ also be thought of as $\Lambda^1 \otimes so(d)$. Given the existence of a G -structure, we can decompose $so(d)$ into a part in the Lie algebra g of $G \subset SO(d)$ and its orthogonal complement $g^\perp = so(d)/g$. The contorsion κ splits accordingly into $\kappa = \kappa^0 + \kappa^g$, where κ^0 - the intrinsic torsion - is the part in $\Lambda^1 \otimes g^\perp$. One can decompose κ^0 into irreducible G representations providing a classification of G -structures in terms of which representations appear in the decomposition. Let us consider the decomposition of T^0 in the case of $SU(3)$ -structure. The relevant representations are $\Lambda^1 \sim 3 \oplus \bar{3}$, $g \sim 8$, $g^\perp \sim 1 \oplus 3 \oplus \bar{3}$. Thus the intrinsic torsion, an element of $\Lambda^1 \oplus su(3)^\perp$, can be decomposed into the following $SU(3)$ representations:

$$\begin{aligned} \Lambda^1 \otimes su(3)^\perp &= (3 \oplus \bar{3}) \otimes (1 \oplus 3 \oplus \bar{3}) \\ &= (1 \oplus 1) \oplus (8 \oplus 8) \oplus (6 \oplus \bar{6}) \oplus (3 \oplus \bar{3}) \oplus (3 \oplus \bar{3})' \equiv W_1 \oplus W_2 \oplus W_3 \oplus W_4 \oplus W_5. \end{aligned} \quad (16)$$

The $SU(3)$ structure torsion classes [50] can be defined in terms of J , Ω , dJ , $d\Omega$ and the contraction operator \lrcorner : $\Lambda^k T^* \otimes \Lambda^n T^* \rightarrow \Lambda^{n-k} T^*$, J being given by:

$$J = e^1 \wedge e^2 + e^3 \wedge e^4 + e^5 \wedge e^6,$$

and the (3,0)-form Ω being given by

$$\Omega = (e^1 + ie^2) \wedge (e^3 + ie^4) \wedge (e^5 + ie^6).$$

The torsion classes are defined in the following way:

- $W_1 \leftrightarrow [dJ]^{(3,0)}$, given by real numbers $W_1 = W_1^+ + W_1^-$ with $d\Omega_+ \wedge J = \Omega_+ \wedge dJ = W_1^+ J \wedge J \wedge J$ and $d\Omega_- \wedge J = \Omega_- \wedge dJ = W_1^- J \wedge J \wedge J$;
- $W_2 \leftrightarrow [d\Omega]_0^{(2,2)}$: $(d\Omega_+)^{(2,2)} = W_1^+ J \wedge J + W_2^+ \wedge J$ and $(d\Omega_-)^{(2,2)} = W_1^- J \wedge J + W_2^- \wedge J$;
- $W_3 \leftrightarrow [dJ]_0^{(2,1)}$ is defined as $W_3 = dJ^{(2,1)} - [J \lrcorner W_4]^{(2,1)}$;
- $W_4 \leftrightarrow J \wedge dJ$: $W_4 = \frac{1}{2} J \lrcorner dJ$;
- $W_5 \leftrightarrow [d\Omega]_0^{(3,1)}$: $W_5 = \frac{1}{2} \Omega_+ \lrcorner d\Omega_+$ (the subscript 0 indicative of the primitivity of the respective forms).

In [29], we saw that the five $SU(3)$ structure torsion classes, in the MQGP limit, satisfied (schematically):

$$T_{SU(3)}^{\text{IIB}} \in W_1 \oplus W_2 \oplus W_3 \oplus W_4 \oplus W_5 \sim \frac{e^{-3\tau}}{\sqrt{g_s N}} \oplus (g_s N)^{\frac{1}{4}} e^{-3\tau} \oplus \sqrt{g_s N} e^{-3\tau} \oplus -\frac{2}{3} \oplus -\frac{1}{2} \quad (17)$$

($r \sim e^{\frac{\tau}{3}}$), such that

$$\frac{2}{3} W_5^{\bar{3}} = W_4^{\bar{3}} \quad (18)$$

in the UV-IR interpolating region/UV, implying a Klebanov-Strassler-like supersymmetry [51]. Locally around $\theta_1 \sim \frac{1}{N^{\frac{1}{5}}}$, $\theta_2 \sim \frac{1}{N^{\frac{3}{10}}}$, the type IIA torsion classes of the delocalized SYZ type IIA mirror metric (??), were shown in [3] to be:

$$T_{SU(3)}^{\text{IIA}} \in W_2 \oplus W_3 \oplus W_4 \oplus W_5 \sim \gamma_2 g_s^{-\frac{1}{4}} N^{\frac{3}{10}} \oplus g_s^{-\frac{1}{4}} N^{-\frac{1}{20}} \oplus g_s^{-\frac{1}{4}} N^{\frac{3}{10}} \oplus g_s^{-\frac{1}{4}} N^{\frac{3}{10}} \approx \gamma W_2 \oplus W_4 \oplus W_5$$

fine tuning: $\gamma \approx 0 \xrightarrow{\quad} \approx W_4 \oplus W_5.$

(19)

Further,

$$W_4 \sim \Re W_5 \quad (20)$$

indicative of supersymmetry after constructing the delocalized SYZ mirror.

Apart from quantifying the departure from $SU(3)$ holonomy due to intrinsic contorsion supplied by the NS-NS three-form H , via the evaluation of the $SU(3)$ structure torsion classes, to our knowledge for the first time in the context of holographic thermal QCD **at finite gauge coupling** in [3]:

(i) the existence of approximate supersymmetry of the type IIB holographic dual of [1] in the MQGP limit near the coordinate branch $\theta_1 = \theta_2 = 0$ was demonstrated, which apart from the existence of a special Lagrangian three-cycle (as shown in [29, 3]) is essential for construction of the local SYZ type

IIA mirror;

(ii) it was demonstrated that the large- N suppression of the deviation of the type IIB resolved warped deformed conifold from being a complex manifold, is lost on being duality-chased to type IIA - it was also shown that one further fine tuning $\gamma_2 = 0$ in W_2^{IIA} can ensure that the local type IIA mirror is complex;

(iii) for the local type IIA $SU(3)$ mirror, the possibility of surviving approximate supersymmetry was demonstrated which is essential from the point of view of the end result of application of the SYZ mirror prescription.

We can get a one-form type IIA potential from the triple T-dual (along x, y, z) of the type IIB $F_{1,3,5}$ in [2] and using which the following $D = 11$ metric was obtained in [2] ($u \equiv \frac{rh}{r}$):

$$ds_{11}^2 = e^{-\frac{2\phi^{\text{IIA}}}{3}} [g_{tt}dt^2 + g_{\mathbb{R}^3}(dx^2 + dy^2 + dz^2) + g_{uu}du^2 + ds_{IIA}^2(\theta_{1,2}, \phi_{1,2}, \psi)] + e^{\frac{4\phi^{\text{IIA}}}{3}} (dx_{11} + A^{F_1} + A^{F_3} + A^{F_5})^2 \equiv \text{Black } M3 - \text{Brane} + \mathcal{O}\left(\left[\frac{g_s M^2 \log N}{N}\right] (g_s M) N_f\right). \quad (21)$$

If V is a seven-dimensional real vector space, then a three-form φ is said to be positive if it lies in the $GL(7, \mathbb{R})$ orbit of φ_0 , where φ_0 is a three-form on \mathbb{R}^7 which is preserved by G_2 -subgroup of $GL(7, \mathbb{R})$. The pair (φ, g) for a positive 3-form φ and corresponding metric g constitute a G_2 -structure. The space of p -forms decompose as following irreps of G_2 [52]:

$$\begin{aligned} \Lambda^1 &= \Lambda_7^1 \\ \Lambda^2 &= \Lambda_7^2 \oplus \Lambda_{14}^2 \\ \Lambda^3 &= \Lambda_1^3 \oplus \Lambda_7^3 \oplus \Lambda_{27}^3 \\ \Lambda^4 &= \Lambda_1^4 \oplus \Lambda_7^4 \oplus \Lambda_{27}^4 \\ \Lambda^5 &= \Lambda_7^5 \oplus \Lambda_{14}^5 \\ \Lambda^6 &= \Lambda_7^6 \end{aligned} \quad (22)$$

The subscripts denote the dimension of representation and components of same representation/dimensionality, are isomorphic to each other. Let M be a 7-manifold with a G_2 -structure (φ, g) . Then the components of spaces of 2-, 3-, 4-, and 5-forms are given in [52, 53]. The metric g defines a reduction of the frame bundle F to a principal $SO(7)$ -sub-bundle Q , that is, a sub-bundle of oriented orthonormal frames. Now, g also defines a Levi-Civita connection ∇ on the tangent bundle TM , and hence on F . However, the G_2 -invariant 3-form φ reduces the orthonormal bundle further to a principal G_2 -subbundle Q . The Levi-Civita connection can be pulled back to Q . On Q , ∇ can be uniquely decomposed as

$$\nabla = \bar{\nabla} + \mathcal{T} \quad (23)$$

where $\bar{\nabla}$ is a G_2 -compatible canonical connection on P , taking values in the sub-algebra $\mathfrak{g}_2 \subset \mathfrak{so}(7)$, while \mathcal{T} is a 1-form taking values in $\mathfrak{g}_2^\perp \subset \mathfrak{so}(7)$; \mathcal{T} is known as the intrinsic torsion of the G_2 -structure - the obstruction to the Levi-Civita connection being G_2 -compatible. Now $\mathfrak{so}(7)$ splits under G_2 as

$$\mathfrak{so}(7) \cong \Lambda^2 V \cong \Lambda_7^2 \oplus \Lambda_{14}^2. \quad (24)$$

But $\Lambda_{14}^2 \cong \mathfrak{g}_2$, so the orthogonal complement $\mathfrak{g}_2^\perp \cong \Lambda_7^2 \cong V$. Hence \mathcal{T} can be represented by a tensor T_{ab} which lies in $W \cong V \otimes V$. Now, since φ is G_2 -invariant, it is $\bar{\nabla}$ -parallel. So, the torsion is determined by $\nabla\varphi$. from Lemma 2.24 of [54]:

$$\nabla\varphi \in \Lambda_7^1 \otimes \Lambda_7^3 \cong W. \quad (25)$$

Due to the isomorphism between the $\Lambda_7^{a=1,\dots,5}$ s, $\nabla\varphi$ lies in the same space as T_{AB} and thus completely determines it. Equation (25) is equivalent to:

$$\nabla_A\varphi_{BCD} = T_A{}^E\psi_{EBCD} \quad (26)$$

where T_{AB} is the full torsion tensor. Equation (26) can be inverted to yield:

$$T_A{}^M = \frac{1}{24}(\nabla_A\varphi_{BCD})\psi^{MBCD}. \quad (27)$$

The tensor $T_A{}^M$, like the space W , possesses 49 components and hence fully defines $\nabla\varphi$. In general T_{AB} can be split into torsion components as

$$T = T_1g + T_7\lrcorner\varphi + T_{14} + T_{27} \quad (28)$$

where T_1 is a function and gives the **1** component of T . We also have T_7 , which is a 1-form and hence gives the **7** component, and, $T_{14} \in \Lambda_{14}^2$ gives the **14** component. Further, T_{27} is traceless symmetric, and gives the **27** component. Writing T_i as W_i , we can split W as

$$W = W_1 \oplus W_7 \oplus W_{14} \oplus W_{27}. \quad (29)$$

From [55], we see that a G_2 structure can be defined as:

$$\varphi_0 = \frac{1}{3!}f_{ABC}e^{ABC} = e^{-\phi^{IIA}}f_{abc}e^{abc} + e^{-\frac{2\phi^{IIA}}{3}}J \wedge e^{x_{10}}, \quad (30)$$

where $A, B, C = 1, \dots, 6, 10; a, b, c = 1, \dots, 6$ and f_{ABC} are the structure constants of the imaginary octonions. Using the same, the G_2 -structure torsion classes were worked out around $\theta_1 \sim \frac{1}{N^{\frac{1}{5}}}, \theta_2 \sim \frac{1}{N^{\frac{3}{10}}}$ in [3] to:

$$T_{G_2} \in W_2^{14} \oplus W_3^{27} \sim \frac{1}{(g_s N)^{\frac{1}{4}}} \oplus \frac{1}{(g_s N)^{\frac{1}{4}}}. \quad (31)$$

Hence, the approach of the seven-fold, locally, to having a G_2 holonomy ($W_1^{G_2} = W_2^{G_2} = W_3^{G_2} = W_4^{G_2} = 0$) is accelerated in the MQGP limit.

As stated earlier, the global uplift to M-theory of the type *IIB* background of [1] is expected to involve a seven-fold of G_2 structure (not G_2 -holonomy due to non-zero G_4). It is hence extremely important to be able to see this, at least locally. It is in this sense that the results of [2] are of great significance as one explicitly sees, for the first time, in the context of holographic thermal QCD **at finite gauge coupling**, though locally, the aforementioned G_2 structure having worked out the non-trivial G_2 -structure torsion classes.

3 $0^{++}(\dots)$ Glueball spectrum from type *IIB* supergravity background

In this section we discuss the 0^{++} glueball spectrum by solving the dilaton wave equation in the type *IIB* background discussed in section 2. The type *IIB* metric as given in equation 4 with the warp factor h given in 7 can be simplified by working around a particular value of θ_1 and θ_2 : $\{\theta_1 = \frac{1}{N^{1/5}}, \theta_2 = \frac{1}{N^{3/10}}\}$, then keeping terms upto (N)ext to (L)eading (O)rder in N in the large N limit. The simplified type *IIB* metric is given as:

$$ds^2 = g_{tt}dt^2 + g_{x_1x_1}(dx_1^2 + dx_2^2 + dx_3^2) + g_{rr}dr^2 + \sqrt{h}r^2d\mathcal{M}_5^2, \quad (32)$$

with the components $g_{tt}, g_{x_1x_1} (= g_{x_2x_2} = g_{x_3x_3}), g_{rr}$ as given below:

$$g_{tt} = \frac{r^2(1-B(r))\left(\frac{r_h^4}{r^4} - 1\right)}{2\sqrt{\pi}\sqrt{N}\sqrt{g_s}} \quad g_{x_1x_1} = \frac{r^2(1-B(r))}{2\sqrt{\pi}\sqrt{N}\sqrt{g_s}} \quad g_{rr} = \frac{2\sqrt{\pi}\sqrt{N}(r^2-3a^2)(B(r)+1)\sqrt{g_s}}{r^4\left(1-\frac{r_h^4}{r^4}\right)}, \quad (33)$$

where $B(r) = \frac{3M^2g_s \log(r)(12N_f g_s \log(r) + 6N_f g_s + N_f g_s(-\log(N)) - 2\log(4)N_f g_s + 8\pi)}{32\pi^2 N}$, and a being the resolution parameter is proportional to the horizon radius r_h . Hence while computing the spectrum with a cut-off in the radial direction and no horizon, we must put both r_h and a to zero in the above equation.

Moreover the dilaton profiles with/without the black-hole are given below as:

$$\begin{aligned} (a) \quad r_h \neq 0: \\ e^{-\Phi} &= \frac{1}{g_s} - \frac{N_f}{8\pi} \log(r^6 + a^2 r^4) - \frac{N_f}{2\pi} \log\left(\sin \frac{\theta_1}{2} \sin \frac{\theta_2}{2}\right), \quad r < \mathcal{R}_{D5/\overline{D5}}, \\ e^{-\Phi} &= \frac{1}{g_s}, \quad r > \mathcal{R}_{D5/\overline{D5}}; \\ (b) \quad r_h = 0: \\ e^{-\Phi} &= \frac{1}{g_s} - \frac{3N_f}{4\pi} \log r - \frac{N_f}{2\pi} \log\left(\sin \frac{\theta_1}{2} \sin \frac{\theta_2}{2}\right), \quad r < |\mu_{\text{Ouyang}}|^{\frac{2}{3}}, \\ e^{-\Phi} &= \frac{1}{g_s}, \quad r > |\mu_{\text{Ouyang}}|^{\frac{2}{3}}. \end{aligned} \quad (34)$$

Again working around the particular choices of θ_1 and θ_2 the above profile can be simplified upto NLO in N . The dilaton equation that has to be solved is given as:

$$\partial_\mu (e^{-2\Phi} \sqrt{g} g^{\mu\nu} \partial_\nu \phi) = 0. \quad (35)$$

To solve the above dilaton equation we assume ϕ in (35) to be of the form $\phi = e^{ik \cdot x} \tilde{\phi}(r)$. Now with this, we adopt the WKB method to get to the final result. The first step towards the WKB method is to convert the glueball equation of motion into a Schrödinger-like equation. Then the WKB quantization condition can be applied on the potential term obtained from the Schrödinger-like equation. For (0^{++}) glueball spectrum with no horizon ($r_h = 0$), one of the solution was obtained by imposing Neumann boundary condition at the cut-off.

3.1 $r_h \neq 0$ using WKB quantization method

In the following we discuss the spectrum of 0^{++} glueball in the type *IIB* background with a black hole, implying a horizon of radius r_h in the geometry. The results corresponding to the coordinate and field redefinitions of [34], are discussed below.

Using the redefinitions of [34] with $r = \sqrt{y}, r_h = \sqrt{y_h}$ and finally $y = y_h(1 + e^z)$, the 0^{++} EOM (35), with $k^2 = -m^2$ can be written as:

$$\partial_z (E_z \partial_z \tilde{\phi}) + y_h^2 E_z m^2 \tilde{\phi} = 0, \quad (36)$$

where at leading order in N , E_z and F_z are given with $L = (4\pi g_s N)^{1/4}$ as:

$$E_z = \frac{1}{128\pi^2 L^5 g_s^2} (e^z + 2) y_h^2 \left(8\pi + g_s N_f \log 256 + 2N_f g_s \log N - 3g_s N_f \log [(e^z + 1) y_h] \right) \left[2 \left(3a^2 \{4\pi + g_s N_f (\log 16 - 6)\} + (e^z + 1) y_h \{8\pi + g_s N_f \log 256\} \right) + 2g_s N_f \log N \{3a^2 + 2(e^z + 1) y_h\} - 3g_s N_f \{3a^2 + 2(e^z + 1) y_h\} \log [(e^z + 1) y_h] \right] \quad (37)$$

$$F_z = \frac{1}{128\pi^2 g_s^2 L y_h (e^z + 1)} e^z \left(4\pi + g_s N_f \log 16 + g_s N_f \log N - \frac{3}{2} g_s N_f \log [(e^z + 1) y_h] \right) \left[(e^z + 1) y_h \left(8\pi + 2g_s N_f \log N + g_s N_f \log 256 - 3g_s N_f \log [(e^z + 1) y_h] \right) - 3a^2 \left(4\pi + 6g_s N_f + g_s N_f \log N + g_s N_f \log 16 - \frac{3}{2} g_s N_f \log [(e^z + 1) y_h] \right) \right] \quad (38)$$

Now, redefining the wave function $\tilde{\phi}$ as $\psi(z) = \sqrt{E_z} \tilde{\phi}(z)$ equation (36) reduces to a Schrödinger-like equation

$$\left(\frac{d^2}{dy^2} + V(z) \right) \psi(z) = 0 \quad (39)$$

where the potential $V(z)$ is a rather cumbersome expression which we will not explicitly write out. The WKB quantization condition becomes: $\int_{z_1}^{z_2} \sqrt{V(z)} dz = (n + \frac{1}{2}) \pi$ where $z_{1,2}$ are the turning points of $V(z)$. We will work below with a dimensionless glueball mass \tilde{m} assumed to be large and defined via: $m = \tilde{m} \frac{r_h}{L^2}$. To determine the turning points of the potential $V(z)$, we consider two limits of the same - $r \in [r_h, \sqrt{3}a(r_h)] \cup [\sqrt{3}br_h, \infty) \equiv (IR, IR/UV \text{ interpolating} + UV)$. In the IR, we have to take the limit $z \rightarrow -\infty$. Now in the large \tilde{m} and large $\log N$ limit this potential at small z can be shown to be given as:

$$V(z \ll 0) = \frac{1}{8} (1 - 3b^2) e^z \tilde{m}^2 + \mathcal{O} \left(e^{2z}, \left(\frac{1}{\tilde{m}} \right)^2, \frac{1}{\log N} \right) < 0 \quad (40)$$

Hence, there are no turning points in the IR.

Now, in the UV, apart from taking the large z limit we also have to take $N_f = M = 0$, to get:

$$V(z \gg 1) = -\frac{3(b^2 + 1)(y_h \tilde{m}^2 + 3)}{4y_h e^{2z}} + \frac{3b^2 + y_h \tilde{m}^2 + 6}{4y_h e^z} - 1 + \mathcal{O}(e^{-3z}). \quad (41)$$

The turning points of (41) are:

$$z_1 = \frac{1}{8} \left(3b^2 - \sqrt{9b^4 - 6b^2(7y_h \tilde{m}^2 + 18) + y_h \tilde{m}^4 - 36y_h \tilde{m}^2 - 108 + y_h \tilde{m}^2 + 6} \right),$$

$$z_2 = \frac{1}{8} \left(3b^2 + \sqrt{9b^4 - 6b^2(7y_h \tilde{m}^2 + 18) + y_h \tilde{m}^4 - 36y_h \tilde{m}^2 - 108 + y_h \tilde{m}^2 + 6} \right) \text{ which in the large } \tilde{m}$$

limit is given as: $\left\{ z_1 = (3 + 3b^2) + \mathcal{O}\left(\frac{1}{\tilde{m}^2}\right), z_2 = \frac{\tilde{m}^2}{4} - \frac{3(2+3b^2)}{4} + \mathcal{O}\left(\frac{1}{\tilde{m}^2}\right) \right\}$.

To obtain a real spectrum, one first notes:

$$\sqrt{V(z \gg 1, N_f = M = 0; b = 0.6)} = \sqrt{0.25e^{-z} - 1.02e^{-2z}}\tilde{m} + \mathcal{O}\left(e^{-3z}, \frac{1}{\tilde{m}^2}\right). \quad (42)$$

and

$$\begin{aligned} \int \sqrt{V(z)}dz &= \frac{\sqrt{e^{-2z}(0.25e^z - 1.0023)}\tilde{m} \left(0.124856e^z \tan^{-1}\left(\frac{0.124856e^z - 1.00115}{\sqrt{0.25e^z - 1.0023}}\right) - 1.\sqrt{0.25e^z - 1.0023}\right)}{\sqrt{0.25e^z - 1.0023}} \\ &= \frac{\sqrt{e^{-2z}(0.25e^z - 1.02)}\tilde{m} \left(0.123768e^z \tan^{-1}\left(\frac{0.123768e^{1.z} - 1.00995}{\sqrt{0.25e^z - 1.02}}\right) - 1.\sqrt{0.25e^z - 1.02}\right)}{\sqrt{0.25e^z - 1.02}} \end{aligned} \quad (43)$$

Therefore

$$\int_{4.08}^{0.25\tilde{m}^2 - 2.31} \sqrt{V(z)} = 0.39\tilde{m} - 2 = \left(n + \frac{1}{2}\right)\pi, \quad (44)$$

yielding:

$$m_n^{0^{++}} = 9.18 + 8.08n. \quad (45)$$

3.2 Glueball Mass for $r_h = 0$ and an IR cut-off r_0

In this background the type *IIB* metric and the dilaton profile has to be modified by the limit $r_h \rightarrow 0$ and hence with $a \rightarrow 0$. This time also we have provided two solutions to the dilaton equation. The first solutions was obtained by first following the redefinition of variables in [33] and then imposing a neumann boundary condition at the radial cut-off. For the other solution we again consider the WKB method after a redefinition of variables as given in [34].

3.2.1 Neumann boundary condition at r_0

Following [33], we redefine the radial coordinate as $z = \frac{1}{r}$. With this change of variable, the radial cut-off now maps to $z = z_0$, with $z_0 = \frac{1}{r_0}$. The dilaton equation using the metric and the dilaton background in the limit $(r_h, a) \rightarrow 0$ is given as:

$$e^{2U} \partial_z \left(e^{-2U} \partial_z \tilde{\phi} \right) + \left(\frac{(4g_s N \pi)(B(z) + 1)}{(1 - B(z))} \right) (m^2) \tilde{\phi} = 0, \quad (46)$$

where upto NLO in N we have,

$$\begin{aligned} e^U &= \frac{8 \times 2^{1/4} g_s^{13/8} \pi^{13/8} N^{5/8} z^{3/2}}{4(\pi \log(4) N_f g_s + \pi) + 2\pi N_f g_s \log(N) + 3N_f g_s \log(z)} \\ &\quad - \frac{15M^2 z^{3/2} g_s^{21/8} \log(z) (-12N_f g_s \log(z) + 6N_f g_s + N_f g_s (-\log(N)) - \log(16) N_f g_s + 8\pi)}{8 \cdot 2^{3/4} \pi^{3/8} N^{3/8} (3N_f g_s \log(z) + 2\pi N_f g_s \log(N) + 4(\pi \log(4) N_f g_s + \pi))}. \end{aligned} \quad (47)$$

Now to convert the above equation in a one-dimensional schrodinger like form we introduce a new field variable $\psi(z)$ as: $\psi(z) = e^{-U} \tilde{\phi}(z)$.

With this one can write the equation in the following schrodinger like form,

$$\frac{\partial^2 \psi(z)}{\partial z^2} = V(z) \psi(z). \quad (48)$$

The potential $V(z)$, in the large- N large- $\log N$ limit is given as:

$$V(z) = 4\pi g_s m^2 N + \frac{6}{\pi z^2 \log(N)} - \frac{15}{4z^2} + \mathcal{O}\left(\frac{1}{(\log N)^2}, \frac{g_s M^2}{N}\right). \quad (49)$$

Hence, the Schrödinger equation becomes:

$$\psi''(z) + \psi(z) \left(4\pi g_s m^2 N + \frac{6}{\pi z^2 \log(N)} - \frac{15}{4z^2}\right) = 0, \quad (50)$$

whose solution is given as under:

$$\psi(z) = c_1 \sqrt{z} J_{\sqrt{\frac{2}{\pi}} \sqrt{\frac{2\pi \log(N)-3}{\log(N)}}} \left(2\sqrt{g_s} m \sqrt{N} \sqrt{\pi} z\right) + c_2 \sqrt{z} Y_{\sqrt{\frac{2}{\pi}} \sqrt{\frac{2\pi \log(N)-3}{\log(N)}}} \left(2\sqrt{g_s} m \sqrt{N} \sqrt{\pi} z\right) \quad (51)$$

Requiring finiteness of $\psi(z)$ at $z = 0$ requires setting $c_2 = 0$. Then imposing Neumann boundary condition on $\tilde{\phi}(z)$ at $z = z_0$ implies:

$$\begin{aligned} \tilde{\phi}'(z_0) &= \frac{1}{\left(-2\pi g_s N_f \log\left(\frac{1}{N}\right) + 3g_s N_f \log(z_0) + 4(\pi g_s N_f \log(4) + \pi)\right)^2} \\ &\times \left\{ 4\sqrt[4]{2\pi^{13/8} g_s^{13/8} N^{5/8} z_0} \left[3 \left(-2\pi g_s N_f \log\left(\frac{1}{N}\right) + 3g_s N_f \log(z_0) - 2g_s N_f + 4\pi g_s N_f \log(4) + 4\pi \right) \right. \right. \\ &\times J_{\sqrt{4 - \frac{6}{\pi \log(N)}}} \left(2\sqrt{g_s} m \sqrt{N} \sqrt{\pi} z_0 \right) + \left(-2\pi g_s N_f \log\left(\frac{1}{N}\right) + 3g_s N_f \log(z_0) + 4(\pi g_s N_f \log(4) + \pi) \right) \\ &\times \left(2\sqrt{\pi} \sqrt{g_s} m \sqrt{N} z_0 J_{\sqrt{4 - \frac{6}{\pi \log(N)}} - 1} \left(2\sqrt{g_s} m \sqrt{N} \sqrt{\pi} z_0 \right) - 2\sqrt{\pi} \sqrt{g_s} m \sqrt{N} z_0 J_{\sqrt{4 - \frac{6}{\pi \log(N)}} + 1} \left(2\sqrt{g_s} m \sqrt{N} \sqrt{\pi} z_0 \right) \right. \\ &\left. \left. + J_{\sqrt{4 - \frac{6}{\pi \log(N)}}} \left(2\sqrt{g_s} m \sqrt{N} \sqrt{\pi} z_0 \right) \right] \right\} = 0, \quad (52) \end{aligned}$$

implying in the large- N large- z (as the Neumann boundary condition will be implemented in the IR) limit:

$$\frac{1}{2} x_0 J_{\sqrt{4 - \frac{6}{\pi \log(N)}} - 1}(x_0) - \frac{1}{2} x_0 J_{\sqrt{4 - \frac{6}{\pi \log(N)}} + 1}(x_0) + 2J_{\sqrt{4 - \frac{6}{\pi \log(N)}}}(x_0) = 0, \quad (53)$$

where $x_0 \equiv 2\sqrt{g_s N \pi} m z_0$. The graphical solution points out that the ground state has a zero mass and the lightest (first excited state) glueball mass is approximately given by $3.71 \frac{r_0}{L^2}$.

3.2.2 WKB method: Including the Non-Conformal/NLO (in N) Corrections

Again following the redefinition of variables as given in [34]: $r = \sqrt{y}$, $y = y_0 (1 + e^z)$, where $r_0 = \sqrt{y_0}$ is the radial cut-off, and using the type IIB metric as well as the dilaton profile in the limit $(rh, a) \rightarrow 0$, the dilaton equation (35) can be written as:

$$\partial_z(C_z \partial_z \tilde{\phi}) + y_h^2 D_z m^2 \tilde{\phi} = 0, \quad (54)$$

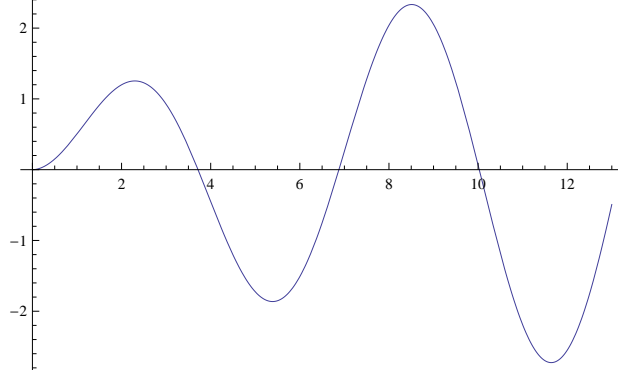


Figure 1: $0^{+++},++++,+++++$ Masses obtained by graphical solution of the Neumann boundary condition in the $r_h = 0$ Limit

where C_z and D_z are given up to NLO in N by,

$$C_z = \frac{1}{32768\sqrt{2} \pi^{21/4} N^{9/4} g_s^{13/4}} e^{-z} (e^z + 1)^3 y_0^3 \left(8\pi + 2g_s N_f \log N + 4g_s N_f \log 4 - 3g_s N_f \log [y_0 (e^z + 1)] \right)^2 \left(128\pi^2 N + 15g_s M^2 \{-8\pi + g_s N_f (\log 16 - 6) + g_s N_f \log N\} \log [(e^z + 1) y_0] - 90M^2 g_s^2 N_f \log [(e^z + 1) y_0]^2 \right) \quad (55)$$

$$D_z = \frac{1}{32768\sqrt{2} \pi^{17/4} N^{5/4} g_s^{9/4}} e^z \left(8\pi + 2g_s N_f \log N + 4g_s N_f \log 4 - 3g_s N_f \log [y_0 (e^z + 1)] \right)^2 \left(128\pi^2 N + 3g_s M^2 \{-8\pi + g_s N_f (\log 16 - 6) + g_s N_f \log N\} \log [(e^z + 1) y_0] - 18M^2 g_s^2 N_f \log [(e^z + 1) y_0]^2 \right) \quad (56)$$

Defining a new variable $\psi(z)$ such that: $\psi(z) = \sqrt{C_z} \tilde{\phi}(z)$, the above equation can be converted into a Schrödinger-like equation,

$$\left(\frac{d^2}{dy^2} + V(z) \right) \psi(z) = 0, \quad (57)$$

where the potential is given up to NLO in N as:

$$V(z) = -\frac{1}{4} - \frac{3e^{2z} g_s^2 \log N M^2 \tilde{m}^2 N_f \log(y_0)}{128\pi^2 N} + \frac{e^{2z} (2(g_s N_f (\log N (\tilde{m}^2 - 3) + \tilde{m}^2 \log(16)) + 12 - 6 \log(4)) + 4\pi (\tilde{m}^2 - 3)) - 3g_s (\tilde{m}^2 - 3) N_f \log(y_0)}{4(2g_s N_f (\log N + \log(16)) - 3g_s N_f \log(y_0) + 8\pi)} + \mathcal{O}\left(\frac{1}{N^2}\right). \quad (58)$$

The domain of integration over which $V(z) > 0$ can be shown to be:

$$\left\{ \log \left(\frac{3g_s^2 M^2 N_f \log(N) \log(y_0)}{64\pi^2 \tilde{m} N} + \frac{1}{\tilde{m}} \right), \log(\delta^2 - 1) \right\}, \text{ where } \mu^{\frac{2}{3}} = \delta \sqrt{y_0}. \text{ Note that the IR cut-off } r_0 \text{ or } y_0$$

is not put in by hand but is proportional to the Ouyang embedding parameter (corresponding to the embedding of the flavor $D7$ -branes) raised to two-third power. The proportionality constant δ could be determined, as discussed in point number 5 in Section 8, by matching with lattice calculations and turns out to be $\mathcal{O}(1)$.

Expanding \sqrt{V} first in N and then in \tilde{m} and then integrating over the above mentioned domain, one gets the following quantization condition,

$$\begin{aligned} & \int_{z=\log\left(\frac{3M^2 g_s^2 N_f \log N \log y_0}{64\pi^2 \tilde{m} N} + \frac{1}{\tilde{m}}\right)}^{\log(\delta^2-1)} \sqrt{V(z)} \\ &= \frac{1}{2} (\delta^2 - 1) \tilde{m} \left(\frac{3M^2 g_s^2 N_f \log N \log y_0}{64\pi^2 N} + 1 \right) - 0.75 + \mathcal{O}\left(\frac{1}{\tilde{m}N}, \frac{1}{\tilde{m}^2}\right) = \left(n + \frac{1}{2}\right) \pi, \end{aligned} \quad (59)$$

yielding:

$$m_n^{0^{++}} = \frac{(6.28319n + 4.64159) \left(1 - \frac{0.00474943g_s^2 \log N M^2 N_f \log(y_0)}{N}\right)}{\delta^2 - 1}. \quad (60)$$

4 Scalar Glueball (0^{-+} (***...)) Masses

As $Tr(F\tilde{F})$ has $P = -, C = +$ and it couples to A_1 in the Wess-Zumino term for the type IIA $D4$ -brane: $\int_{\Sigma_{4,1}} A \wedge F \wedge F$, one considers A_1 's EOM:

$$\partial_\nu \left(\sqrt{g^{\text{IIA}}} g_{\text{IIA}}^{\mu\sigma} g_{\text{IIA}}^{\nu\rho} (\partial_{[\sigma} A_{\rho]}) \right) = 0, \quad (61)$$

where $\mu, \nu, \dots = a(\equiv 0, 1, 2, 3), r, \alpha(\equiv 5, \dots, 9)$. Like [56], assume $A_\mu = \delta_\mu^{\theta_2} a_{\theta_2}(r) e^{ik \cdot x}$, $k^2 = -m^2$ as the fluctuation about the type IIA A_1 that was worked out in [2]. The 0^{-+} EOM then reduces to:

$$\sqrt{g^{\text{IIA}}} g_{\text{IIA}}^{\theta_2\theta_2} g_{\text{IIA}}^{rr} a_{\theta_2}''(r) + \partial_r \left(\sqrt{g^{\text{IIA}}} g_{\text{IIA}}^{\theta_2\theta_2} g_{\text{IIA}}^{rr} \right) a_{\theta_2}'(r) + \sqrt{h} m^2 \sqrt{g^{\text{IIA}}} g_{\text{IIA}}^{\theta_2\theta_2} a_{\theta_2}(r) = 0. \quad (62)$$

4.1 Neumann/Dirichlet Boundary Conditions

4.1.1 $r_h \neq 0$

Then taking the large- N limit followed by a small- θ_1 small- θ_2 limit one can show that the equation of motion (62) yields::

$$-\frac{8\pi (r^4 - r_h^4) a_{\theta_2}''(r)}{\sqrt{3}} + \frac{32\pi (r^4 - 2r_h^4) a_{\theta_2}'(r)}{\sqrt{3}r} - 32\sqrt[6]{3}\pi^2 g_s m^2 N a_{\theta_2}(r) = 0. \quad (63)$$

Working near $r = r_h$, approximating (64) by:

$$-\frac{32\pi r_h^3 (r - r_h) a_{\theta_2}''(r)}{\sqrt{3}} + \left(\frac{160\pi r_h^2 (r - r_h)}{\sqrt{3}} - \frac{32\pi r_h^3}{\sqrt{3}} \right) a_{\theta_2}'(r) - 32\sqrt[6]{3}\pi^2 g_s m^2 N a_{\theta_2}(r) = 0 \quad (64)$$

whose solution is given as under:

$$a_{\theta_2}(r) = c_1 U \left(-\frac{3^{2/3} g_s m^2 N \pi}{5r_h^2}, 1, \frac{5r}{r_h} - 5 \right) + c_2 L_{\frac{3^{2/3} \pi g_s m^2 N}{5r_h^2}} \left(\frac{5r}{r_h} - 5 \right) \quad (65)$$

Imposing Neumann boundary condition: $a'_{\theta_2}(r = r_h) = 0$, utilizing:

$$\begin{aligned}
U \left(1 - \frac{3^{2/3} \pi g_s m^2 N}{5|r_h|^2}, 2, \frac{5r}{r_h} - 5 \right) = \\
-\frac{r_h^3}{3^{2/3} \pi g_s m^2 N (r - r_h) \Gamma \left(-\frac{3^{2/3} g_s m^2 N \pi}{5r_h^2} \right)} + \frac{\psi^{(0)} \left(1 - \frac{3^{2/3} g_s m^2 N \pi}{5r_h^2} \right) + \log \left(\frac{5r}{r_h} - 5 \right) + 2\gamma - 1}{\Gamma \left(-\frac{3^{2/3} g_s m^2 N \pi}{5r_h^2} \right)} \\
+ \frac{(r - r_h) (5r_h^2 - 3^{2/3} \pi g_s m^2 N) \left(2\psi^{(0)} \left(2 - \frac{3^{2/3} g_s m^2 N \pi}{5r_h^2} \right) + 2 \log(r - r_h) + 2 \log \left(\frac{5}{r_h} \right) + 4\gamma - 5 \right)}{4r_h^3 \Gamma \left(-\frac{3^{2/3} g_s m^2 N \pi}{5r_h^2} \right)} \\
+ \mathcal{O}((r - r_h)^2), \tag{66}
\end{aligned}$$

$r_h = T\sqrt{4\pi g_s N}$ - up to LO in N - requires $c_2 = 0$ and

$$\frac{3^{2/3} m^2}{20T^2} = n, \tag{67}$$

implying:

$$m_n^{0-+} = \frac{2\sqrt{5}\sqrt{n}T}{\sqrt[3]{3}}. \tag{68}$$

One can show that imposing Dirichlet boundary condition $a_{\theta_2}(r = r_h) = 0$, yields the same spectrum as (68). If the temperature T gets identified with a of [56], then the ground state, unlike [56], is massless; the excited states for lower n 's are closer to $a = 0$ and the higher excited states are closer to $a \rightarrow \infty$ in [56].

4.1.2 $r_h = 0$ Limit of (63)

The $r_h = 0$ limit of (63) gives:

$$\sqrt{3}r^4 a_{\theta_2}''(r) - 4\sqrt{3}r^3 a_{\theta_2}'(r) + 3\sqrt[6]{3}\tilde{m}^2 r_0^2 a_{\theta_2}(r) = 0, \tag{69}$$

which near $r = r_0$ yields:

$$a_{\theta_2}(r) = (4r - 3\tilde{m})^{5/4} \left(c_1 U \left(\frac{5}{4} - \frac{\tilde{m}^2}{4\sqrt[3]{3}}, \frac{9}{4}, \frac{3r}{\tilde{m}} - \frac{9}{4} \right) + c_2 L^{\frac{5}{12}} \frac{1}{(3^{2/3}\tilde{m}^2 - 15)} \left(\frac{3r}{\tilde{m}} - \frac{9}{4} \right) \right). \tag{70}$$

Imposing Neumann boundary condition on (70) yields:

$$\begin{aligned}
m^{0-+}(r_h = 0) &= 0 \\
m^{0-+*}(r_h = 0) &\approx 3.4 \frac{r_0}{L^2} \\
m^{0-+***}(r_h = 0) &\approx 4.35 \frac{r_0}{L^2}. \tag{71}
\end{aligned}$$

One can similarly show that imposing Dirichlet boundary condition on (70) for $c_2 = 0$ yields:

$$\begin{aligned}
m^{0-+}(r_h = 0) &= 0 \\
m^{0-+*}(r_h = 0) &\approx 3.06 \frac{r_0}{L^2} \\
m^{0-+***}(r_h = 0) &\approx 4.81 \frac{r_0}{L^2}. \tag{72}
\end{aligned}$$

4.1.3 WKB Quantization for $r_h \neq 0$

The potential corresponding to the Schrödinger-like equation a la [34], substituting $m = \tilde{m} \frac{\sqrt{y_h}}{L^2}$, is given by:

$$V = \frac{e^z (4 \cdot 3^{2/3} \tilde{m}^2 (3e^z + e^{2z} + 2) - 64e^z - 108e^{2z} - 25e^{3z} + 96)}{16 (e^z + 1)^2 (e^z + 2)^2}. \quad (73)$$

Therefore, in the IR:

$$V(z \ll 0) = \left(-\frac{3}{16} 3^{2/3} \tilde{m}^2 - \frac{11}{2} \right) e^{2z} + \left(\frac{1}{8} 3^{2/3} \tilde{m}^2 + \frac{3}{2} \right) e^z + \mathcal{O}(e^{-3z}), \quad (74)$$

the turning points being given by $-\infty$ and $\log \left(\frac{2 \cdot 3^{2/3} \tilde{m}^2 + 24}{3 \cdot 3^{2/3} \tilde{m}^2 + 88} \right) \approx -0.405$. But only $z \in (-\infty, -2.526]$ corresponds to the IR in our calculations. So,

$$\int_{-\infty}^{-2.526} \sqrt{V} = 0.283 \tilde{m} = \left(n + \frac{1}{2} \right) \pi, \quad (75)$$

which obtains:

$$m_n^{0^-+}(T, IR) = 5.56(1 + 2n) \frac{r_h}{L^2}. \quad (76)$$

Similarly, in the UV:

$$V(UV, T) = \left(\frac{1}{4} 3^{2/3} \tilde{m}^2 + \frac{21}{8} \right) e^{-z} + \left(\frac{9}{16} - \frac{3}{4} 3^{2/3} \tilde{m}^2 \right) e^{-2z} - \frac{25}{16} + \mathcal{O}(e^{-3z}), \quad (77)$$

whose turning points are: $\log \left(\frac{1}{25} \left(2 \cdot 3^{2/3} \tilde{m}^2 \pm \sqrt{6} \sqrt{2 \cdot 3^{3/3} \tilde{m}^4 - 36 \cdot 3^{2/3} \tilde{m}^2 + 111 + 21} \right) \right)$
 $= \log(3 + \mathcal{O}(\frac{1}{\tilde{m}^2})), \log(0.33\tilde{m}^2 - 1.32 + \mathcal{O}(\frac{1}{\tilde{m}^2}))$. Now: $\sqrt{V(UV, T)} = \frac{1}{2} \sqrt[3]{3} \tilde{m} e^{-z} \sqrt{e^z - 3} + \mathcal{O}(\frac{1}{\tilde{m}})$.
Therefore,

$$\int_{\log 3}^{\log(0.33\tilde{m}^2 - 1.32)} \sqrt{V(UV, T)} = 0.654 \tilde{m} - 2.5 = \left(n + \frac{1}{2} \right) \pi, \quad (78)$$

which obtains:

$$m_n^{0^-+}(UV, T) = (6.225 + 4.804n) \pi T. \quad (79)$$

4.1.4 WKB Quantization at $r_h = 0$

The ‘potential’ is given by:

$$V(0^-+, r_h = 0) = \frac{43^{2/3} \tilde{m}^2 e^{2z} + \frac{e^{2z}(e^z+1)(5e^z+12)^2}{(e^z+2)^2} - 2(e^z+1)(14e^z+25e^{2z}+4)}{16(e^z+1)^3} + \mathcal{O}\left(\frac{g_s M^2}{N}\right). \quad (80)$$

Therefore, in the IR:

$$V(IR, r_h = 0) = -\frac{1}{2} - \frac{3}{4} e^z + \left(\frac{9}{8} + \frac{3^{2/3}}{4} \tilde{m}^2 \right) e^{2z} + \mathcal{O}(e^{3z}), \quad (81)$$

and in the IR, the domain of integration becomes: $[\log\left(\frac{\sqrt{2}}{3^{\frac{1}{3}}\tilde{m}}\right), \log(\delta^2-1)]: \int_{\log\left(\frac{\sqrt{2}}{3^{\frac{1}{3}}\tilde{m}}\right)}^{\log(\delta^2-1)} \sqrt{V(IR, r_h=0)} = \frac{3^{\frac{1}{3}}(\delta^2-1)}{2}\tilde{m} - 1.1126$, yielding:

$$m_n^{0^{-+}}(IR, r_h=0) = \frac{(3.72 + 4.36n)}{(\delta^2 - 1)} \frac{r_0}{L^2}. \quad (82)$$

Also, in the UV:

$$V(UV, r_h=0) = \left(-\frac{3}{4}3^{2/3}\tilde{m}^2 - \frac{103}{16}\right)e^{-2z} + \left(\frac{1}{4}3^{2/3}\tilde{m}^2 + \frac{21}{8}\right)e^{-z} - \frac{25}{16}, \quad (83)$$

whose turning points are: $\frac{1}{25}\left(23^{2/3}\tilde{m}^2 \pm \sqrt{12\sqrt{3}\tilde{m}^4 - 2163^{2/3}\tilde{m}^2 - 2134 + 21}\right) = \left(3 + \mathcal{O}\left(\frac{1}{\tilde{m}^2}\right), \frac{4}{25}3^{\frac{2}{3}}\tilde{m}^2 - \frac{33}{25}\right)$, yielding: $\int_3^{\frac{4}{25}3^{2/3}\tilde{m}^2 - \frac{33}{25}} \sqrt{V(UV, r_h=0)} = \frac{\pi}{43^{\frac{1}{6}}} = \left(n + \frac{1}{2}\right)\pi$ which obtains:

$$m_n^{0^{-+}}(UV, r_h=0) = 4.804 \left(n + \frac{1}{2}\right) \frac{r_0}{L^2}. \quad (84)$$

5 Glueball ($0^{--(***)}$) Masses

5.1 $r_h \neq 0$ and Neumann/Dirichlet Boundary Conditions at $r = r_h$

Given the Weiss-Zumino term $A^{\mu\nu} d^{abc} \text{Tr}\left(F_{\mu\rho}^a F_{\lambda}^b{}^\rho F_{\nu}^c{}^\lambda\right)$ and the two-form potential $A_{\mu\nu}$ is dual to a pseudo-scalar, for $r_h \neq 0$, corresponding to QCD₃, one writes down the EOM for the fluctuation δA^{23} . The B_{MN}, C_{MN} EOMs are:

$$\begin{aligned} D^M H_{MNP} &= \frac{2}{3} F_{NPQRS} F^{QRS}, \\ D^M F_{MNP} &= -\frac{2}{3} F_{NPQRS} H^{QRS}, \end{aligned} \quad (85)$$

or defining $A_{MN} = B_{MN} + iC_{MN}$, (85) can be rewritten as:

$$D^M \partial_{[M} A_{NP]} = -\frac{2i}{3} F_{NPQRS} \partial^{[Q} A^{RS]}. \quad (86)$$

Now, $A_{MN} \rightarrow A_{MN}^{(0)} + \delta A_{MN}$ with $\delta A^{MN} = \delta_2^M \delta_3^N \delta A_{23}$, the EOM satisfied by $\delta A_{23}(x^{0,1,2,3}, r) = \int \frac{d^4 k}{(2\pi)^4} e^{ik \cdot x} g_{22} G(r)$ reduces to:

$$\partial_\mu (\sqrt{-g} g^{22} g^{33} g^{\mu\nu} \partial_\nu \delta A_{23}) = 0. \quad (87)$$

Assuming $a = \left(\alpha + \beta \frac{g_s M^2}{N} + \gamma \frac{g_s M^2}{N} \log r_h \right) r_h$ [41, 5] for $(\alpha, \beta, \gamma) = (0.6, 4, 4)$ [5] and $k^\mu = (\omega, k_1, 0, 0) : k^2 = -m^2$, and defining $\mathcal{G}(r) \equiv g_{22} G(r)$ the EOM for $G(r)$ is:

$$\begin{aligned}
& \mathcal{G}''(r) \\
& + \mathcal{G}'(r) \left(\frac{3g_s M^2 (g_s N_f (\log N - 6 + \log(16))) - 24g_s N_f \log(r) - 8\pi}{64\pi^2 N r} \right. \\
& \left. - \frac{75.r_h^2 (4.g_s M^2 \log(r_h) + 4.g_s M^2 + 0.6N)^2}{N^2 r^3} + \frac{5r^4 - r_h^4}{r^5 - r r_h^4} \right) \\
& - \frac{g_s m^2 \mathcal{G}(r)}{4\pi r^2 (r^4 - r_h^4)} \left(\frac{3r_h^2 (4.g_s M^2 \log(r_h) + 4.g_s M^2 + 0.6N)^2}{N^2} - r^2 \right) \\
& \times \left[36g_s^2 M^2 N_f \log^2(r) - 3g_s M^2 \log(r) (g_s N_f (\log N - 6 + \log(16))) - 8\pi + 16\pi^2 N \right] = 0.
\end{aligned} \tag{88}$$

The EOM (88), near $r = r_h$ can be approximated as:

$$\mathcal{G}''(r) + \left(b_1 + \frac{1}{r - r_h} \right) \mathcal{G}'(r) + \mathcal{G}(r) \left(\frac{a_2}{r - r_h} + b_2 \right) = 0, \tag{89}$$

where

$$\begin{aligned}
b_1 &= \frac{g_s M^2 (g_s (0.005 \log N - 0.015) N_f + (-0.114 g_s N_f - 360.) \log(r_h) - 360.119)}{N r_h} - \frac{24.5}{r_h}, \\
a_2 &= \frac{0.02 g_s^2 m^2 M^2 (\log(r_h) (g_s (0.24 \log N - 0.775) N_f - 2279.99) - 2.88 g_s N_f \log^2(r_h) - 2273.96)}{r_h^3} - \frac{0.251 g_s m^2 N}{r_h^3}, \\
b_2 &= \frac{0.04 g_s^2 m^2 M^2 (\log(r_h) (g_s N_f (8.158 - 3.42 \log N) + 4065.38) + g_s (0.12 \log N - 0.387) N_f + 41.04 g_s N_f \log^2(r_h) + 3976.41)}{r_h^4} \\
& + \frac{7.163 g_s m^2 N}{r_h^4}.
\end{aligned} \tag{90}$$

The solution to (89) is given by:

$$\begin{aligned}
\mathcal{G}(r) &= e^{\frac{1}{2}r(-\sqrt{b_1^2 - 4b_2} - b_1)} \left[c_1 U \left(-\frac{2a_2 - b_1 - \sqrt{b_1^2 - 4b_2}}{2\sqrt{b_1^2 - 4b_2}}, 1, \sqrt{b_1^2 - 4b_2} r - \sqrt{b_1^2 - 4b_2} r_h \right) \right. \\
& \left. + c_2 L_{\frac{2a_2 - \sqrt{b_1^2 - 4b_2} - b_1}{2\sqrt{b_1^2 - 4b_2}}} \left(r \sqrt{b_1^2 - 4b_2} - r_h \sqrt{b_1^2 - 4b_2} \right) \right],
\end{aligned} \tag{91}$$

implying:

$$G'(r) = \left(\frac{\mathcal{G}(r)}{g_{22}} \right)' = \frac{1}{\Gamma \left(\frac{-2a_2 + b_1 + \sqrt{b_1^2 - 4b_2}}{2\sqrt{b_1^2 - 4b_2}} \right)} \sum_{n=-1}^{\infty} a_n(N, M, N_f, g_s, r_h) (r - r_h)^n. \tag{92}$$

Assuming $c_2 = 0$, the Neumann boundary condition at $r = r_h$ can be satisfied by setting the argument of the gamma function to a negative integer n . It runs out setting $\frac{-2a_2 + b_1 + \sqrt{b_1^2 - 4b_2}}{2\sqrt{b_1^2 - 4b_2}} = -n \in \mathbb{Z}^- \cup \{0\}$

produces a negligible ground state 0^{--} mass. Hence, we consider $\frac{-2a_2+b_1+3\sqrt{b_1^2-4b_2}}{2\sqrt{b_1^2-4b_2}} = -n \in \mathbb{Z}^- \cup \{0\}$, which gives a finite ground state mass. This condition up to LO in N yields:

$$\frac{T^2 \left(1.5 \sqrt{\frac{1.82719 \times 10^{12} T^2 - 1.66774 \times 10^9 m^2}{T^2}} - 675867. \right) + 265.153 m^2}{T \sqrt{1.82719 \times 10^{12} T^2 - 1.66774 \times 10^9 m^2}} = -n \in \mathbb{Z}^- \cup \{0\}, \quad (93)$$

the solution to which are given below:

$$\begin{aligned} m_{0^{--}} &= 32.461T \\ m_{0^{--}}^* &= 32.88T \\ m_{0^{--}}^{**} &= 32.989T \\ m_{0^{--}}^{***} &= 33.033T \\ m_{0^{--}}^{****} &= 33.055T. \end{aligned} \quad (94)$$

One can show that one obtains the same spectrum as in (94) after imposing Dirichlet boundary condition $G(r = r_h) = 0$.

5.2 $r_h = 0$ limit of (88)

$$\begin{aligned} \mathcal{G}''(r) + \frac{\mathcal{G}'(r) \left(\frac{3g_s M^2 (g_s N_f (\log N - 6 + \log(16)) - 24g_s N_f \log(r) - 8\pi)}{\pi^2 N} + 320 \right)}{64r} \\ + \frac{g_s m^2 (36g_s^2 M^2 N_f \log^2(r) - 3g_s M^2 \log(r) (g_s N_f (\log N - 6 + \log(16)) - 8\pi) + 16\pi^2 N)}{4\pi r^4} \mathcal{G}(r) = 0. \end{aligned} \quad (95)$$

The EOM (95) near $r = r_0$ - IR cut-off at $r_h = 0$, reduces to:

$$\mathcal{G}''(r) + (\alpha_1 + \beta_1(r - r_0))\mathcal{G}'(r) + (\alpha_2 + \beta_2(r - r_0))\mathcal{G}(r) = 0 \quad (96)$$

where

$$\begin{aligned} \alpha_1 &= \frac{3g_s^2 \log N M^2 N_f + 320}{64r_0}, \\ \beta_1 &= -\frac{3g_s^2 M^2 N_f}{64\pi^2 N r_0^2} - \frac{5}{r_0^2}, \\ \alpha_2 &= \frac{4\pi g_s m^2 N}{r_0^4} - \frac{3g_s^3 m^2 M^2 N_f \log(r_0)}{4\pi r_0^4}, \\ \beta_2 &= \frac{3g_s^3 \log N m^2 M^2 N_f (4 \log(r_0) - 1)}{4\pi r_0^5} - \frac{16\pi g_s m^2 N}{r_0^5}. \end{aligned} \quad (97)$$

The solution to (96) is given by:

$$\begin{aligned} \mathcal{G}(r) = e^{-\alpha_1 r + \frac{\beta_2 r}{\beta_1} - \frac{\beta_1 r^2}{2} + \beta_1 r r_0} \left[c_2 {}_1F_1 \left(\frac{\beta_1^3 - \alpha_2 \beta_1^2 + \alpha_1 \beta_2 \beta_1 - \beta_2^2}{2\beta_1^3}; \frac{1}{2}; \frac{((r - r_0)\beta_1^2 + \alpha_1 \beta_1 - 2\beta_2)^2}{2\beta_1^3} \right) \right. \\ \left. + c_1 H_{\frac{-\alpha_1 \beta_1 \beta_2 + \alpha_2 \beta_1^2 - \beta_1^3 + \beta_2^2}{\beta_1^3}} \left(\frac{\alpha_1 \beta_1 + \beta_1^2 (r - r_0) - 2\beta_2}{\sqrt{2}\beta_1^{3/2}} \right) \right]. \end{aligned} \quad (98)$$

One can then work out $G'(r = r_0) = \left(\frac{g(r)}{g_{22}} \right)' \Big|_{r=r_0}$. Now, setting $c_2 = 0$, defining \tilde{m} via: $m = \tilde{m} \frac{r_0}{L^2}$, and using the large \tilde{m} -limit of Hermite functions:

$$H_{\frac{-\alpha_1\beta_1\beta_2 + \alpha_2\beta_1^2 - (1 \text{ or } 2)\beta_1^3 + \beta_2^2}{\beta_1^3}} \left(\frac{\alpha_1\beta_1 - 2\beta_2}{\sqrt{2}\beta_1^{3/2}} \right) \longrightarrow H_{-\frac{16\tilde{m}^4}{125}} \left(\frac{2^{\frac{5}{2}}}{5^{\frac{3}{2}}} \tilde{m}^2 \right), \quad (99)$$

and

$$H_n(x) \xrightarrow{n \gg 1} \frac{2^{\frac{n}{2} + \frac{1}{2}} e^{\frac{x^2}{2}} \left(\frac{n}{e} \right)^{n/2} \cos \left(\frac{\pi n}{2} - x \sqrt{2n - \frac{x^2}{3} + 1} \right)}{\sqrt[4]{1 - \frac{x^2}{2n}}}, \quad (100)$$

one can show that the Neumann(/Dirichlet: $G(r = r_0) = 0$) boundary condition at $r = r_0$ is equivalent to the condition:

$$\frac{8}{375} \left(\sqrt{6\tilde{m}^2} \sqrt{375 - 64\tilde{m}^4} - 6i\pi\tilde{m}^4 \right) = i\pi(2n + 1), \quad (101)$$

yielding:

$$m_n^{0--}(r_h = 0) = \frac{1}{2} 5^{3/4} \sqrt[4]{\frac{-2 \left(\sqrt{6} \sqrt{\pi^2 (16n^2 + 22n + 7) + 6} + 6 \right) - 3\pi^2(2n + 1)}{3\pi^2 - 32}} \frac{r_0}{L^2}. \quad (102)$$

5.3 0^{--} Glueball Spectrum from WKB Method for $r_h \neq 0$

Using the variables of [34], the potential in the IR is given as:

$$V(IR, T) = (6 - 0.01\tilde{m}^2) e^z + (0.15\tilde{m}^2 - 16.1875) e^{2z} + \mathcal{O}(e^{3z}), \quad (103)$$

where in the ‘large’ \tilde{m} -limit, $V(IR, T) > 0$ for (i) $z : e^z > \frac{2.31799 \times 10^{31} - 3.86332 \times 10^{28} \tilde{m}^2}{6.25374 \times 10^{31} - 5.79497 \times 10^{29} \tilde{m}^2} = 0.067 + \mathcal{O}\left(\frac{1}{\tilde{m}^2}\right)$ if $\tilde{m} > 24.495$ and (ii) $0 < e^z < \frac{2.31799 \times 10^{31} - 3.86332 \times 10^{28} \tilde{m}^2}{6.25374 \times 10^{31} - 5.79497 \times 10^{29} \tilde{m}^2} = 0.067 + \mathcal{O}\left(\frac{1}{\tilde{m}^2}\right)$ if $10.388 < \tilde{m} < 24.495$. One can show that: $\int_{\log(0.067)}^{-2.526} \sqrt{V(IR, T)} = \int_{-\infty}^{\log(0.067)} \sqrt{V(IR, T)} \approx 0$, implying there is no contribution to the WKB quantization condition in the IR.

Now, consider:

$$V(UV, T) = (-1.02\tilde{m}^2 - 22.5) e^{-2z} + (0.25\tilde{m}^2 + 8.25) e^{-z} - 1 + \mathcal{O}(e^{-3z}). \quad (104)$$

For $\tilde{m} > 4.29$ the turning points of $V(UV, T)$ are $0.125\tilde{m}^2 - 0.025\sqrt{25\tilde{m}^4 + 18\tilde{m}^2 - 8775} + 4.125 = 4.08 + \mathcal{O}\left(\frac{1}{\tilde{m}^2}\right) < e^z < 0.125\tilde{m}^2 + 0.025\sqrt{25\tilde{m}^4 + 18\tilde{m}^2 - 8775} + 4.125 = 0.25\tilde{m}^2 + 4.17 + \mathcal{O}\left(\frac{1}{\tilde{m}^2}\right)$. Hence,

$$\begin{aligned} \int_{\log(4.08)}^{\log(0.25\tilde{m}^2 + 4.17)} \sqrt{V(UV, T)} &= \int_{\log(4.08)}^{\log(0.25\tilde{m}^2 + 4.17)} e^{-z} \sqrt{0.25e^z - 1.02} + \mathcal{O}\left(\frac{1}{\tilde{m}}\right) \\ &= 0.389\tilde{m} - 2 + \mathcal{O}\left(\frac{1}{\tilde{m}}\right) = \left(n + \frac{1}{2}\right) \pi. \end{aligned} \quad (105)$$

Hence one obtains isospectrality with 0^{++} ; for large n , there is also isospectrality with 2^{++} .

5.4 WKB Method at $r_h = 0$

In this section we will discuss obtaining the spectrum at $r_h = 0$ using WKB quantization condition at LO in N in **5.3.1** and up to NLO in N in **5.3.2**.

5.4.1 LO in N

In the IR, the WKB ‘potential’ can be shown to be given by:

$$V(IR, r_h = 0) = -\frac{1}{4} + \frac{1}{4}(-3 + \tilde{m}^2) e^{2z} + \mathcal{O}(e^{3z}), \quad (106)$$

with turning points: $(\log\left(\frac{1}{m_0} + \mathcal{O}\left(\frac{1}{m_0^3}\right)\right) \approx -\log(m_0), \log(\delta^2 - 1))$. Further dropping $\mathcal{O}\left(\frac{1}{m_0^3}\right)$ terms, $\int_{-\log m_0}^{-2.526} \sqrt{V(IR, r_h = 0)} = \frac{(\delta^2 - 1)}{2} \tilde{m} - 0.785 = (n + \frac{1}{2}) \pi$ yielding:

$$m_n^{0--}(IR, r_h = 0) = \frac{(3 + 4n)\pi r_0}{2(\delta^2 - 1)L^2} = \left(\frac{4.71 + 6.28n}{\delta^2 - 1}\right) \frac{r_0}{L^2}. \quad (107)$$

In the UV,

$$V(UV, r_h = 0) = -\frac{3}{4}(\tilde{m}^2 + 3) e^{-2z} + \frac{1}{4}(\tilde{m}^2 + 6) e^{-z} - 1, \quad (108)$$

with turning points: $(\log(3 + \mathcal{O}(\frac{1}{\tilde{m}^2})), \log(\frac{\tilde{m}^2}{4} - \frac{3}{2} + \mathcal{O}(\frac{1}{\tilde{m}^2})))$, and $\sqrt{V(UV, r_h = 0)} = \frac{e^{-z}}{2} \sqrt{e^z - 3\tilde{m}} + \mathcal{O}(\frac{1}{\tilde{m}})$:

$$\int_{\log 3}^{\log(\frac{\tilde{m}^2}{4} - \frac{3}{2})} \frac{e^{-z}}{2} \sqrt{e^z - 3\tilde{m}} = \left(n + \frac{1}{2}\right) \pi, \quad (109)$$

implying:

$$m_n^{0--}(UV, r_h = 0) = (7.87 + 6.93n) \frac{r_0}{L^2}. \quad (110)$$

5.4.2 NLO (in N)/Non-Conformal Corrections

Up to NLO in N , in the IR, the potential ‘ $V(IR, r_h = 0)$ ’ is given by:

$$V(IR, r_h = 0) = \frac{1}{256\pi^2 N} \left\{ e^{2z} \left(-g_s^2 M^2 N_f (6\log N - 72 + \log(16777216)) + 36g_s^2 M^2 \tilde{m}^2 N_f \log^2(y_0) + g_s M^2 \log(y_0) \right. \right. \\ \left. \left. \times (g_s N_f (72 - \tilde{m}^2 (6\log N - 36 + \log(16777216))) + 48\pi \tilde{m}^2) + 48\pi g_s M^2 + 64\pi^2 (\tilde{m}^2 - 3) N \right) \right\} - \frac{1}{4} + \mathcal{O}(e^{-3z}). \quad (111)$$

The turning points of (111) up NLO in N are given by:

$\left[\log\left(\frac{1}{\tilde{m}} \left[1 - \frac{g_s M^2 \log(y_0) (-g_s N_f (6\log N - 36 + \log(16777216)) + 36g_s N_f \log(y_0) + 48\pi)}{128\pi^2 N} \right] \right), \log(\delta^2 - 1) \right]$. After evaluation of the integral of $\sqrt{V(IR, r_h = 0)}$ between the aforementioned turning points, in the large- \tilde{m} -limit, one obtains the following quantization condition:

$$\left(\frac{(\delta^2 - 1)}{2} - \frac{3(\delta^2 - 1)g_s M^2 (g_s N_f) \log N \log r_0}{64\pi^2 N} \right) \tilde{m} - \frac{\pi}{4} = \left(n + \frac{1}{2} \right) \pi, \quad (112)$$

which yields:

$$m_n^{0--}(r_h = 0) = \frac{6.28319n + 4.71239}{\delta^2 - 1} \left(1 + \frac{0.01g_s^2 \log NM^2 N_f \log(r_0)}{N} \right). \quad (113)$$

6 Glueball Masses from M theory

The glueball spectrum for spin $0^{++}, 1^{++}$ and 2^{++} is calculated in this section from the M-theory perspective both by considering $r_h \neq 0$ and an IR radial cut-off (for $r_h = 0$) in the background. The 11 dimensional M-theory action is given as:

$$S_M = \frac{1}{16\pi} \int_M d^{11}x \sqrt{G} R - \frac{1}{4} \sqrt{G} \int_M d^{11}x G_4 \wedge *_{11} G_4, \quad (114)$$

where $G_4 = dC_3 + A_1 \wedge dB_2 + dx_{10} \wedge dB_2$, and $C_{\mu\nu 10}^M = B_{\mu\nu}^{IIA}, C_{\mu\nu\rho}^M = C_{\mu\nu\rho}^{IIA}$. Now, as shown in [2], no F_4^{IIA} (to be obtained via a triple T-dual of type IIB $F_{1,3,5}$ where $F_1 \sim F_{x/y/z}, F_3 \sim F_{xyr/\theta_1/\theta_2}, F_{x zr/\theta_1/\theta_2}, F_{y zr/\theta_1/\theta_2}$ and $F_5 \sim F_{xyz\beta_1\beta_2}$ where $\beta_i = r/\theta_i$) can be generated.⁵ Thus, the four-form flux $G_4 = d(C_{\mu\nu 10} dx^\mu \wedge dx^\nu \wedge dx_{10}) + (A_1^{F_1} + A_1^{F_3} + A_1^{F_5}) \wedge H_3 = H_3 \wedge dx_{10} + A \wedge H_3$, where $C_{\mu\nu 10} \equiv B_{\mu\nu}$.

$$\int G_4 \wedge *_{11} G_4 = \int (H_3 \wedge dx_{10} + A \wedge H_3) \wedge *_{11} (H_3 \wedge dx_{10} + A \wedge H_3). \quad (115)$$

Now, $H_3 \wedge dx_{10} \wedge *_{11} (H_3 \wedge A) = 0$ as neither H_3 nor A has support along x_{10} . Hence,

$$\begin{aligned} & H_3 \wedge dx_{10} \wedge *_{11} (H_3 \wedge dx_{10}) \\ &= \sqrt{G} H_{\mu\nu\rho 10} G^{\mu\mu_1} G^{\nu\nu_1} G^{\rho\rho_1} G^{10\lambda_1} H_{\mu_1\nu_1\rho_1\lambda_1} dt \wedge \dots dx_{10} \\ &= \sqrt{G} H_{\mu\nu\rho 10} \left(-G^{\mu 10} G^{\nu\nu_1} G^{\rho\rho_1} G^{10\lambda_1} H_{\nu_1\rho_1\lambda_1} + G^{\mu\mu_1} G^{\nu 10} G^{\rho\rho_1} G^{10\lambda_1} H_{\mu_1\rho_1\lambda_1} \right. \\ &\quad \left. - G^{\mu\mu_1} G^{\nu\nu_1} G^{\rho 10} G^{10\lambda_1} H_{\mu_1\nu_1\lambda_1} + G^{\mu\mu_1} G^{\nu\nu_1} G^{\rho\rho_1} G^{10 10} H_{\mu_1\nu_1\rho_1} \right) dt \wedge \dots dx_{10}, \end{aligned} \quad (116)$$

where $H_{\mu\nu\rho 10} = H_{\mu\nu\rho}$, and

$$(H \wedge A) \wedge *_{11} (H \wedge A) = \sqrt{G} H_{[\mu\nu\rho} A_{\lambda]} G^{\mu\mu_1} G^{\nu\nu_1} G^{\lambda\lambda_1} H_{[\mu_1\nu_1\rho_1} A_{\lambda_1]}, \quad (117)$$

with $H_{[\mu_1\mu_2\mu_3} A_{\mu_4]} \equiv H_{\mu_1\mu_2\mu_3} A_{\mu_4} - (H_{\mu_2\mu_3\mu_4} A_{\mu_1} - H_{\mu_3\mu_4\mu_1} A_{\mu_2} + H_{\mu_4\mu_1\mu_2} A_{\mu_3})$.

It was shown in [2] that in the MQGP limit (11), in equation (116), contribution of $H_3 \wedge dx^{11} \wedge *_{11} (H_3 \wedge dx^{11})$ is always dominated by $\sqrt{G} H_{\mu\nu\omega} G^{\mu\sigma} G^{\nu\psi} G^{\omega\alpha} G^{10 10} H_{\sigma\psi\alpha}$ term and in equation (117), contribution of $(H \wedge A) \wedge *_{11} (H \wedge A)$ is dominated by $\sqrt{G} H_{\theta_1\theta_2 y} A_\psi G^{\theta_1\alpha} G^{\theta_2\rho} G^{y\sigma} G^{\psi\beta} H_{\alpha\rho\beta}$ term. Therefore, for simplicity in calculations, we assume that leading contribution in equations (116) and (117) are governed by aforementioned terms.

⁵Consider T_x followed by T_y followed by T_z where T_i means T-dualizing along i-th direction. As an example, $T_x F_x^{IIB} \rightarrow$ non-dynamical 0-form field strength^{IIA}[72], $T_y T_x F_x^{IIB} \rightarrow F_y^{IIB}$, $T_z F_y^{IIB} \rightarrow F_{yz}^{IIA}$ implying one can never generate F_4^{IIA} from F_1^{IIB} . As also an example consider $T_x F_{xy\beta_i}^{IIB} \rightarrow F_{y\beta_i}^{IIA}, T_y F_{y\beta_i}^{IIA} \rightarrow F_{\beta_i}^{IIB}, T_z F_{\beta_i}^{IIB} \rightarrow F_{\beta_i z}^{IIA}$ again not generating F_4^{IIA} ; $T_x F_{xyz\beta_1\beta_2}^{IIB} \rightarrow F_{yz\beta_1\beta_2}^{IIA}, T_y F_{yz\beta_1\beta_2}^{IIA} \rightarrow F_{z\beta_1\beta_2}^{IIB}, T_z F_{z\beta_1\beta_2}^{IIB} \rightarrow F_{\beta_1\beta_2}^{IIB}$; thus one can not generate F_4^{IIA} .

The relevant inverse components of the 11-dimensional metric, in the MQGP limit (11), as worked out in [2] using which the most dominant contribution near $\theta_{1,2} = 0$ in the equations (116) and (117), as shown in [2], are given by the following analytical expressions:

$$H_3 \wedge dx^{11} \wedge *_{11} (H_3 \wedge dx^{11}) \Big|_{\theta_1 \sim \frac{\alpha_{\theta_1}}{N^{\frac{1}{5}}}, \theta_2 \sim \frac{\alpha_{\theta_2}}{N^{\frac{3}{10}}}} = \frac{\sqrt{3} (-4\alpha_{\theta_2}^2 + 27\alpha_{\theta_1}^6) r^3 N^{\frac{9}{10}}}{2\alpha_{\theta_1}^3 \alpha_{\theta_2}^6 g_s^{\frac{11}{4}} \pi^{\frac{3}{4}}} + \frac{\alpha_{\theta_1} (82r^4 - r_h^4) N^{\frac{1}{4}}}{2\sqrt{3} \alpha_{\theta_2}^4 g_s^{\frac{11}{4}} \pi^{\frac{3}{4}} r} \quad (118)$$

and

$$(H \wedge A) \wedge *_{11} (H \wedge A) \Big|_{\theta_1 \sim \frac{\alpha_{\theta_1}}{N^{\frac{1}{5}}}, \theta_2 \sim \frac{\alpha_{\theta_2}}{N^{\frac{3}{10}}}} = \mathcal{F}(\alpha_{\theta_1}, \alpha_{\theta_2}; a; g_s, M, N_f) N^{\frac{17}{20}}, \quad (119)$$

where $\mathcal{F}(\alpha_{\theta_1}, \alpha_{\theta_2}; a; g_s, M, N_f)$ is a well-defined function of the parameters indicated. One hence notes that $\lim_{r_\Lambda \rightarrow \infty} \int_0^{r_h} \frac{\sqrt{4\pi g_s N}}{r_h} \int_{r_h}^{r_\Lambda} (H \wedge A) \wedge *_{11} (H \wedge A) \sim \frac{r_\Lambda}{r_h} N^{\frac{27}{20}}$, and is UV-divergent. Also, this yields a large cosmological constant in the IR because: $\frac{G_4 \wedge *G_4}{\sqrt{G}} \supseteq \frac{|H \wedge A|^2}{\sqrt{G}} \sim \frac{N^{\frac{17}{20}}}{r^3 N^{\frac{17}{20}}} = \frac{1}{r^3}$. To take care of both these issues, from the discussion on holographic renormalizability of the $D = 11$ supergravity action in [2], one sees that this term can be cancelled by a boundary counter term: $\int_{r=r_\Lambda} \sqrt{G} |G_4|^2$.

Now, using:

$$\sqrt{G} \Big|_{\theta_1 \sim \frac{\alpha_{\theta_1}}{N^{\frac{1}{5}}}, \theta_2 \sim \frac{\alpha_{\theta_2}}{N^{\frac{3}{10}}}} = \frac{2N^{17/20} r^3}{27 \cdot 3^{5/6} \sqrt[4]{\pi} \alpha_{\theta_1}^4 \alpha_{\theta_2} g_s^{35/12}}, \quad (120)$$

and (118), one sees that one obtains a large- N suppressed cosmological constant from the second term in $\frac{|H \wedge dx^{10}|^2}{\sqrt{G}}$ that remains small $\forall r > r_h$. To ensure one does not generate an N -enhanced cosmological

constant from the first term in (118), one imposes the condition: $-4\alpha_{\theta_2}^2 + 27\alpha_{\theta_1}^6 = 0$, i.e., $\alpha_{\theta_2} = \frac{3^{\frac{3}{4}} \alpha_{\theta_1}^{\frac{3}{2}}}{\sqrt{2}}$.

One hence obtains the following flux-generated cosmological constant (with a slight abuse of notation):

$$\frac{G_4 \wedge *G_4}{\sqrt{G}} \Big|_{\theta_1 \sim \frac{1}{N^{\frac{1}{5}}}, \theta_2 \sim \frac{1}{N^{\frac{3}{10}}}} = \frac{3^{\frac{13}{12}} \sqrt{\alpha_{\theta_1}} g_s^{\frac{1}{6}} (82r^4 - r_h^4)}{N^{\frac{3}{5}} \sqrt{2\pi} r^4}. \quad (121)$$

Metric Fluctuations: The background metric $g_{\mu\nu}^{(0)}$ is linearly perturbed as $g_{\mu\nu} = g_{\mu\nu}^{(0)} + h_{\mu\nu}$. With this perturbation the equation of motion follows from the action (114) as:

$$R_{\mu\nu}^{(1)} = \frac{-1}{12} \frac{G_4^2}{\sqrt{G}} h_{\mu\nu}, \quad (122)$$

Now we assume the perturbation to have the following form: $h_{\mu\nu} = \epsilon_{\mu\nu}(r) e^{ikx_1}$. Clearly there is a $SO(2)$ rotational symmetry in the $x_2 - x_3$ plane which allow us to classify different perturbations into three categories, namely tensor, vector and scalar type of metric perturbations.

The mass spectrum was obtained by (i) solving equation (122) and applying Neumann/Dirichlet boundary condition near r_h/r_0 , (ii) following the redefinition of variables in [34] and then considering the WKB quantization condition.

6.1 0^{++} Glueball spectrum

The 0^{++} glueball in M-theory corresponds to scalar metric perturbations [73]:

$$\begin{aligned} h_{tt} &= g_{tt} e^{iqx_1} q_1(r), \\ h_{x_1 r} &= h_{rx_1} = iq g_{x_1 x_1} e^{iqx_1} q_3(r), \\ h_{rr} &= g_{rr} e^{iqx_1} q_2(r), \end{aligned} \quad (123)$$

where g_{tt} , $g_{x_i x_i}$ and g_{rr} are the metric components of the M-theory and is given in equation (21).

6.1.1 M-theory background with $r_h \neq 0$

Considering these components at leading order in N , and taking into account the above perturbation, we get the following differential equation for $q_3(r)$ with $q^2 = -m^2$ from (122):

$$\begin{aligned} q_3''(r) + \frac{q_3'(r)}{12\pi g_s N r^3 (r^4 - r_h^4)} &\left\{ \left[r^2 \left(16\pi^2 g_s^2 m^2 N^2 r^2 + 12\pi g_s N (9r^4 - r_h^4) - 3r (r^4 - r_h^4)^2 \right) \right. \right. \\ &\left. \left. - 3a^2 \left(16\pi^2 g_s^2 m^2 N^2 r^2 + 36\pi g_s N (r^4 - r_h^4) + 3r (r^4 - r_h^4)^2 \right) \right] \right\} \\ + \frac{q_3(r)}{12\pi g_s N r^4 (r^4 - r_h^4)} &\left\{ \left[r^2 \left(32\pi^2 g_s^2 m^2 N^2 r^2 + 12\pi g_s N (15r^4 + r_h^4) - 3r (5r^8 - 6r^4 r_h^4 + r_h^8) \right) \right. \right. \\ &\left. \left. - 36a^2 \left(4\pi^2 g_s^2 m^2 N^2 r^2 + \pi g_s N (11r^4 + r_h^4) + r^9 - r^5 r_h^4 \right) \right] \right\} = 0. \end{aligned} \quad (124)$$

(a) Spectrum from Neumann/Dirichlet Boundary Condition: Equation (124), for $a = 0.6r_h$ near $r = r_h$ (writing $m = \tilde{m} \frac{r_h}{L^2}$) simplifies to:

$$q_3''(r) + \frac{(2 - 0.00666667\tilde{m}^2) q_3'(r)}{r - r_h} + \frac{(0.76 - 0.103333\tilde{m}^2) q_3(r)}{r_h(r - r_h)} = 0. \quad (125)$$

Lets write the above equation of the following form,

$$h''(r) + \frac{p}{r - r_h} h'(r) + \frac{s}{r - r_h} h(r) = 0, \quad (126)$$

where we have, $p = (2 - 0.00666667\tilde{m}^2)$, $s = \frac{(0.76 - 0.103333\tilde{m}^2)}{r_h}$.

The solution to (126) is given by:

$$\begin{aligned} h(r) &= c_1 (2r - 2r_h)^{p/2} (r - r_h)^{-p/2} (-s(r - r_h))^{\frac{1}{2} - \frac{p}{2}} I_{p-1} \left(2\sqrt{-s(r - r_h)} \right) \\ &+ (-1)^{1-p} c_2 (2r - 2r_h)^{p/2} (r - r_h)^{-p/2} (-s(r - r_h))^{\frac{1}{2} - \frac{p}{2}} K_{p-1} \left(2\sqrt{-s(r - r_h)} \right). \end{aligned} \quad (127)$$

Setting $c_2 = 0$, one can verify that one satisfy the Neumann boundary condition: $h'(r = r_h) = 0$ provided:

$$p = -n \in \mathbb{Z}^- \cup \{0\}, \quad (128)$$

implying:

$$\tilde{m} = 12.25\sqrt{2+n}. \quad (129)$$

One can similarly show that by imposing Dirichlet boundary condition: $h(r = r_h) = 0$:

$$\tilde{m} = 12.25\sqrt{1+n}. \quad (130)$$

(b) Spectrum using WKB method: Following the redefinition of ([34]), equation (124) can be rewritten as a Schrodinger like form, where for $a = 0.6r_h$ and setting $g_s = 0.9$, $N \sim (g_s)^{-39} \sim 100$ - in the MQGP limit of [2] - the ‘potential’ in the IR can be shown to be given by:

$$V_{IR}(z) = e^z \left(-0.00576389\tilde{m}^4 - 0.0708333\tilde{m}^2 + 0. \right) + 0.00201389\tilde{m}^4 + 0.00333333\tilde{m}^2 - 0.25 + \mathcal{O}(e^{2z}) \quad (131)$$

The potential (131) is positive for $z \in (-\infty, \log(0.349)]$, but to remain within the IR, one truncates this domain to $z \in (-\infty, -2.526]$ and the same yields:

$$\int_{-\infty}^{-2.626} \sqrt{V_{IR}(z)} = 0.0898\tilde{m}^2 \log(\tilde{m}) - 0.0439\tilde{m}^2 = \pi \left(n + \frac{1}{2} \right) = \left(n + \frac{1}{2} \right) \pi, \quad (132)$$

or

$$m_n^{0^{++}} = \frac{\sqrt{70.0055n + 35.0027}}{\sqrt{\mathcal{P}\mathcal{L}(26.3065n + 13.1533)}}. \quad (133)$$

In the UV, one can show that:

$$V_{UV}(z) = \frac{-0.00694444\tilde{m}^4 + 0.295\tilde{m}^2 + 1.62}{e^{2z}} + \frac{-0.0833333\tilde{m}^2 - 0.54}{e^z} - 0.25 < 0, \quad (134)$$

implying no turning points in the UV.

6.1.2 M-theory background with IR Cut-Off r_0

In this case, equation (124) is modified only by the limit $(r_h, a) \rightarrow 0$. The equation in this limit is given as,

$$q_3''(r) + q_3'(r) \left(\frac{4\pi g_s m^2 N}{3r^3} - \frac{r^4}{4\pi g_s N} + \frac{9}{r} \right) + q_3(r) \left(\frac{8\pi g_s m^2 N}{3r^4} - \frac{5r^3}{4\pi g_s N} + \frac{15}{r^2} \right) = 0. \quad (135)$$

(a) Spectrum from Neumann/Dirichlet Boundary Condition: Near the cut-off at $r = r_0$, equation (135) is given by:

$$q_3''(r) + \left(\frac{4\tilde{m}^2 + 108}{12r_0} - \frac{(\tilde{m}^2 + 9)(r - r_0)}{r_0^2} \right) q_3'(r) + q_3(r) \left(\frac{8\tilde{m}^2 + 180}{12r_0^2} - \frac{(32\tilde{m}^2 + 360)(r - r_0)}{12r_0^3} \right) = 0, \quad (136)$$

whose solution is given by:

$$q_3(r) = e^{-\frac{2(4\tilde{m}^2+45)r}{3(\tilde{m}^2+9)r_0}} \left[c_1 H_{-\frac{2\tilde{m}^6+71\tilde{m}^4+828\tilde{m}^2+2835}{9(\tilde{m}^2+9)^3}} \left(\frac{3(\tilde{m}^2+9)^2 r - 2(2\tilde{m}^4+37\tilde{m}^2+153)r_0}{3\sqrt{2}(\tilde{m}^2+9)^{3/2} r_0} \right) \right. \\ \left. + c_2 {}_1F_1 \left(\frac{2\tilde{m}^6+71\tilde{m}^4+828\tilde{m}^2+2835}{18(\tilde{m}^2+9)^3}; \frac{1}{2}; \frac{\left(3(\tilde{m}^2+9)^2 r - 2(2\tilde{m}^4+37\tilde{m}^2+153)r_0 \right)^2}{18(\tilde{m}^2+9)^3 r_0^2} \right) \right]. \quad (137)$$

Thus:

$$\begin{aligned}
q_3'(r = r_0) = & \frac{1}{27r_0^2} \left\{ e^{-\frac{2(4\tilde{m}^2+45)}{3(\tilde{m}^2+9)}} \left([2\tilde{m}^6 + 71\tilde{m}^4 + 828\tilde{m}^2 + 2835] \right. \right. \\
& \times \left[-\frac{3\sqrt{2}c_1r_0H_{-\frac{11\tilde{m}^6+314\tilde{m}^4+3015\tilde{m}^2+9396}{9(\tilde{m}^2+9)^3}} \left(-\frac{\tilde{m}^4+20\tilde{m}^2+63}{3\sqrt{2}(\tilde{m}^2+9)^{3/2}} \right)}{(\tilde{m}^2+9)^{5/2}} \right. \\
& \left. \left. - \frac{c_2(\tilde{m}^4+20\tilde{m}^2+63)r_0 {}_1F_1 \left(\frac{2\tilde{m}^6+71\tilde{m}^4+828\tilde{m}^2+2835}{18(\tilde{m}^2+9)^3} + 1; \frac{3}{2}; \frac{(\tilde{m}^4+20\tilde{m}^2+63)^2}{18(\tilde{m}^2+9)^3} \right)}{(\tilde{m}^2+9)^4} \right] \right. \\
& \left. - \frac{1}{\tilde{m}^2+9} \left\{ 18(4\tilde{m}^2+45)r_0 \left(c_1H_{-\frac{2\tilde{m}^6+71\tilde{m}^4+828\tilde{m}^2+2835}{9(\tilde{m}^2+9)^3}} \left(-\frac{\tilde{m}^4+20\tilde{m}^2+63}{3\sqrt{2}(\tilde{m}^2+9)^{3/2}} \right) \right. \right. \right. \\
& \left. \left. \left. + c_2 {}_1F_1 \left(\frac{2\tilde{m}^6+71\tilde{m}^4+828\tilde{m}^2+2835}{18(\tilde{m}^2+9)^3}; \frac{1}{2}; \frac{(\tilde{m}^4+20\tilde{m}^2+63)^2}{18(\tilde{m}^2+9)^3} \right) \right) \right\} \right\}. \tag{138}
\end{aligned}$$

Numerically/graphically we see that for $c_1 = -0.509c_2$, one gets $q_3(r = r_0, \tilde{m} \approx 4.1) = 0$. We hence estimate the ground state of 0^{++} from metric fluctuations in M-theory to be $4.1 \frac{r_0}{L^2}$.

(b) Spectrum using WKB method: Defining $m = \tilde{m} \frac{\sqrt{y_0}}{L^2}$ and following [34], the potential term in the Schrödinger-like equation from (135) is given as,

$$\begin{aligned}
V(z) = & \frac{1}{2304\pi^2 g_s^2 N^2 (e^z + 1)^4} \left\{ -16\pi^2 g_s^2 N^2 (12(\tilde{m}^2 + 12)e^{3z} + (\tilde{m}^4 + 12\tilde{m}^2 + 216)e^{2z} + 144e^z + 36e^{4z} + 36) \right. \\
& \left. + 24\pi g_s N y_0^{5/2} e^{2z} (e^z + 1)^{7/2} (\tilde{m}^2 + 9e^z + 9) - 9y_0^5 e^{2z} (e^z + 1)^7 \right\}. \tag{139}
\end{aligned}$$

We hence see that in the large- N limit, $V(z) < 0$ and hence has no turning points. The WKB method a la [34] does not work in this case.

6.2 2^{++} Glueball spectrum

To study the spectrum of spin 2^{++} glueball, we consider the tensor type of metric perturbations where the non-zero perturbations are given as:

$$\begin{aligned}
h_{x_2 x_3} = h_{x_3 x_2} = g_{x_1 x_1} H(r) e^{ikx_1} \\
h_{x_2 x_2} = h_{x_3 x_3} = g_{x_1 x_1} H(r) e^{ikx_1}, \tag{140}
\end{aligned}$$

where $g_{x_1 x_1}$ is as given in (21).

6.2.1 M-theory background with $r_h \neq 0$

Considering the tensor modes of metric perturbations and the M-theory metric components corrected upto NLO in N , as given in (21), we obtain a second order differential equation in $H(r)$ from (122),

$$\begin{aligned}
& H''(r) + H'(r) \left(-\frac{3a^2}{r^3} + \frac{15g_s M^2 (g_s N_f \log(N) - 24g_s N_f \log(r) - 6g_s N_f + g_s N_f \log(16) - 8\pi)}{64\pi^2 N r} \right. \\
& \left. + \frac{5r^4 - r_h^4}{r^5 - r r_h^4} \right) + \left(\frac{1}{4\pi r^4 (r^4 - r h^4)} \left[8\pi \left\{ 3a^2 (-2\pi g_s N m^2 r^2 - r^4 + r_h^4) + 2\pi g_s N m^2 r^4 + 4r^6 \right\} \right. \right. \\
& \left. \left. - 3g_s^2 M^2 m^2 r^2 (r^2 - 3a^2) \log(r) \left\{ g_s N_f \log(N) + g_s N_f (\log(16) - 6) - 8\pi \right\} \right. \right. \\
& \left. \left. + 36g_s^3 M^2 N_f m^2 r^2 (r^2 - 3a^2) \log^2(r) \right] \right) H(r) = 0, \tag{141}
\end{aligned}$$

where we assume $k^2 = -m^2$ with m being the mass of the corresponding glueball.

(a) Spectrum from Neumann/Dirichlet Boundary Condition: Near $r = r_h$, the solution to the above equation will be given on the same lines as **5.1** for 0^{--} glueballs, and the analog of (93) is:

$$\frac{T^2 \left(\frac{1.5\sqrt{0.0536698T^2 - 0.00186263m^2}}{T} - 0.115834 \right) + 0.00018196m^2}{T\sqrt{0.0536698T^2 - 0.00186263m^2}} = -n, \tag{142}$$

the solutions to which are given as:

$$\begin{aligned}
m_{2^{++}} &= 5.086T \\
m_{2^{++}}^* &= 5.269T \\
m_{2^{++}}^{**} &= 5.318T \\
m_{2^{++}}^{***} &= 5.338T \\
m_{2^{++}}^{****} &= 5.348T
\end{aligned} \tag{143}$$

One can impose Dirichlet boundary condition: $H(r = r_h) = 0$, and show that,

$$m_n^{2^{++} \text{ (Neumann)}} = m_{n+1}^{2^{++} \text{ (Dirichlet)}}, \text{ for } n = 0, 1, 2, \dots$$

(b) Spectrum from WKB method: Using the variables of [34], The potential term in the schrodinger like equation for 2^{++} glueball can be obtained from (141) and in the IR region written in terms of $m = \tilde{m} \frac{r_h}{L^2} = \tilde{m} \frac{\sqrt{y_h}}{L^2}$, can be shown to given by:

$$V_{IR}(z) = e^z (0.52 - 0.01\tilde{m}^2) + (0.15\tilde{m}^2 - 1.0275) e^{2z} + \mathcal{O} \left(\frac{g_s M^2}{N}, e^{3z} \right). \tag{144}$$

Now, negative z implies being closer to the IR and the boundary would correspond to $r \leq \sqrt{3}a = 0.6\sqrt{3}r_h$ corresponding to $z = -2.53$. It can be shown that for $\tilde{m} > 7.211$ $V(z \in [-2.71, -2.53]) > 0$. Now $\int_{z=-2.71}^{z=-2.53} \sqrt{V_{IR}(z)} \approx 0$. Hence, the IR does not contribute to the 2^{++} glueball spectrum.

In the UV we must consider the limit ($z \rightarrow \infty$). Moreover, in the UV $N_f = M = 0$.

$$V_{UV}(z) = e^{-2z} (6.56 - 1.02\tilde{m}^2) + (0.25\tilde{m}^2 - 2.77) e^{-z} + 1. + \mathcal{O}\left(\frac{1}{\tilde{m}}, e^{-3z}\right), \quad (145)$$

whose turning points are: $\{\log(4.08 + \mathcal{O}(\frac{1}{\tilde{m}^2})), \infty\}$, giving the WKB quantization as:

$$\int_{\log 4.08}^{\infty} \sqrt{V_{UV}(z)} = 0.39\tilde{m} = \left(n + \frac{1}{2}\right) \pi, \quad (146)$$

implying:

$$m_n^{2^{++}}(T) = 8.08 \left(n + \frac{1}{2}\right) \frac{r_h}{L^2}. \quad (147)$$

6.2.2 M-theory background with an IR Cut-Off r_0

Considering the limit ($r_h, a \rightarrow 0$) equation (141) is given by,

$$\begin{aligned} H''(r) + & \left(\frac{5(3M^2g_s(-24N_f g_s \log(r) - 6N_f g_s + N_f g_s \log(N) + \log(16)N_f g_s - 8\pi) + 64\pi^2 N)}{64\pi^2 N r} \right) H'(r) \\ & + \frac{1}{4\pi r^4} \left(36m^2 M^2 N_f g_s^3 \log^2(r) - 3m^2 M^2 g_s^2 \log(r) (N_f g_s \log(N) + (\log(16) - 6)N_f g_s - 8\pi) \right. \\ & \left. + 16\pi (\pi m^2 N g_s + 2r^2) \right) H(r) = 0 \end{aligned} \quad (148)$$

(a) Neumann/Dirichlet Boundary Condition at $r = r_0$: Up to LO in N near $r = r_0$, the above equation is given by:

$$H''(r) + \left(\frac{5}{r_0} - \frac{5(r-r_0)}{r_0^2} \right) H'(r) + H(r) \left(\frac{\tilde{m}^2 + 8}{r_0^2} - \frac{4(\tilde{m}^2 + 4)(r-r_0)}{r_0^3} \right) = 0. \quad (149)$$

The solution of (149) is given by:

$$\begin{aligned} H(r) = & e^{-\frac{4(\tilde{m}^2+4)r}{5r_0}} \left(c_1 H_{\frac{1}{125}(16\tilde{m}^4+53\tilde{m}^2+56)} \left(\frac{2(4\tilde{m}^2-9)r_0+25r}{5\sqrt{10}r_0} \right) \right. \\ & \left. + c_2 {}_1F_1 \left(\frac{1}{250} (-16\tilde{m}^4 - 53\tilde{m}^2 - 56); \frac{1}{2}; \frac{(25r+2(4\tilde{m}^2-9)r_0)^2}{250r_0^2} \right) \right). \end{aligned} \quad (150)$$

The Neumann boundary condition $H'(r = r_0) = 0$, numerically yields that for $c_1 = -0.509c_2$, the lightest 2^{++} glueball has a mass $1.137 \frac{r_0}{L^2}$. Similarly, by imposing Dirichlet boundary condition: $H(r = r_h) = 0$, for $c_1 = -0.509c_2$, the lightest 2^{++} glueball has a mass $0.665 \frac{r_0}{L^2}$.

(b) Spectrum using WKB method: Following [34], the ‘potential’ term, in the IR region, up to leading order in N with $m = \tilde{m} \frac{r_0}{L^2} = \tilde{m} \frac{\sqrt{y_0}}{L^2}$ is given as:

$$V_{IR}(z) = \frac{1}{4} (\tilde{m}^2 + 5) e^{2z} - \frac{1}{4} + \mathcal{O}(e^{3z}), \quad (151)$$

and $V_{IR}(z) > 0$ for $z \in [\log(\frac{1}{\tilde{m}} + \frac{1}{\tilde{m}^3}), \log(\delta^2 - 1)] \approx [-\log \tilde{m}, \log(\delta^2 - 1)]$. Hence WKB quantization condition gives,

$$\int_{-\log \tilde{m}}^{-2.526} \sqrt{\frac{1}{4} (\tilde{m}^2 + 5) e^{2z} - \frac{1}{4}} = \frac{(\delta^2 - 1)}{2} \tilde{m} - 0.785 + \mathcal{O}\left(\frac{1}{\tilde{m}^3}\right) = \left(n + \frac{1}{2}\right) \pi, \quad (152)$$

implying:

$$m_n^{2^{++}}(IR, r_h = 0) = m_n^{0^{--}}(IR, r_h = 0). \quad (153)$$

In the UV, we have:

$$\begin{aligned} V_{UV}(z) &= \frac{1}{4} (\tilde{m}^2 - 10) e^{-z} - \frac{3}{4} (\tilde{m}^2 - 5) e^{-2z} + 1 + \mathcal{O}(e^{-3z}) \\ &= \frac{e^{-z}}{2} \sqrt{e^z - 3\tilde{m}} + \mathcal{O}\left(e^{-3z}, \frac{1}{\tilde{m}}\right), \end{aligned} \quad (154)$$

and $V_{UV}(z) > 0$ for $z > \log\left(\frac{1}{8}(-\tilde{m}^2 + \sqrt{\tilde{m}^4 + 28m_0^2 - 140} + 10)\right) = \log\left(3 + \mathcal{O}\left(\frac{1}{\tilde{m}^2}\right)\right)$. Further, $\int_{\log 3}^{\infty} \sqrt{V_{UV}(z)} = \frac{\pi \tilde{m}}{8\sqrt{3}}$, implying:

$$m_n^{2^{++}}(UV) = (3.46 + 6.93) \frac{r_0}{L^2}. \quad (155)$$

(c) NLO-in- N /Non-Conformal Corrections using WKB method: The ‘potential’ inclusive of NLO-in- N terms, in the IR region in the $r_h = 0$ limit, is given by:

$$\begin{aligned} V(IR, r_h = 0) &= \frac{1}{512\pi^2 N} \left\{ e^{2z} \left(-60g_s^2 M^2 N_f (\log N - 12 + \log(16)) + 72g_s^2 M^2 m_0^2 N_f \log^2(y_0) + g_s M^2 \log(y_0) \right) \right. \\ &\times \left. \left(g_s N_f (m_0^2 (-12 \log N + 72 + \log(4096) - 15 \log(16)) + 720) + 96\pi m_0^2 \right) + 480\pi g_s M^2 + 128\pi^2 (m_0^2 + 5) N \right\} \\ &- \frac{1}{4} + \mathcal{O}(e^{-3z}), \end{aligned} \quad (156)$$

whose turning points are given by:

$\left[\log \left\{ \frac{1 - \frac{g_s M^2 \log(y_0) (g_s N_f (-12 \log N + 72 + \log(4096) - 15 \log(16)) + 72 g_s N_f \log(y_0) + 96\pi)}{256\pi^2 N}}{m_0} \right\}, \log(\delta^2 - 1) \right]$. The integral of $\sqrt{V(IR, r_h = 0)}$ between these turning points, in the large- \tilde{m} limit, yields the same spectrum as 0^{--} up to NLO in N .

6.3 Spin-1⁺⁺ Glueball spectrum

Here we need to consider the vector type of metric perturbation with the non-zero components given as: $h_{ti} = h_{it} = g_{x_1 x_1} G(r) e^{ikx_1}$, $i = x_2, x_3$.

6.3.1 M theory background with $r_h \neq 0$

Substituting the above ansatz for the perturbation in (122), the differential equation in $G(r)$ is given with $k^2 = -m^2$ as,

$$\begin{aligned}
& G''(r) + G'(r) \left(-\frac{3a^2}{r^3} - \frac{15g_s M^2 (-g_s N_f \log(N) + 24g_s N_f \log(r) + 6g_s N_f - 2g_s N_f \log(4) + 8\pi)}{64\pi^2 N r} + \frac{5}{r} \right) \\
& + \frac{G(r)}{4\pi r^4 (r^4 - r_h^4)} \left\{ \left(36g_s^3 M^2 N_f m^2 r^2 (r^2 - 3a^2) \log^2(r) - 3g_s^2 M^2 m^2 r^2 (r^2 - 3a^2) \log(r) (g_s N_f \log(N) + g_s N_f (\log(16) - 6) - 8\pi) \right. \right. \\
& \left. \left. + 8\pi (3a^2 (-2\pi g_s N m^2 r^2 - r^4 + r_h^4) + 2\pi g_s N m^2 r^4 + 4r^6) \right) \right\} = 0. \tag{157}
\end{aligned}$$

(a) Neumann/Diriclet boundary condition at $r = r_h$: Near $r = r_h$, equation (157) up to LO in N , is given by:

$$G''(r) + \left(\frac{3.92}{r_h} \right) G'(r) + \left(\frac{2 - 0.02\tilde{m}^2}{r_h(r - r_h)} + \frac{-1.16 + 0.57\tilde{m}^2}{r_h^2} \right) G(r) = 0, \tag{158}$$

whose solution is given by:

$$\begin{aligned}
G(r) &= e^{\left(\frac{0.5r(-2\sqrt{5.0016-0.57\tilde{m}^2}-3.92)+r_h \log(r-r_h)}{r_h} \right)} \\
&\times \left[c_1 U \left(-\frac{-0.01\tilde{m}^2 - \sqrt{5.0016 - 0.57\tilde{m}^2} + 1}{\sqrt{5.0016 - 0.57\tilde{m}^2}}, 2, \frac{2\sqrt{5.0016 - 0.57\tilde{m}^2}r}{r_h} - 2\sqrt{5.0016 - 0.57\tilde{m}^2} \right) \right. \\
&\left. + c_2 L^1_{-\frac{1}{\sqrt{5.0016-0.57\tilde{m}^2}}, \frac{-1\sqrt{5.0016-0.57\tilde{m}^2}-0.01\tilde{m}^2+1}{\sqrt{5.0016-0.57\tilde{m}^2}}} \left(\frac{2r\sqrt{5.0016-0.57\tilde{m}^2}}{r_h} - 2\sqrt{5.0016-0.57\tilde{m}^2} \right) \right]. \tag{159}
\end{aligned}$$

Imposing Neumann boundary condition at $r = r_h$ yields:

$$\begin{aligned}
& \lim_{z \rightarrow 0} \frac{1}{r_h} \left\{ e^{-\sqrt{5.0016-0.57\tilde{m}^2}z} \left[0.140858c_1 r_h U \left(\frac{0.01\tilde{m}^2}{\sqrt{5.0016-0.57\tilde{m}^2}} - \frac{1}{\sqrt{5.0016-0.57\tilde{m}^2}} + 1, 2, z \right) \right. \right. \\
& \left. \left. + 0.140858c_2 r_h L^1_{-\frac{1}{\sqrt{5.0016-0.57\tilde{m}^2}}, \frac{0.01\tilde{m}^2}{\sqrt{5.0016-0.57\tilde{m}^2}} + \frac{1}{\sqrt{5.0016-0.57\tilde{m}^2}}} - 1(z) \right] \right\}. \tag{160}
\end{aligned}$$

Considering $p = \frac{0.01\tilde{m}^2}{\sqrt{5.0016-0.57\tilde{m}^2}} - \frac{1}{\sqrt{5.0016-0.57\tilde{m}^2}} + 1$ and setting $c_2 = 0$ in (160), and then using $\lim_{z \rightarrow 0} U(p, 2, z \sim 0) \sim \frac{z^{-1} {}_1F_1(p-1; 0; z)}{\Gamma(p)}$, one notes that one can satisfy the Neumann boundary condition at $r = r_h$ provided $\lim_{z \rightarrow 0} {}_1F_1(p-1; 0; z) = \lim_{b \rightarrow 0} \lim_{z \rightarrow 0} {}_1F_1(p-1; b; z)$ (i.e. first set z to 0 and then b), $p = -n \in \mathbb{Z}^-$. Hence:

$$\begin{aligned}
m^{1^{++}}(T) &= 2.6956\pi T \\
m^{1^{+++}}(T) &= 2.8995\pi T \\
m^{1^{++++}}(T) &= 2.9346\pi T \\
m^{1^{++++}}(T) &= 2.9467\pi T. \tag{161}
\end{aligned}$$

One can show that one obtains the same spectrum as (161) even upon imposing Dirichlet boundary condition: $G(r = r_h) = 0$.

(b) Spectrum using WKB method: Following [34], the ‘potential’ V in the Schrödinger-like equation working with the dimensionless mass variable \tilde{m} defined via: $m = \tilde{m} \frac{r_h}{L^2} = \tilde{m} \frac{\sqrt{y_h}}{L^2}$, in the IR, can be shown to be given by:

$$V_{IR}(z) = e^{2z} (0.15\tilde{m}^2 - 1.52) + e^z (1 - 0.01\tilde{m}^2) - \frac{1}{4} + \mathcal{O}\left(e^{3z}, \frac{1}{N}\right). \quad (162)$$

The zeros of the potential as function of e^z , in (162) are given by:

$$\frac{-1.8765 \times 10^{14} \tilde{m}^2 \pm 6.022232598554301 \times 10^{-7} \sqrt{9.70917 \times 10^{40} \tilde{m}^4 + 1.26219 \times 10^{44} \tilde{m}^2 - 5.04877 \times 10^{44} + 1.8765 \times 10^{16}}}{5.70456 \times 10^{16} - 5.6295 \times 10^{15} \tilde{m}^2} = -\frac{25}{\tilde{m}^2} + \mathcal{O}\left(\frac{1}{\tilde{m}^2}\right),$$

$0.07 + \mathcal{O}\left(\frac{1}{\tilde{m}^2}\right)$; the first not being permissible. Now, in the IR $r \in [r_h, \sqrt{3}a \approx 0.6\sqrt{3}r_h]$ or in terms of $z : (-\infty, -2.526]$. Therefore the allowed domain of integration is: $[\log(0.07), -2.526]$. Thus, in the IR:

$$\int_{z=-2.704}^{z=-2.526} \sqrt{e^{2z} (0.15\tilde{m}^2 - 1.52) + e^z (1 - 0.01\tilde{m}^2) - \frac{1}{4}} \approx 0, \quad (163)$$

implying a null contribution to the WKB quantization condition in the IR.

In the UV, the potential is given by:

$$V_{UV}(z) = \frac{e^{3z} (-3b^2 + \tilde{m}^2 + 10) + e^{2z} (-3b^2 (\tilde{m}^2 + 2) + 2\tilde{m}^2 + 9) + e^z ((1 - 3b^2) \tilde{m}^2 + 1) + 4e^{4z} - 2}{4(e^z + 1)^3 (e^z + 2)}, \quad (164)$$

which for $b = 0.6$ obtains:

$$V(N_f = M = 0, UV) = e^{-2z} (6.56 - 1.02\tilde{m}^2) + (0.25\tilde{m}^2 - 2.77) e^{-z} + 1 + \mathcal{O}(e^{-3z}). \quad (165)$$

The zeros of the potential in the UV, as a function of e^z , in (165) are given by:

$-0.125\tilde{m}^2 \pm 0.005\sqrt{625.\tilde{m}^4 + 26950.\tilde{m}^2 - 185671} + 1.385 = (-0.25\tilde{m}^2 - 1.31, 4.08 + \mathcal{O}\left(\frac{1}{\tilde{m}^2}\right))$; the former not being permissible. Hence, the allowed domain of integration over which the potential is positive, is: $([\log(4.08), \infty)$. Performing a large- \tilde{m} -expansion, one obtains:

$$\begin{aligned} & \int_{\log(4.08)}^{\infty} \sqrt{e^{-2z} (6.56 - 1.02\tilde{m}^2) + (0.25\tilde{m}^2 - 2.77) e^{-z} + 1} = \int_{z=\log(4.08)}^{\infty} e^{-z} \sqrt{0.25e^z - 1.02} + \mathcal{O}\left(\frac{1}{\tilde{m}}\right) \\ & = 0.389\tilde{m} = \left(n + \frac{1}{2}\right) \pi, \end{aligned} \quad (166)$$

yielding:

$$m_n^{1++}(T) = 4.04 (1 + 2n) \frac{r_h}{L^2}. \quad (167)$$

6.3.2 M theory background with an IR Cut-Off r_0

(a) Neumann/Diriclet boundary condition at $r = r_0$: Considering the limit of $(r_h, a) \rightarrow 0$ in equation (157) up to LO in N and imposing Neumann boundary condition at the IR cut-off $r = r_0$, yields isospectrality with 2^{++} glueball spectrum at $r_h = 0$.

(b) Spectrum using WKB method: Using the redefinition of [34], the ‘potential’ up to leading order in N is given by:

$$V(z) = \frac{(\tilde{m}^2 + 2) e^{2z} - 3e^z + 4e^{3z} - 1}{4(e^z + 1)^3} + \mathcal{O}\left(\frac{g_s M^2}{N}\right). \quad (168)$$

In the IR region we get the potential as:

$$V_{IR}(z) = -\frac{1}{4} + \frac{1}{4}(5 + \tilde{m}^2)e^{2z} + \mathcal{O}(e^{3z}), \quad (169)$$

giving the turning points as, $z \in [\log(\frac{1}{\tilde{m}} + \mathcal{O}(\frac{1}{\tilde{m}^3})) \approx -\log \tilde{m}, \log(\delta^2 - 1)]$ and the WKB quantization condition becomes:

$$\int_{-\log \tilde{m}}^{\log(\delta^2 - 1)} \sqrt{V_{IR}(z)} = \frac{(\delta^2 - 1)}{2} \tilde{m} - \frac{\pi}{4} = \left(n + \frac{1}{2}\right) \pi. \quad (170)$$

Therefore:

$$m_n^{1^{++}}(IR, r_h = 0) = m_n^{2^{++}}(IR, r_h = 0) = m_n^{0^{--}}(IR, r_h = 0). \quad (171)$$

Further, in the UV:

$$V_{UV}(z) = \frac{1}{4}(\tilde{m}^2 - 10)e^{-z} - \frac{3}{4}(\tilde{m}^2 - 5)e^{-2z} + 1 + \mathcal{O}(e^{-3z}), \quad (172)$$

implying that $V_{UV}(z) > 0$ for $z \in [\log\left(\frac{1}{8}\left(-\tilde{m}^2 + \sqrt{\tilde{m}^4 + 28\tilde{m}^2 - 140} + 10\right)\right) = \log\left(3 + \mathcal{O}\left(\frac{1}{\tilde{m}^2}\right)\right), \infty)$. This yields the following WKB quantization condition:

$$\int_{\log 3}^{\infty} \sqrt{V_{UV}(z)} = \frac{\pi \tilde{m}}{4\sqrt{3}} = \left(n + \frac{1}{2}\right) \pi, \quad (173)$$

which obtains:

$$m_n^{1^{++}}(UV, r_h = 0) = (3.46 + 6.93n) \frac{r_0}{L^2}. \quad (174)$$

(c) NLO in N /Non-Conformal Corrections using WKB method: In the IR region, the ‘potential’ including NLO-in- N corrections in the $r_h = 0$ limit, is given by:

$$\begin{aligned} V(IR, r_h = 0) &= \frac{1}{4}e^{2z}(\tilde{m}^2 + 5) \\ &+ \frac{1}{512\pi^2 N} \left\{ g_s M^2 e^{2z} \left(\log(y_0) (g_s N_f (\tilde{m}^2(-12\log N + 72 + \log(4096) - 15\log(16)) + 720) + 96\pi\tilde{m}^2) \right. \right. \\ &\left. \left. + 60(8\pi - g_s N_f (\log N - 12 + \log(16))) + 72g_s \tilde{m}^2 N_f \log^2(y_0) \right) \right\} - \frac{1}{4}, \end{aligned} \quad (175)$$

whose turning points are:

$\left[\log\left(\frac{1}{\tilde{m}} \left[1 - \frac{g_s M^2 \log(y_0) (g_s N_f (-12\log N + 72 + \log(4096) - 15\log(16)) + 72g_s N_f \log(y_0) + 96\pi)}{256\pi^2 N} \right] \right), \log(\delta^2 - 1) \right]$, and the integral of $\sqrt{V(IR, r_h = 0)}$ between these turning points yields an isospectrality with the 0^{--} and 2^{++} NLO-in- N spectrum.

7 2^{++} Glueball Masses from Type IIB

7.1 $r_h \neq 0$

The 10-dimensional type IIB supergravity action in the low energy limit is given by,

$$\frac{1}{2k_{10}^2} \left\{ \int d^{10}x e^{-2\phi} \sqrt{-G} \left(R - \frac{1}{2} H_3^2 \right) - \frac{1}{2} \int d^{10}x \sqrt{-G} \left(F_1^2 + \widetilde{F}_3^2 + \frac{1}{2} \widetilde{F}_5^2 \right) \right\}, \quad (176)$$

where ϕ is the dilaton, G_{MN} is the 10-d metric and F_1 , H_3 , \widetilde{F}_3 , \widetilde{F}_5 are different fluxes.

The five form flux \widetilde{F}_5 and the three form flux \widetilde{F}_3 are defined as,

$$\widetilde{F}_5 = F_5 + \frac{1}{2} B_2 \wedge F_3, \quad \widetilde{F}_3 = F_3 - C_0 \wedge H_3, \quad (177)$$

where F_5 and F_3 are sourced by the D_3 and D_5 branes respectively. B_2 is the NS-NS two form and C_0 is the axion. The three form fluxes \widetilde{F}_3 , H_3 , the two form B_2 and the axion C_0 are given as [1] - see (9). Now varying the action in (176) with respect to the metric $g_{\mu\nu}$ one get the following equation of motion,

$$\begin{aligned} R_{\mu\nu} = & \left(\frac{5}{4} \right) e^{2\phi} \widetilde{F}_{\mu p_2 p_3 p_4 p_5} \widetilde{F}_{\nu}^{p_2 p_3 p_4 p_5} - \left(\frac{g_{\mu\nu}}{8} \right) e^{2\phi} \widetilde{F}_5^2 + \left(\frac{3}{2} \right) H_{\mu\alpha_2\alpha_3} H_{\nu}^{\alpha_2\alpha_3} \\ & - \left(\frac{g_{\mu\nu}}{8} \right) H_3^2 + \left(\frac{3}{2} \right) e^{2\phi} \widetilde{F}_{\mu\alpha_2\alpha_3} \widetilde{F}_{\nu}^{\alpha_2\alpha_3} - \left(\frac{g_{\mu\nu}}{8} \right) e^{2\phi} \widetilde{F}_3^2 + \left(\frac{1}{2} \right) e^{2\phi} F_{\mu} F_{\nu}. \end{aligned} \quad (178)$$

we consider the following linear perturbation of the metric,

$$g_{\mu\nu} = g_{\mu\nu}^{(0)} + h_{\mu\nu}, \quad (179)$$

where as before $\mu, \nu = \{t, x_1, x_2, x_3, r, \theta_1, \theta_2, \phi_1, \phi_2, \psi\}$. Here the only non zero component according to the tensor mode of metric fluctuation is $h_{x_2 x_3}$. Since the non zero components of F_1 , \widetilde{F}_3 and H_3 has no indices as $\{x_2, x_3\}$, the final equation of motion gets simplified and can be shown to be given as:

$$\begin{aligned} R_{x_2 x_3}^{(1)} = & \left(\frac{5}{4} \right) e^{2\phi} \left(4 \widetilde{F}_{x_2 x_3 p_3 p_4 p_5} \widetilde{F}_{x_2 x_3 q_3 q_4 q_5} g^{p_3 q_3} g^{p_4 q_4} g^{p_5 q_5} h^{x_2 x_3} \right) - \left(\frac{h_{x_2 x_3}}{8} \right) e^{2\phi} \widetilde{F}_5^2 \\ & - \left(\frac{h_{yz}}{8} \right) H_3^2 - \left(\frac{h_{x_2 x_3}}{8} \right) e^{2\phi} \widetilde{F}_3^2. \end{aligned} \quad (180)$$

Working at a particular value of θ_1 and θ_2 given as: $\theta_1 = N^{-1/5}$ and $\theta_2 = N^{-3/10}$, the square of different fluxes figuring in (180) at the lowest-order in N , are given in (A1). Writing the perturbation $h_{x_2 x_3}$ as $h_{x_2 x_3} = \frac{r^2}{2(g_s \pi N)^{1/2}} H(r) e^{ikx_1}$, (180) reduces to the following second order differential equation

in $H(r)$:

$$\begin{aligned}
& H''(r) + \left(\frac{5r^4 - r_h^4}{r(r^4 - r_h^4)} - \frac{9a^2}{r^3} + \left\{ \frac{3}{256\pi^2 N^{2/5} r^3} \left[-54a^2 g_s^2 M^2 N_f - 72\pi a^2 g_s M^2 + 768\pi^2 a^2 + 12g_s^2 M^2 N_f r^2 + \right. \right. \right. \\
& 9a^2 g_s^2 M^2 N_f \log(16) - 2g_s^2 M^2 N_f r^2 \log(16) + 16\pi g_s M^2 r^2 + g_s^2 M^2 N_f (9a^2 - 2r^2) \log(N) - 24g_s^2 M^2 N_f \\
& \left. \left. \left. (9a^2 - 2r^2) \log(r) \right] \right\} \right) H'(r) + \left(\frac{1}{4\pi r^4 (r^4 - r_h^4)} \left\{ 8\pi (a^2 (6\pi g_s N q^2 r^2 - 9r^4 + 9r_h^4) - 2\pi g_s N q^2 r^4 + 4r^6) \right. \right. \\
& \left. \left. + 3g_s^2 M^2 q^2 r^2 (r^2 - 3a^2) \log(r) (g_s N_f \log(16N) - 6g_s N_f - 8\pi) - 36g_s^3 M^2 N_f q^2 r^2 (r^2 - 3a^2) \log^2(r) \right\} - \right. \\
& \left. \frac{g_s^2}{512\pi^3} \left\{ \frac{34992a^2 g_s M^2 (\sqrt[5]{N} + 3) N_f^2 \log(r)}{r^3} + 9a^2 g_s N_f \left(\frac{7831552\pi^5}{(r^4 - r_h^4) (g_s N_f \log(16N) - 3g_s N_f \log(r) + 4\pi)^3} - \frac{81M^2 (7\sqrt[5]{N} - 1) N_f}{r^4} \right) \right. \right. \\
& \left. \left. + \frac{2 \left(243g_s M^2 (\sqrt[5]{N} + 1) N_f^2 + \frac{3915776\pi^5 r^4}{(r^4 - r_h^4) (g_s N_f \log(16N) - 3g_s N_f \log(r) + 4\pi)^2} \right)}{r^2} \right\} \right) H(r) = 0. \tag{181}
\end{aligned}$$

7.1.1 Mass Spectrum from Neumann Boundary Condition at $r = r_h$

To get a sensible answer, one has to perform a small- T expansion when one rewrites and solves (181) around $r = r_h$. This time around the analog of (93) becomes:

$$0.5 - \frac{0.174071m^2 \left(1 - \frac{3(g_s M^2 (2 \log(N) + 11.8963) + 4g_s M^2 \log(T) + 0.6N)^2}{N^2} \right)}{T \sqrt{-m^2 \left(4 - 7 \left(1 - \frac{3(g_s M^2 (2 \log(N) + 11.8963) + 4g_s M^2 \log(T) + 0.6N)^2}{N^2} \right) \right)}} = -n, \tag{182}$$

which for $g_s = 0.8$, $N = g_s^{-39} \sim 6000$, $M = 3$ yields:

$$\begin{aligned}
m_{2^{++}} &= 4.975T \\
m_{2^{++}}^* &= 14.925T \\
m_{2^{++}}^{**} &= 24.876T \\
m_{2^{++}}^{***} &= 34.826T \\
m_{2^{++}}^{****} &= 44.776T
\end{aligned} \tag{183}$$

So, one obtains an approximate match between the ground state 2^{++} mass from M theory and type IIB string theory.

7.1.2 WKB Quantization Method

Using the variables of [34], the ‘potential’, defining $m = \tilde{m} \frac{\sqrt{y_h}}{L^2}$, yields:

$$\begin{aligned}
V(2^{++}, IIB, r_h \neq 0) &= \frac{1}{4(e^z + 1)^3 (e^z + 2)^2} \left\{ e^z \left(3b^2 (e^z + 2) (-\tilde{m}^2 - 6) e^z - \tilde{m}^2 + 3e^{2z} + 6 \right) \right. \\
& \left. + (-e^z - 1) \left((25 - 3\tilde{m}^2) e^z - (\tilde{m}^2 - 18) e^{2z} - 2(\tilde{m}^2 - 6) + 4e^{3z} \right) \right\} + \mathcal{O}\left(\frac{g_s M^2}{N}\right). \tag{184}
\end{aligned}$$

In the IR, the potential is given by:

$$V(IR, T) = e^z \left((0.15\tilde{m}^2 - 1.3375) e^z - 0.01\tilde{m}^2 + 0.06 \right) + \mathcal{O}(e^{3z}), \quad (185)$$

and in the IR, for $\tilde{m} > 2.986$, $V(IR < T) > 0$ for $z \in [\log(0.067 + \mathcal{O}(\frac{1}{\tilde{m}^2})) \approx -2.708, -2.526]$ and: $\int_{2.708}^{-2.526} \sqrt{V(IR, T)} \approx 0$ - hence the IR provides no contribution to the WKB quantization.

In the UV:

$$V(UV, T) = \frac{1}{4} (\tilde{m}^2 + 9.24) e^{-z} - \frac{3}{4} (\tilde{m}^2 + 0.36 (\tilde{m}^2 + 9) + 3) + \mathcal{O}(e^{-3z}), e^{-2z} - 1 \quad (186)$$

the turning points for $\tilde{m} > 7.141$ are $(\log(4.08 + \mathcal{O}(\frac{1}{\tilde{m}^2})), 0.25\tilde{m}^2 - 1.77)$. Hence,

$$\begin{aligned} \int_{1.406}^{\log(0.25\tilde{m}^2 - 1.77)} \sqrt{V(UV, T)} &= \int_{1.406}^{\log(0.25\tilde{m}^2 - 1.77)} \frac{e^{-z}}{2} \sqrt{e^z - 4.08\tilde{m}} + \mathcal{O}\left(\frac{1}{\tilde{m}}\right) \\ &= 0.389\tilde{m} - 2 = \left(n + \frac{1}{2}\right) \pi, \end{aligned} \quad (187)$$

which obtains:

$$m_n^{2^{++}}(T) = (9.18 + 8.08n) \frac{r_h}{L^2}. \quad (188)$$

Hence, the string theory 2^{++} glueball is isospectral with 0^{++} ; in the large n -limit of the spectrum, the M-theory and type IIB spectra coincide.

7.2 $r_h = 0$

7.2.1 WKB Method

Once again defining $r = \sqrt{y}$, $r_h = \sqrt{y_0}$, $y = y(1 + e^z)$ analogous to their $r_h \neq 0$ redefinitions of [34], the ‘potential’ in the IR, is given by:

$$V(r_h = 0) = -\frac{1}{4} + \frac{1}{4} (1 + \tilde{m}^2) e^{2z} + \mathcal{O}(e^{-3z}). \quad (189)$$

The domain in the IR over which $V(r_h = 0) > 0$ is: $[-\frac{1}{2} \log(5 + \tilde{m}^2), \log(\delta^2 - 1)]$ and:

$$\int_{-\frac{1}{2} \log(5 + \tilde{m}^2)}^{-2.526} \sqrt{-\frac{1}{4} + \frac{1}{4} (1 + \tilde{m}^2) e^{2z}} = \frac{(\delta^2 - 1) \tilde{m}}{2} - \frac{\pi}{4} = \left(n + \frac{1}{2}\right) \pi, \quad (190)$$

yielding:

$$m_n^{2^{++}}(IR, IIB, r_h = 0) = m_n^{2^{++}}(IR, M \text{ theory}, r_h = 0). \quad (191)$$

In the UV

$$V(UV, r_h = 0) = \frac{1}{4} (\tilde{m}^2 - 10) e^{-z} - \frac{3}{4} (\tilde{m}^2 - 5) e^{-2z} + 1 + \mathcal{O}(e^{-3z}), \quad (192)$$

the zeros of which, as functions of e^z , are at $(\frac{1}{8} (-\tilde{m}^2 \pm \sqrt{\tilde{m}^4 + 28\tilde{m}^2 - 140} + 10)) = (-\frac{\tilde{m}^2}{4} - \frac{1}{2}, 3 + \mathcal{O}(\frac{1}{\tilde{m}^2}))$. Hence the domain of integration over which $V(UV, r_h = 0) > 0$ is: $[\log 3, \infty)$. Therefore:

$$\int_{\log 3}^{\infty} \sqrt{V(UV, r_h = 0)} = \frac{1}{2} \int_{\log 3}^{\infty} e^{-z} \sqrt{e^z - 3\tilde{m}} + \mathcal{O}\left(\frac{1}{\tilde{m}}\right) = \frac{\tilde{m}\pi}{4\sqrt{3}} = \left(n + \frac{1}{2}\right) \pi, \quad (193)$$

yielding:

$$m_n^{2^{++}}(r_h = 0) = (3.464 + 6.928n) \frac{r_0}{L^2}. \quad (194)$$

7.2.2 NLO-in- N /Non-Conformal Corrections in the IR in the $r_h = 0$ Limit

The ‘potential’ inclusive of the NLO-in- N corrections in the IR in the $r_h = 0$ limit, reads as:

$$V(IR, r_h = 0) = e^{2z} \left(\frac{g_s M^2 \left(\frac{1}{N}\right)^{2/5} (g_s N_f (6 \log N - 72 + \log(16777216)) - 72 g_s N_f \log(y_0) - 48\pi)}{512\pi^2} + \frac{1}{4} (\tilde{m}^2 - 3) \right) - \frac{1}{4} + \mathcal{O}(e^{-3z}), \quad (195)$$

whose turning points, in the large- \tilde{m} limit are: $[\log \{ \frac{1}{\tilde{m}} + \mathcal{O}(\frac{1}{\tilde{m}^3}) \}, \log(\delta^2 - 1)] \approx [-\log \tilde{m}, \log(\delta^2 - 1)]$. Now,

$$\int_{-\log \tilde{m}}^{\log(\delta^2 - 1)} \sqrt{V(IR, r_h = 0)} = \frac{(\delta^2 - 1)}{2} \tilde{m} - \frac{\pi}{4} + \mathcal{O}\left(\frac{1}{\tilde{m}}\right) = \left(n + \frac{1}{2}\right), \quad (196)$$

which yields the same LO spectrum as $0^{--}, 1^{++}$ and the 2^{++} spectrum obtained from M theory. Hence, the type IIB at $r_h = 0$ is unable to capture the non-conformal NLO-in- N corrections in the 2^{++} corrections, as the same either precisely cancel out or are $\frac{1}{\tilde{m}}$ -suppressed in the large- \tilde{m} limit, in a IIB computation.

8 Summary and Discussion

Supergravity calculations of glueball spectra in top-down holographic duals of large- N thermal QCD at *finite string/gauge coupling* and not just $g_s N \gg 1$, have thus far, been missing in the literature. Such a limit is particularly relevant to sQGP [4]. This work fills in this gap by working out the spectra of $0^{++}, 0^{-+}, 0^{--}, 1^{++}, 2^{++}$ glueballs in a type IIB/delocalized SYZ IIA mirror/(its) M-theory (uplift) model corresponding to the top-down holographic dual of [1] in the MQGP limit introduced in [2]. As discussed in **2.1**, towards the end of a Seiberg duality cascade in the IR, despite setting $M (= N_c$ in the IR) to three in the MQGP limit, due a flavor-color enhancement of the length scale as compared to the KS model, one can trust supergravity calculations without worrying about stringy corrections. Further, in the MQGP limit, all physical quantities as seen in all calculations in [5], receive non-conformal corrections that appear at the NLO in N and display a universal $\frac{g_s M^2 (g_s N_f)}{N}$ -suppression.

It should be noted that a numerical computation like the ‘shooting computation’ used in a lot of holographic glueball spectrum computations will not be feasible to use for the following reason. In the ‘shooting method’, like [61], one can first solve the EOMs in the UV using the infinite series/Frobenius method and then numerically (via Euler’s method, etc.) obtain the solution at the horizon where one imposes a Neumann boundary condition. By matching the value obtained by numerically ‘shooting’ from the UV to the horizon in the IR and matching the radial derivative of the solution so obtained to zero, one can obtain quantized values of the glueball masses. The caveat is that one should have at hand the exact radial profile of the effective number of fractional $D3$ -branes ($D5$ -branes wrapping the small two-cycle) and the number of flavor branes which would correctly interpolate between $(M, N_f) = (0, 0)$ in the UV and $(M = 3, N_f = 2)$ in the IR. But, we do not have this information - we know the values in the IR and the UV but not for the interpolating region. Hence, numerical methods such as the ‘shooting method’ could at best be used, to obtain only the LO-in- N results, not the NLO-in- N results which is one of the main objectives of our computations.

The summary of all calculations is given in tables 1 (and Fig. 2) and 3 - the former table/graph having to do with a WKB quantization calculation using the coordinate/field redefinitions of [34] and the latter table having to do with obtaining the mass spectrum by imposing Neumann/Dirichlet boundary condition at r_h /IR cut-off r_0 . Some of the salient features of the results are given as separate bullets.

It should be noted that the last two columns in Tables 1 and 3 have been prepared in the same spirit as the last columns in Table 2 of [75].

S. No.	Glueball	\tilde{m} using WKB $r_h \neq 0$ (units of πT , up to LO in N) (large- \tilde{m} limit)	\tilde{m} using WKB $r_h = 0$ (units of $\frac{r_0}{L^2}$, up to NLO in N) (large- \tilde{m} limit)
1	0^{++} (Fluctuations: $h_{00,rx_1,rr}$ in M-theory metric)	(M theory) $\frac{\sqrt{35+70n}}{\sqrt{\mathcal{P}\mathcal{L}(13.15+26.31n)}}$ ▲	(M theory) No turning points
	0^{++} (Dilaton Fluctuations)	(Type IIB) $9.18 + 8.08n$ ▲	(Type IIB) $\frac{(4.64+6.28n)}{(\delta^2-1)} \left[1 - 0.01 \frac{g_s M^2}{N} (g_s N_f) \log N \log r_0 \right]$
2	0^{-+} (1-form fluctuation a_{θ_2})	(Type IIA) $11.12 (n + \frac{1}{2}), n = 0$ ■ $(6.22 + 4.80n), n \in \mathbb{Z}^+$ ▲	(Type IIA) $\frac{3.72+4.36n}{(\delta^2-1)}, n = 0$ $4.8 (n + \frac{1}{2}), n \in \mathbb{Z}^+$
3	0^{--} 2-form fluctuation A_{23}	(Type IIB) $= m_n^{0^{++}}$ (dilaton, T) ▲	(Type IIB) $\frac{6.28n+4.71}{(\delta^2-1)} \left(1 + \frac{0.01 g_s^2 \log N M^2 N_f \log(r_0)}{N} \right), n = 0$ $(7.87 + 6.93n), n \in \mathbb{Z}^+$
4	1^{++} (Fluctuations: $h_{it} = h_{ti}, i = x_{2,3}$ in M-theory metric)	(M theory) $8.08 (n + \frac{1}{2})$ ▲	(M theory) $m_n^{1^{++}} (n = 0, r_h = 0) = m_n^{0^{--}} (n = 0, r_h = 0)$ $(3.46 + 6.93n), n \in \mathbb{Z}^+$
5	2^{++} (Fluctuations: $h_{x_2x_3} = h_{x_3x_2},$ $h_{x_2x_2} = h_{x_3x_3}$ in M-theory metric)	(M theory) $8.08 (n + \frac{1}{2}) = m_n^{1^{++}} (T)$ ▲	(M theory) $= m_n^{1^{++}} (r_h = 0)$
	2^{++} (Fluctuation $h_{x_2x_3} = h_{x_3x_2}$ in type IIB metric)	(Type IIB) $9.18 + 8.08n = m_n^{0^{++}} (IIB, T)$ ▲	(Type IIB) $= m_n^{1^{++}} (r_h = 0)$

Table 1: Summary of Glueball Spectra: $m = \tilde{m} \frac{r_h}{L^2}$ from Type IIB, IIA and M Theory using WKB quantization condition for $r_h \neq 0$, and $m = \tilde{m} \frac{r_0}{L^2}$ for $r_h = 0$ (equalities in the $r_h = 0$ column, are valid up to NLO in N); the colored triangles/square in the third column correspond to the colored triangles/square that appear in Fig. 2 in the combined plot of $r_h \neq 0$ supergravity calculations of glueballs

The $r_h \neq 0$ glueball spectra is plotted in Figure 2.

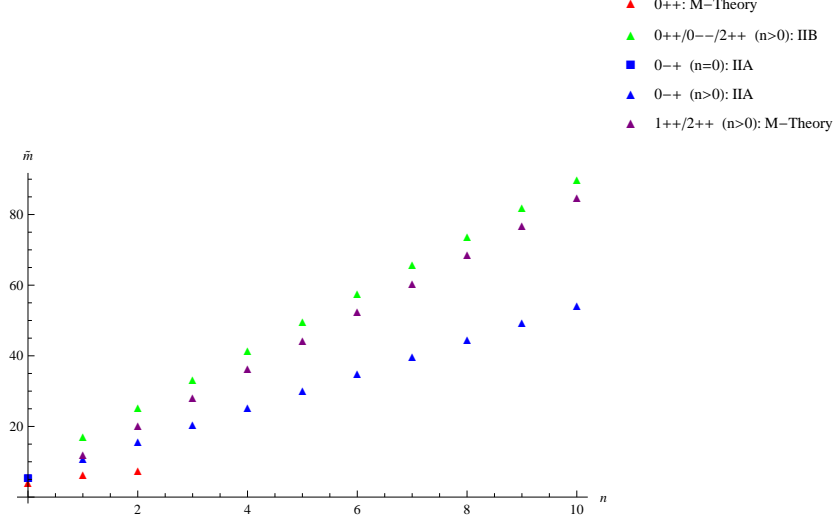


Figure 2: Plots of Supergravity $0^{++}, 0^{-+}, 0^{--}, 1^{++}$ Glueball Spectra for $r_h \neq 0$

Some of the salient features of Table 1 and Figure 2 are presented below:

1. Interestingly, via a WKB quantization condition using coordinate/field redefinitions of [34], the lightest 0^{++} glueball spectrum for $r_h \neq 0$ coming from scalar metric fluctuations in M theory compares rather well with the $N \rightarrow \infty$ lattice results of [57] - refer to Table 2. Also, similar to [58], the 0^{++} coming from the scalar fluctuations of the M theory metric is lighter than the 0^{++} coming from type IIB dilaton fluctuations. Further, interestingly, one can show that by using the coordinate and field redefinitions of [33] when applied to the EOM for dilaton fluctuation to yield a WKB quantization condition, for $a = 0.6r_h$ - as in [5] - one obtains a match with the UV limit of the 0^{++} glueball spectrum as obtained in [34]. For our purpose, the method based on coordinate/field redefinitions of [33], is no good for obtaining the 0^{++} glueball ground state and was not used for any other glueball later on in subsequent calculations in this paper.

State	$N \rightarrow \infty$ Entry in Table 34 Of [57] in units of square root of string tension	M-theory scalar metric perturbations (6.1.2 - in units of $\frac{r_h}{T_2}$)	Type IIB Dilaton fluctuations of [61] in units of reciprocal of temporal circle's diameter
0^{++}	4.065 ± 0.055	4.267	4.07 (normalized to match lattice)
0^{++*}	6.18 ± 0.13	6.251	7.02
0^{++**}	7.99 ± 0.22	7.555	9.92
0^{++***}	-	8.588	12.80
0^{++****}	-	9.464	15.67

Table 2: Comparison of [57]'s $N \rightarrow \infty$ lattice results for 0^{++} glueball with our supergravity results obtained using WKB quantization condition and redefinitions of [34] for M theory scalar metric fluctuations

2. Also, from Table 1/Figure 2, $m_{n>0}^{2^{++}} > m_{n>0}^{0^{++}}$ (scalar metric perturbations), similar to [58].

3. The higher excited states of the type IIA 0^{-+} glueball, for both $r_h \neq 0$ and $r_h = 0$, are isospectral. This is desirable because large- n corresponds to the UV and that takes one away from the BH geometry, i.e., towards $r_h = 0$.
4. The non-conformal corrections up to NLO in N , have a semi-universal behavior of $\frac{(g_s M^2)(g_s N_f) \log r_0}{N}$ and turn out to be multiplied by a numerical pre-factor of $\mathcal{O}(10^{-2})$; we could disregard the same in the MQGP limit.
5. As per a more recent lattice calculation [59]⁶, the 0^{++} -glueball has a mass $4.16 \pm 0.11 \pm 0.04$ (in units of the reciprocal of the ‘hadronic scale parameter’ of [60]), which compares rather well with $m_{n=0}^{0^{++}} = 4.267$ (in units of $\frac{r_h}{L^2}$) of Table 2 coming from scalar fluctuations of the M theory metric. Similarly, the 0^{-+} -glueball in [59] has a mass $6.25 \pm 0.06 \pm 0.06$ and from Table 1, which matches rather nicely with $m_{n=0}^{0^{-+}}(\delta = 1.26) = 6.25$ (in units of $\frac{r_0}{L^2}$) of Table 1 coming from type IIA one-form fluctuation.
6. The ground state and the $n \gg 1$ excited states of 1^{++} and 0^{--} glueballs are isospectral.
7. The higher excited $r_h \neq 0$ 2^{++} glueball states corresponding to metric fluctuations of the M-theory metric and the ones corresponding to fluctuations of the type IIB metric, are isospectral. The $r_h = 0$ 2^{++} glueball states corresponding to metric fluctuations of the M-theory/type IIB string theory, are isospectral. Further, it turns out that due to internal cancellation of terms and $\frac{1}{m}$ -suppression, a type IIB $r_h = 0$ 2^{++} glueball spectrum, unlike an M-theoretic computation, is unable to capture the NLO-in- N corrections to the LO-in- N type IIB 2^{++} glueball spectrum.
8. $m_n^{2^{++}}(\text{NLO}, r_h = 0) = m_n^{1^{++}}(\text{NLO}, r_h = 0) \xrightarrow{n \gg 1} m_n^{0^{--}}(\text{NLO}, r_h = 0)$, where the ‘NLO’ implies equality with the inclusion of NLO-in- N corrections.

⁶We thank P.Majumdar for bringing this reference to our attention.

S. No.	Glueball	Spectrum Using N(eumann)/D(irichlet) b.c., $r = r_h$ (units of πT)	Spectrum Using N(eumann)/D(irichlet) b.c., $r = r_0$ (units of $\frac{r_0}{l^2}$)
1	0^{++}	(M theory) (N) $12.25\sqrt{2+n}$ (D) $12.25\sqrt{1+n}$	(M theory) (N) 4.1
2	0^{-+}	(Type IIA) (N/D) $\frac{3.1}{\pi}\sqrt{n}$	(Type IIA) (N) $m_{n=0}^{0^{-+}} = 0, m_{n=1}^{0^{-+}} \approx 3.4, m_{n=2}^{0^{-+}} \approx 4.35$ (D) $m_{n=0}^{0^{-+}} = 0, m_{n=1}^{0^{-+}} \approx 3.06, m_{n=2}^{0^{-+}} \approx 4.81$
3	0^{--}	(Type IIB) (N/D) $m_{n=0}^{0^{--}}(T) = 0, m_{n=1}^{0^{--}}(T) = \frac{32.46}{\pi},$ $m_{n=2}^{0^{--}}(T) = \frac{32.88}{\pi}$	(Type IIB) (large n) (N/D) $\frac{1}{2}5^{3/4}\sqrt[4]{\frac{2(\sqrt{6}\sqrt{\pi^2(16n^2+22n+7)+6+6})+3\pi^2(2n+1)}{32-3\pi^2}}$
4	1^{++}	(M theory) (N/D) $m_{n=0}^{1^{++}}(T) = 2.6956, m_{n=1}^{1^{++}}(T) = 2.8995$ $m_{n=2}^{1^{++}}(T) = 2.9346$	(M theory) (N) $m_{n=0}^{1^{++}}(r_h = 0) \approx 1.137$ (D) $m_{n=0}^{1^{++}}(r_h = 0) \approx 0.665$
5	2^{++}	(M theory) (N) $m_{n=0}^{2^{++}}(T) = \frac{5.086}{\pi}, m_{n=1}^{2^{++}}(T) = \frac{5.269}{\pi}$ $m_{n=2}^{2^{++}}(T) = \frac{5.318}{\pi}$ $m_{n=0}^{2^{++}}(D, T) = 0, m_{n+1}^{2^{++}}(D, T) = m_n^{2^{++}}(N, T)$	(M theory) $= m_n^{1^{++}}(r_h = 0)$

Table 3: Summary of Glueball Spectra from Type IIB, IIA and M Theory for $r_h \neq 0/r_h = 0$ using Neumann/Dirichlet boundary conditions at the horizon r_h /IR cut-off r_0

Some salient features of Table 3 are presented below:

- The following is the comparison of ratios of 0^{--} glueball masses obtained in this work from Neumann/Dirichlet boundary conditions at the horizon, with [61]:

Ratio	Our Results	[61]'s Results
$\frac{m_{0^{--}}^*}{m_{0^{--}}}$	1.0129	1.5311
$\frac{m_{0^{--}}^{**}}{m_{0^{--}}^*}$	1.0033	1.3244
$\frac{m_{0^{--}}^{***}}{m_{0^{--}}^{**}}$	1.0013	1.2393
$\frac{m_{0^{--}}^{****}}{m_{0^{--}}^{***}}$	1.0007	1.1588

Table 4: Comparison of ratios of 0^{--} glueball masses obtained from Neumann/Dirichlet boundary conditions at the horizon, with [61]

Hence, for higher excited states, the ratio of masses of successive excited states approaches unity faster as per our results as compared to [61].

- From a comparison of results in Tables 1/2 or Figures 2 with $N \rightarrow \infty$ lattice results, it appears that WKB quantization-based spectra are closer to $N \rightarrow \infty$ lattice results than the computations involving imposing Neumann/Dirichlet boundary conditions at the horizon/IR cut-off. In particular, it is pleasantly surprising that the WKB quantization method applied to the $0^{++}, 0^{-+}$ glueball spectra, is able to provide a good agreement (in fact for the lightest 0^{++} glueball spectrum, better than the classic computations of [61]) with lattice results even for the ground and the lower excited states.

Acknowledgements

KS is supported by is supported by a senior research fellowship (SRF) from the Ministry of Human Resource and Development (MHRD), Govt. of India. VY is supported by a junior research fellowship (JRF) from the University Grants Commission, Govt. of India. We would like to thank P. Majumdar and S. Gupta for useful communications, H. B. Filho for a useful clarification, and R. Das for participating in the material in **3.2.1** as part of his Masters' project work. One of us (AM) would like to dedicate this work to the memory of his father, the late R. K. Misra who was and (whose memory) still remains a true driving force and inspiration for him.

A $\widetilde{F}_5^2, \widetilde{F}_3^2, H_3^2$

The expressions of squares of various fluxes that figure in the EOM (180) are given below for ready reference:

$$\begin{aligned}
\widetilde{F}_5^2 &= -\frac{8}{\sqrt{\pi}\sqrt{N}\sqrt{g_s}} - \frac{1}{254803968\pi^{13/2}N^{7/10}} \\
&\times \left[M^4 r^6 N_f^4 g_s^{11/2} (r^4 - r_h^4) (\phi_1 + \phi_2 - \psi)^2 \left(N_f g_s \log(N) (2(r+1)\log(r) + 1) + 2 \left\{ -9(r+1)N_f g_s \log^2(r) \right. \right. \right. \\
&\left. \left. \left. - 2(r+1)\log(r) (2\pi - \log(4)N_f g_s) + \log(4)N_f g_s \right\} \right)^2 \right] \\
&+ a^2 \left[+\frac{\pi^{3/2} r^{10} g_s^{3/2}}{956593800 N^{7/10}} - \frac{24}{\sqrt{\pi}\sqrt{N}\sqrt{g_s} r^2} - \frac{1}{84934656\pi^{13/2} N^{7/10}} \right. \\
&\times \left\{ M^4 r^6 N_f^4 g_s^{11/2} (r^4 - r_h^4) (\phi_1 + \phi_2 - \psi)^2 (24r \log r - 1) \left(N_f g_s \log(N) (2(r+1)\log(r) + 1) \right. \right. \\
&\left. \left. + 2 \left\{ -9(r+1)N_f g_s \log^2(r) - 2(r+1)\log(r) (2\pi - \log(4)N_f g_s) + \log(4)N_f g_s \right\} \right)^2 \right\} \left. \right]; \\
\widetilde{F}_3^2 &= \frac{729 M^2 N_f^2 \sqrt{g_s} (r^4 - r_h^4) (72 a^2 N^{2/5} \log(r) + a^2 (- (3 N^{2/5} + 4)) + 2 N^{2/5} r^2)}{128 \pi^{7/2} N^{11/10} r^6}; \\
H_3^2 &= \frac{243 M^2 N_f^2 g_s^{5/2} (r^4 - r_h^4) (144 a^2 (\sqrt[5]{N} + 3) r \log(r) + a^2 (9 - 15 \sqrt[5]{N}) + 2 (\sqrt[5]{N} + 1) r^2)}{256 \pi^{7/2} \sqrt{N} r^6}; \\
\widetilde{F}_{x_2 x_3 p_3 p_4 p_5} \widetilde{F}_{x_2 x_3 q_3 q_4 q_5} g^{p_3 q_3} g^{p_4 q_4} g^{p_5 q_5} h^{x_2 x_3} &= \frac{60 r^4}{\pi^{3/2} N^{3/2} g_s^{3/2}} - \frac{1}{169869312 \pi^{13/2} N^{7/10}} \\
&\times \left[5 M^4 r^{10} N_f^4 g_s^{9/2} (r^4 - r_h^4) (\phi_1 + \phi_2 - \psi)^2 \left(N_f g_s \log(N) (2(r+1)\log(r) + 1) + 2 \left\{ -9(r+1)N_f g_s \log^2(r) \right. \right. \right. \\
&\left. \left. \left. - 2(r+1)\log(r) (2\pi - \log(4)N_f g_s) + \log(4)N_f g_s \right\} \right)^2 \right] + a^2 \left[\frac{180 r^2}{\pi^{3/2} N^{3/2} g_s^{3/2}} + \frac{1}{56623104 \pi^{15/2} N^{17/10}} \right. \\
&\times \left\{ 5 M^4 r^{10} N_f^4 g_s^{9/2} (r^4 - r_h^4) (\phi_1 + \phi_2 - \psi)^2 (24r \log r - 1) \left(N_f g_s \log(N) (2(r+1)\log(r) + 1) \right. \right. \\
&\left. \left. + 2 \left\{ -9(r+1)N_f g_s \log^2(r) - 2(r+1)\log(r) (2\pi - \log(4)N_f g_s) + \log(4)N_f g_s \right\} \right)^2 \right\} \left. \right]. \tag{A1}
\end{aligned}$$

References

- [1] M. Mia, K. Dasgupta, C. Gale and S. Jeon, *Five Easy Pieces: The Dynamics of Quarks in Strongly Coupled Plasmas*, Nucl. Phys. B **839**, 187 (2010) [arXiv:hep-th/0902.1540].
- [2] M. Dhuria and A. Misra, *Towards MQGP*, JHEP 1311 (2013) 001, [arXiv:hep-th/1306.4339].

- [3] K. Sil and A. Misra, *On Aspects of Holographic Thermal QCD at Finite Coupling*, Nucl. Phys. B **910**, 754 (2016) [arXiv:1507.02692 [hep-th]].
- [4] M. Natsuume, *String theory and quark-gluon plasma*, hep-ph/0701201.
- [5] K. Sil and A. Misra, *New Insights into Properties of Large- N Holographic Thermal QCD at Finite Gauge Coupling at (the Non-Conformal/Next-to) Leading Order in N* , Eur. Phys. J. C **76**, no. 11, 618 (2016) doi:10.1140/epjc/s10052-016-4444-7 [arXiv:1606.04949 [hep-th]].
- [6] Juan M. Maldacena, *The Large N Limit of Superconformal Field Theories and Supergravity*, Adv.Theor.Math.Phys.2:231-252,(1998), doi:10.1023/A:1026654312961 [arXiv:hep-th/9711200]
- [7] G. Boyd, J. Engels, F. Karsch, E. Laermann, C. Legeland, M. Luetgemeier, B. Petersson *Thermodynamics of $SU(3)$ Lattice Gauge Theory*, Nucl.Phys. B469 (1996) 419-444, [arXiv:hep-lat/9602007]
- [8] P. Colangelo, F. Giannuzzi and S. Nicotri, *Holographic Approach to Finite Temperature QCD: The Case of Scalar Glueballs and Scalar and Scalar Mesons*, Phys. rev. D **80**, 094019 (2009) doi:10.1103/PhysRevD.80.094019 [arXiv:0909.1534 [hep-ph]].
- [9] S. Nicotri, *Scalar glueball in a holographic model of QCD*, Nuovo Cim. B bf 123,796 (2008) [Nuovo Cim. B **123**, 851 (2008)] doi:10.1393/ncb/i2008-10579-5, 10.1393/ncb/i2008-10580-0 [arXiv:0807.4377 [hep-ph]].
- [10] H. Forkel, *Glueball correlators as holograms*, arXiv:0808.0304 [hep-ph]].
- [11] H. Forkel, *Holographic glueball structure*, Phys. Rev. D **78**, 025001 (2008) doi:10.1103/PhysRevD.78.025001 [arXiv:071101179 [hep-ph]].
- [12] D. Li and M. Huang, *Dynamical holographic QCD model for glueball and light meson spectra*, JHEP **1311**, 088 (2013) doi:10.1007/JHEP11(2013)088 [arXiv:1303.6929 [hep-ph]].
- [13] E. Folco Capossoli and H. Boschi-Filho, *Renormalized AdS_5 Mass for even Spin Glueball and Pomeron Trajectory from a Holographic softwall model*, arXiv:1611.09817[hep-ph].
- [14] F. Jugeau, *Holographic description of glueballs in a deformed AdS-dilaton background*, AIP Conf. Proc. **964** (2007) 151 doi:10.1063/1.2823842 [arXiv:0709.1093 [hep-ph]].
- [15] P. Colangelo, F. De Fazio, F. Jugeau and S. Nicotri, *On the light glueball spectrum in a holographic description of QCD*, Phys. Lett. B **652**, 73 (2007) doi:10.1016/j.physletb.2007.06.072 [hep-th/0703316].
- [16] W. H. Huang, *Holographic Description of Glueball and Baryon in Noncommutative Dipole Gauge Theory*, JHEP **0806**, 006 (2008) doi:10.1088/1126-6708/2008/06/006 [arXiv:0805.0985 [hep-ph]].
- [17] Y. Chen and M. Huang, *Two-gluon and trigluon glueballs from dynamical holography QCD*, Chin. Phys. C **40**, no. 12, 123101 (2016) doi:10.1088/1674-1137/40/12/123101 [arXiv:1511.07018 [hep-ph]].
- [18] I. Gordeli and D. Melnikov, *Calculation of glueball spectra in supersymmetric theories via holography*, arXiv:1311.6537 [hep-ph]].

- [19] K. Hashimoto, C. I. tan and S. Terashima, *Glueball decay in holographic QCD*, Phys. Rev. D **77**, 086001 (2008) doi:10.1103/PhysRevD.77.086001 [arXiv:0709.2208 [hep-th]].
- [20] F. Brunner and A. Rebhan, *Holographic QCD predictions for production and decay of pseudoscalar glueballs*, arXiv:1610.10034 [hep-ph].
- [21] A. Rebhan, F. Brunner and D. Parganlija, *Glueball decay patterns in top-down holographic QCD* PoS EPS **-HEP2015**, 421 (2015) [arXiv:1511.01391 [hep-ph]].
- [22] D. Parganlija *Scalar Glueball in a Top-Down Holographic Approach to QCD*, Acta Phys. Polon. Supp. **8**, no. 1, 219(2015) doi:10.5506/APhysPolBSupp.8.219 [arXiv:1503.00550 [hep-ph]].
- [23] F. Brunner, D. Parganlija and A. Rebhan, *Top-down Holographic Glueball Decay Rates*, AIP Conf. Proc. **1701**, 090007 (2016) doi:10.1063/1.4938709 [arXiv:1502.00456 [hep-ph]].
- [24] F. Brunner, D. Parganlija and A. Rebhan, *Holographic Glueball Decay*, Acta Phys. Polon. Supp. **7**, no. 3, 533 (2014) doi:10.5506/APhysPolBSupp.7.533 [arXiv:1407.6914 [hep-ph]].
- [25] D. Parganlija, *Tensor Glueball in a Top-Down Holographic Approach to QCD*, Acta Phys. Polon. Supp. **8**, no. 2, 289(2015) doi:10.5506/APhysPolBSupp.8.289 [arXiv:1506.03000 [hep-ph]].
- [26] E. Folco Capossoli and H. Boschi-Filho, *Glueball spectra and Regge trajectories from a modified holographic softwall model*, Phys. Lett. B **753**, 419 (2016) doi:10.1016/j.physletb.2015.12.034 [arXiv:1510.03372 [hep-ph]].
- [27] E. Witten, *Anti-de Sitter space, thermal phase transition and confinement in gauge theories*, Adv. Theor. Math. Phys. **2** (1998) 505 [hep-th/9803131].
- [28] J. Polchinski and M.J. Strassler, *Hard scattering and gauge/string duality*, Phys. Rev. Lett. **88** (2002) 031601 [hep-th/0109174].
- [29] M. Dhuria and A. Misra, *Transport Coefficients of Black MQGP M3-Branes*, Eur. Phys. J. C **75**, no. 1, 16 (2015) [arXiv:1406.6076 [hep-th]].
- [30] Igor R. Klebanov and Edward Witten, *Superconformal Field Theory on Threebranes at a Calabi-Yau Singularity*, Nucl. Phys. B **536**, 199 (1998)[arXiv:hep-th/9807080].
- [31] S. S. Gubser, *Einstein manifolds and conformal field theories*, Phys. Rev. D **59**, 025006 (1999) doi:10.1103/PhysRevD.59.025006 [hep-th/9807164].
- [32] N. Kochelev, *Ultralight glueballs in Quark-Gluon Plasma*, Phys. Part. Nucl. Lett. **13**, no. 2, 149 (2016) doi:10.1134/S1547477116020138 [arXiv:1501.07002 [hep-ph]].
- [33] A. S. Miranda, C. A. Ballon Bayona, H. Boschi-Filho and N. R. F. Braga, *Black-hole quasinormal modes and scalar glueballs in a finite-temperature AdS/QCD model*, JHEP **0911**, 119 (2009) [arXiv:0909.1790 [hep-th]].4
- [34] J. A. Minahan, *Glueball mass spectra and other issues for supergravity duals of QCD models* JHEP **9901**, 020 (1999) doi:10.1088/1126-6708/1999/01/020 [hep-th/9811156].
- [35] I.R. Klebanov and A. Tseytlin, *Gravity Duals of Supersymmetric $SU(N) \times SU(M + N)$ Gauge Theories*, [hep-th/0002159].

- [36] I. R. Klebanov and M. J. Strassler, *Supergravity and a Confining Gauge Theory: Duality Cascades and XSB-Resolution of Naked Singularities*, JHEP 0008:052,2000 [arXiv:hep-th/0007191].
- [37] P. Ouyang, *Holomorphic D7-Branes and Flavored N=1 Gauge Theories*, Nucl.Phys.B 699:207-225 (2004), [arXiv:hep-th/0311084].
- [38] A. Buchel, *Finite temperature resolution of the Klebanov-Tseytlin singularity*, Nucl. Phys. B **600**, 219 (2001) [hep-th/0011146].
- [39] S. S. Gubser, C. P. Herzog, I. R. Klebanov and A. A. Tseytlin, *Restoration of chiral symmetry: A Supergravity perspective*, JHEP **0105**, 028 (2001) [hep-th/0102172]; A. Buchel, C. P. Herzog, I. R. Klebanov, L. A. Pando Zayas and A. A. Tseytlin, *Nonextremal gravity duals for fractional D-3 branes on the conifold*, JHEP **0104**, 033 (2001)[hep-th/0102105].
- [40] M. Mahato, L. A. Pando Zayas and C. A. Terrero-Escalante, *Black Holes in Cascading Theories: Confinement/Deconfinement Transition and other Thermal Properties*, JHEP **0709**, 083 (2007) [arXiv:0707.2737 [hep-th]].
- [41] M. Mia, F. Chen, K. Dasgupta, P. Franche and S. Vaidya, *Non-Extremality, Chemical Potential and the Infrared limit of Large N Thermal QCD*, Phys. Rev. D **86**, 086002 (2012)[arXiv:1202.5321 [hep-th]].
- [42] M. Mia, K. Dasgupta, C. Gale and S. Jeon, *Toward Large N Thermal QCD from Dual Gravity: The Heavy Quarkonium Potential*, Phys. Rev. D **82**, 026004 (2010) [arXiv:1004.0387 [hep-th]].
- [43] A. Strominger, S. T. Yau and E. Zaslow, *Mirror symmetry is T duality*, Nucl. Phys. B **479**, 243 (1996) [hep-th/9606040].
- [44] M. Ionel and M. Min-OO, *Cohomogeneity One Special Lagrangian 3-Folds in the Deformed and the Resolved Conifolds*, Illinois Journal of Mathematics, Vol. 52, Number 3 (2008).
- [45] S. Alexander, K. Becker, M. Becker, K. Dasgupta, A. Knauf and R. Tatar, *In the realm of the geometric transitions*, Nucl. Phys. B **704**, 231 (2005) [hep-th/0408192].
- [46] F. Chen, K. Dasgupta, P. Franche, S. Katz and R. Tatar, *Supersymmetric Configurations, Geometric Transitions and New Non-Kahler Manifolds*, Nucl. Phys. B **852**, 553 (2011) [arXiv:hep-th/1007.5316].
- [47] D. Tong, *NS5-branes, T duality and world sheet instantons*, JHEP **0207**, 013 (2002) [hep-th/0204186].
- [48] A. Sen, *Dynamics of multiple Kaluza-Klein monopoles in M and string theory*, Adv. Theor. Math. Phys. **1**, 115 (1998)[hep-th/9707042].
- [49] F. Chen, K. Dasgupta, P. Franche, S. Katz and R. Tatar, *Supersymmetric Configurations, Geometric Transitions and New Non-Kahler Manifolds*, Nucl. Phys. B **852**, 553 (2011) [arXiv:1007.5316 [hep-th]].
- [50] G. Lopes Cardoso, G. Curio, G. Dall'Agata, D. Lust, P. Manousselis and G. Zoupanos, *NonKahler string backgrounds and their five torsion classes*, Nucl. Phys. B **652**, 5 (2003) [hep-th/0211118].

- [51] A. Butti, M. Grana, R. Minasian, M. Petrini and A. Zaffaroni, *The baryonic branch of Klebanov-Strassler solution: A supersymmetric family of $SU(3)$ structure backgrounds*, JHEP 0503, 069 (2005) [arXiv:hep-th/0412187].
- [52] S. Grigorian, *Deformations of G_2 -Structures with Torsion*, arXiv:1108.2465.
- [53] R. L. Bryant, *Some remarks on $G(2)$ -structures*, math/0305124 [math-dg].
- [54] S. Karigiannis, *Geometric Flows on Manifolds with G_2 Structure*, [arXiv:math/0702077].
- [55] P. Kaste, R. Minasian, M. Petrini and A. Tomasiello, *Kaluza-Klein bundles and manifolds of exceptional holonomy*, JHEP **0209**, 033 (2002) [hep-th/0206213].
- [56] C. Csaki, Y. Oz, J. Russo and J. Terning, *Large N QCD from rotating branes*, Phys. Rev. D **59**, 065012 (1999) doi:10.1103/PhysRevD.59.065012 [hep-th/9810186].
- [57] M. J. Teper, *$SU(N)$ gauge theories in $(2+1)$ -dimensions*, Phys. Rev. D **59**, 014512 (1999) doi:10.1103/PhysRevD.59.014512 [hep-lat/9804008].
- [58] R. C. Brower, S. D. Mathur and C. I. Tan, *Discrete spectrum of the graviton in the AdS_5 black hole background* Nucl. Phys. B **574**, 219 (2000) doi:10.1016/S0550-3213(99)00802-0 [hep-th/9908196].
- [59] Y. Chen *et al.*, *Glueball spectrum and matrix elements on anisotropic lattices*, Phys. Rev. D **73**, 014516 (2006) doi:10.1103/PhysRevD.73.014516 [hep-lat/0510074].
- [60] R. Sommer, *A New way to set the energy scale in lattice gauge theories and its applications to the static force and alpha-s in $SU(2)$ Yang-Mills theory*, Nucl. Phys. B **411**, 839 (1994) doi:10.1016/0550-3213(94)90473-1 [hep-lat/9310022].
- [61] C. Csaki, H. Ooguri, Y. Oz and J. Terning, *Glueball mass spectrum from supergravity*, JHEP **9901**, 017 (1999) doi:10.1088/1126-6708/1999/01/017 [hep-th/9806021].
- [62] Frederic. Brunner, Denis. Parganlija and Anton. Rebhan, *Glueball decay patterns in top-down holographic QCD*, [arXiv:1511.01391].
- [63] Elena. Caceres and Rafel. Hernandez, *Glueball Masses for the Deformed Conifold Theory*, [arXiv:hep-th/0011204].
- [64] Elena. Caceres and Xavier. Amador, *Spin two glueball mass and glueball regge trajectory from supergravity* ,JHEP**11**(2004) 022.
- [65] H. Boschi-Filho and N. R. F. Braga, *QCD/string holographic mapping and glueball mass spectrum*, Eur. Phys. J. C **32**, 529 (2004) doi:10.1140/epjc/s2003-01526-4 [hep-th/0209080].
- [66] N. R. Constable and R. C. Myers, *Spin two glueballs, positive energy theorems and the AdS/CFT correspondence*, JHEP **9910**, 037 (1999) doi:10.1088/1126-6708/1999/10/037 [hep-th/9908175].
- [67] R. C. Brower, S. D. Mathur and C. I. Tan, *Glueball spectrum for QCD from AdS supergravity Duality*, Nucl. Phys. B **587**, 249 (2000) doi:10.1016/S0550-3213(00)00435-1 [hep-th/0003115].
- [68] C. Csaki, H. Ouguri, Y. Oz, J. Terning, *Glueball mass spectrum from supergravity*, JHEP **9901**, 017 (1999) doi:10.1088/1126-6708/1999/01/017 [hep-th/9806021].

- [69] , I.R. Klebanov and N. Nekrasov, *Gravity Duals of Fractional Branes and Logarithmic RG Flow*, [hep-th/9911096].
- [70] B. A. Burrington, J. T. Liu, L. A. Pando Zayas and D. Vaman, *Holographic duals of flavored $N=1$ super Yang-mills: Beyond the probe approximation*, JHEP **0502**, 022 (2005)[hep-th/0406207].
- [71] R. C. Brower, S. D. Mathur and C. I. Tan, *Glueball spectrum for QCD from AdS supergravity duality*, Nucl. Phys. B **587**, 249 (2000) doi:10.1016/S0550-3213(00)00435-1 [hep-th/0003115].
- [72] *String Theory in a Nutshell*, E. Kiritsis, Princeton University Press (2007).
- [73] R. C. Brower, S. D. Mathur and C. I. Tan, *Discrete spectrum of the graviton in the AdS(5) black hole background*, Nucl. Phys. B **574**, 219 (2000) doi:10.1016/S0550-3213(99)00802-0 [hep-th/9908196].
- [74] S. Chiossi, S. Salamon, *The Intrinsic Torsion of $SU(3)$ and G_2 Structures*, arXiv:math/0202282 [math.DG].
- [75] *Gauge/string duality and scalar glueball mass ratios*, Henrique Boschi-Filho, Nelson R. F. Braga, JHEP0305:009,2003 [hep-th/0212207].